Substrate Specificity and Metal Requirements of 3-Deoxy-D-manno-octulosonate 8-Phosphate Synthase (KDOPS)

by

Jingjing Li

A dissertation submitted in partial fulfillment
of the requirements for the degree of
Doctor of Philosophy
(Chemistry)
in The University of Michigan
2008

Doctoral Committee:

Professor Ronald W. Woodard, Chair
Professor E. Neil G. Marsh
Professor Henry I. Mosberg
Professor Edwin Vedejs

This manuscript is dedicated to my dear parents and grandparents for their hope and dream.

ACKNOWLEDGEMENTS

I would particularly like to thank Professor Woodard for providing both guidance and laboratory environment that have been necessary for my PhD study. I would also like to thank my thesis committee members for their helpful suggestions and insight. I want to express my gratitude to members in the Woodard laboratory for accompanying and helping me.

I finally would like to thank my husband since it would not be possible for me to complete this thesis without his love, support, patience, and understanding.

TABLE OF CONTENTS

LIST OF TABLES

Table

LIST OF FIGURES

Figure

CHAPTER 1

INTRODUCTION

1.1. BACTERIAL PATHOGENESIS

Historically, a major human health problem has been microorganisms that are pathogenic bacteria. Thousands of antibiotics have been designed to treat this problem, but it continues, due to the ability of these microorganisms to survive through mutations and become resistant to antibiotic treatment. This increases the importance of finding novel antibiotics.

Present antibiotics can be divided into five categories based on their inhibition targets: cell wall formation, protein synthesis , nucleic acid synthesis, cell membrane or cell spindle functions [1]. To date, the majority of cell wall antibiotics function by inhibiting the enzymes involved in the biosynthesis of peptidoglycan portion of the cell wall. These antibiotics are effective mainly against Gram-positive (G+) microorganisms, which contain 50-80% of peptidoglycan [2]. In Gram-negative (G-) microorganisms, the lower peptidoglycan content (8-10%), as well as several other differences in cell wall composition, often renders peptidoglycan-type inhibitors less effective [2]. However, many of the more deadly organisms are G- species. For example, *Francisella tularemia*, which causes tularemia, is one of the most infectious pathogenic bacteria known [3]; fleas

carried by rodents infected with *Yersinia pestis* transmitted the infection to humans to cause the Black Death/Plague [4]; pathogenic *E. coli* strains O157:H7 and CFT073 also cause millions of illnesses, which are not lethal but quite debilitating [5]. Those organisms are all G- bacteria. Therefore, a real need exists to develop effective antibiotics against G- microorganisms that function via a different mechanism of action.

In the cell envelope of G- bacteria, the peptidoglycan layer is surrounded by an outer membrane that contains phospholipids, proteins, and lipopolysaccharide (Figure 1-1) [2]. Lipopolysaccharide (LPS) is a fundamental constituent of the G- cell envelope consisting of several distinct regions. The inner core region of the LPS contains 2-3 residues of the unique octulose—3-deoxy-D-*manno*-octulosonate (KDO). KDO serves to join the lipid A, the membrane imbedded component of the LPS, to the remaining outer core and O-antigen elements of the LPS [6]. The requirement of KDO incorporation into LPS for proper cellular growth was first demonstrated by Rick and Osborn [7]. Inhibition of the biosynthesis of LPS with subsequent arrest in cell growth has been attributed to specific mutations in the *Salmonella typhimurium* KDO biosynthesis. Munson et al. [8], showed that two molecules of KDO are necessary for the maturation of the LPS structure in *E. coli*. Microorganisms producing incomplete LPS should be non-viable and/or more susceptible to antibiotics. Therefore, several key enzymes in the KDO biosynthetic pathway are considered to be ideal chemotherapeutic targets for the development of novel G- antibiotics.

The KDO biosynthetic pathway is responsible for incorporation of KDO into the LPS in G- bacteria, and consists of several important enzymes including: (1) arabinose 5-phosphate (A5P) isomerase, (2) 3-deoxy-D-*manno*-octulosonate 8-phosphate

synthase (KDOPS), (3) 3-deoxy-D-*manno*-octulosonate 8-phosphate (KDO8P) phosphatase, (4) CMP-KDO synthase, and (5) CMP-KDO transferase (Figure 1-2). The first three enzymes in this biosynthetic pathway are studied in the Woodard laboratory as targets for the development of antibacterial agents.

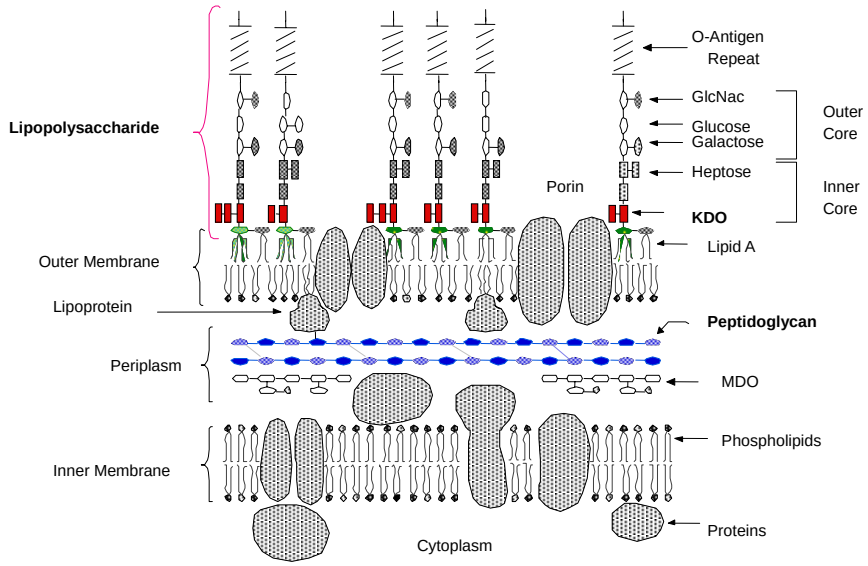

Figure 1-1. Representation of the cell wall of G- bacteria of *E. coli* [2].

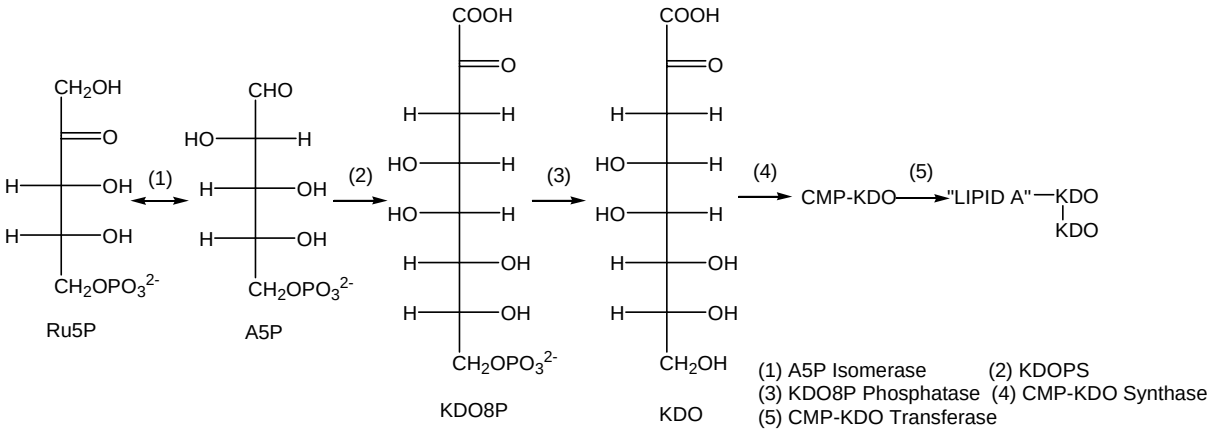

Figure 1-2. KDO biosynthetic pathway.

1.2. KDOPS

The second product in the LPS biosynthetic pathway is KDO8P, the phosphorylated precursor of KDO. The enzyme KDOPS catalyzes the irreversible condensation of arabinose 5-phosphate (A5P) and phospho*enol*pyruvate (PEP) to yield inorganic phosphate and monosaccharide KDO8P (Figure 1-3) [9].

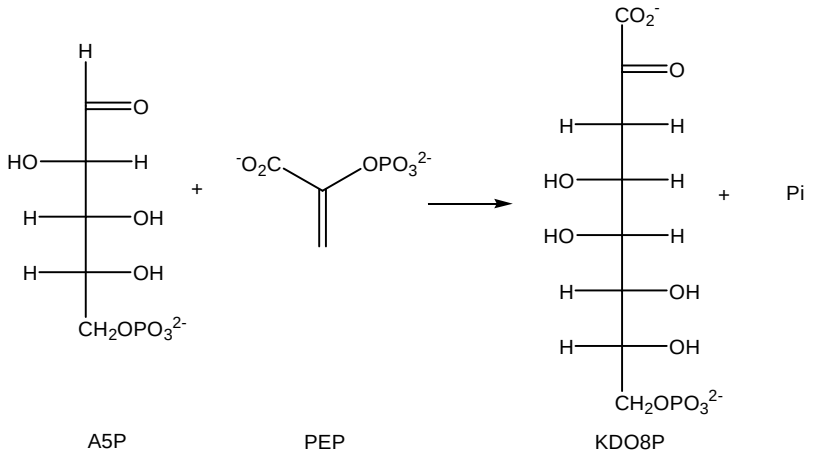

Figure 1-3. Reaction catalyzed by KDOPS.

In addition to its importance in G- bacteria, much is known about the structure and mechanism of KDOPS.

The crystal structure of *E. coli* KDOPS ($KDOPS^{Ec}$) has been determined in collaboration between Professor Domenico Gatti at Wayne State University and our laboratory [10]. KDOPS is a homotetramer in which each monomer folds into a $(\beta/\alpha)_8$ barrel (Figure 1-4).

The structures of *Aquifex aeolicus* KDOPS ($KDOPS^{Aq}$) with various combinations of substrates and metal have also been obtained (Figure 1-5) [11]. The enzyme active site is located at the C-terminal end of the barrel in each subunit at the interface with the adjacent subunit. Three loops L2, L7, and L8 control the access to the

active site. The loop L7 becomes ordered and isolates the active site from bulk solvent only after both substrates (A5P and PEP) are bound. The PEP binds to the bottom of the active site cavity, while A5P binds at the top. The two substrates are mainly stabilized by a network of hydrogen bonds and salt bridges between their phosphate and carboxylate/aldehyde moieties and several active site residues.

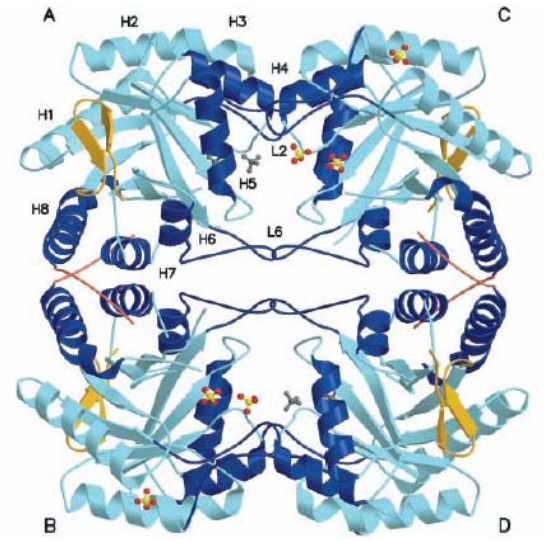

Figure 1-4. Overall structure of one asymmetric unit in KDOPS^{Ec} at 2.4 Å [10].

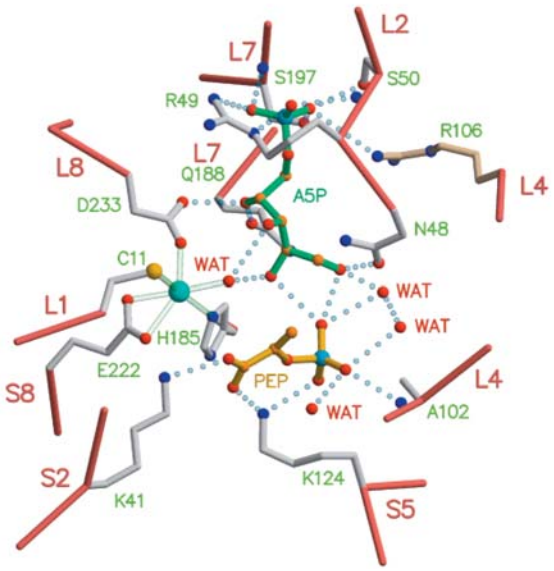

Figure 1-5. Crystal structure of KDOPS^{Aa} active site with PEP, A5P and metal bound [11].

Earlier studies have determined that the reaction of KDOPS is a sequentially ordered process in which the binding of PEP precedes the binding of A5P and the release of inorganic phosphate precedes the release of KDO8P [12]. The condensation step of the reaction is stereospecific, which involves the addition of the *si* face of C3 of PEP to the *re* face of the A5P carbonyl [13]. The conclusion was deduced from the stereochemistry of the product KDO8P and by using 3-substituted PEP analogues. Based on the information from these studies as well as crystal structures, a mechanism has been proposed for the reaction of KDOPS: an activated active site water molecule attacks at C2 of PEP, coincident with the addition of C3 of PEP to the electrophilic aldehyde of A5P, to yield a linear intermediate, followed by the release of inorganic phosphate (Figure 1-6) [14].

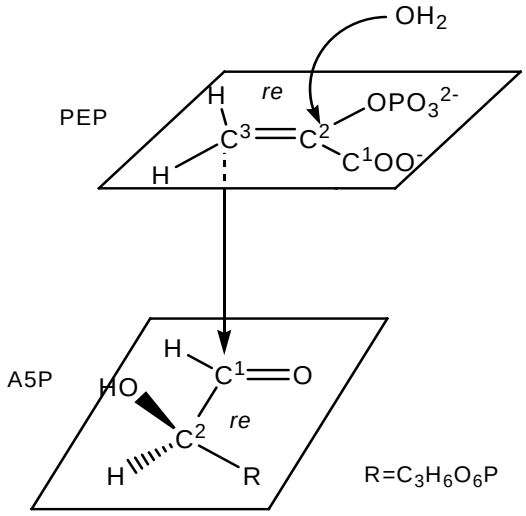

Figure 1-6. Stereochemical mechanism of KDOPS.

It has also been established that phosphate release in the KDOPS catalyzed reaction occurs by cleavage of the C-O bond of PEP [15], as opposed to the more

conventional cleavage of the P-O bond in PEP utilizing enzymes [16]. Only five known PEP utilizing enzymes catalyze the breakage of the C-O bond during their reaction. Two of them catalyze the transfer of the intact *enol*ether moiety of PEP: *enol*pyruvylshikimate phosphate (EPSP) synthase [EC 2.5.1.7] and UDP-*N*-acetylglucosamine *enol*pyruvyl transferase (EPTase) [EC 2.5.1.7]. The other three catalyze the aldol-type condensation reaction between PEP and a phosphorylated monosaccharide: KDOPS, 3-deoxy-D-*arabino*-heptulosonate 7-phosphate synthase (DAHPS) [17] and *N*-acetylneuraminate 9-phosphate synthase [EC 4.1.2.20] [18].

DAHPS, which is considered to be a functionally related enzyme to KDOPS, is also under investigation in the Woodard laboratory. DAHPS catalyzes the first committed step in the Shikimate pathway. The Shikimate pathway is responsible for the generation of aromatic amino acids and aromatic vitamins [19]. DAHPS catalyzes a similar condensation reaction of PEP with a phosphorylated monosaccharide, erythrose 4-phosphate (E4P), to form 3-deoxy-D-*arabino*-heptulosonate 7-phosphate (DAH7P) (Figure 1-7) [17]. E4P is one -CHOH- unit shorter than A5P, the substrate of KDOPS.

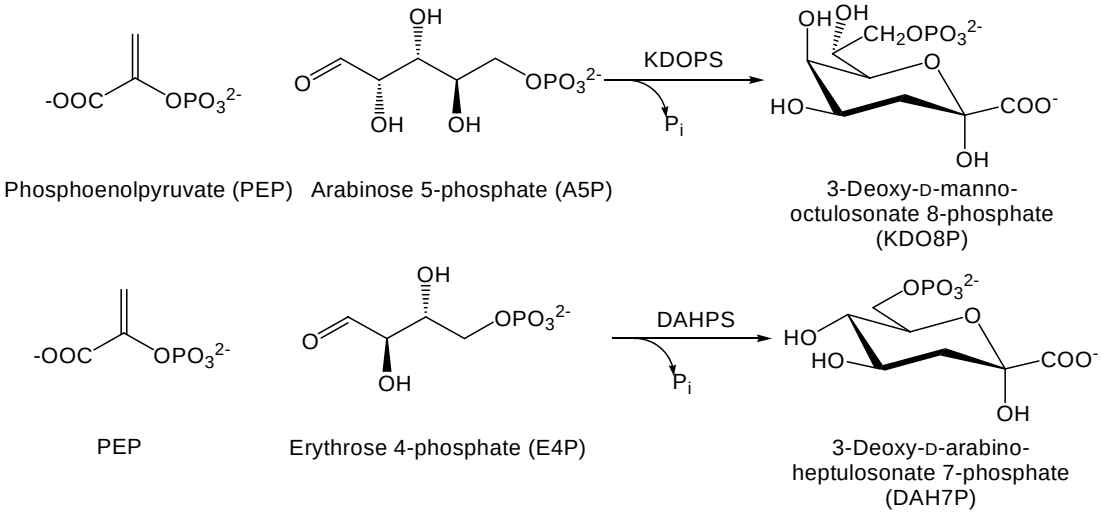

Figure 1-7. Reactions catalyzed by KDOPS and DAHPS.

The crystal structure of DAHPS from several different organisms has also been obtained. Both KDOPS and DAHPS fold into a $(\beta/\alpha)_8$ barrel topology [10, 20], and their composition and architecture in the active sites bear a striking resemblance (Figure 1-8) [10]. These similarities suggest a divergent evolutionary relationship between KDOPS and DAHPS, and potentially a common mechanism for these two enzymes.

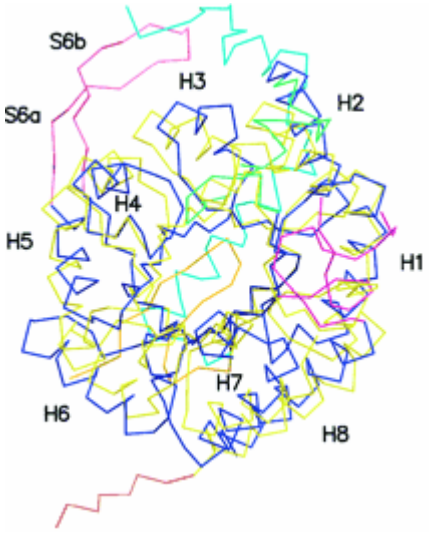

Figure 1-8. Least-square superposition of the monomers of the KDOPS^{Ec} and DAHPS^{Ec} [10]. The KDOPS^{Ec} is in yellow, the DAHPS^{Ec} is in blue. The root mean square deviation for 205 aligned Cα atoms is 1.8 Å.

1.3. DISSERTATION RATIONALE

The ultimate goal of this dissertation is to study the substrate specificity and metal requirements of KDOPS in order to gain more mechanistic insight into KDOPS.

Multiple approaches were undertaken to study and characterize KDOPS, utilizing a combination of techniques in molecular biology, enzymology, biochemistry, and analytical chemistry.

Chapter 2 describes altering the substrate specificity of KDOPS from A5P to E4P in order to gather mechanistic information in substrate binding. Three types of

methodology from both rational design and random mutagenesis were conducted, including structure-based engineering, domain swapping and directed evolution.

Chapter 3 focuses on choosing alternate substrates for KDOPS from a series of A5P analogues. The results from this approach may give useful information on the substrate binding mechanism of KDOPS.

Chapter 4 describes the importance of metal in KDOPS mechanism. Interconversion between metallo and non-metallo KDOPSs was performed. The results from X-ray crystallography study were utilized to determine the role and function of metal and amino acid residues involved in metal binding.

1.4. REFERENCES

1. Zahner, H. and W.K. Maas, *Biology of Antibiotics*. 1972, New York: Springer Verlag.

2. Raetz, C.R. and C. Whitfield, *Lipopolysaccharide endotoxins.* Annu Rev Biochem, 2002. **71**: p. 635-700.

3. Oyston, P.C., A. Sjostedt, and R.W. Titball, *Tularaemia: bioterrorism defence renews interest in Francisella tularensis.* Nat Rev Microbiol, 2004. **2**(12): p. 967-78.

4. Bockemuhl, J., *[100 years after the discovery of the plague-causing agent--importance and veneration of Alexandre Yersin in Vietnam today].* Immun Infekt, 1994. **22**(2): p. 72-5.

5. Hooton, T.M. and W.E. Stamm, *Diagnosis and treatment of uncomplicated urinary tract infection.* Infect Dis Clin North Am, 1997. **11**(3): p. 551-81.

6. Duewel, H.S., et al., *Functional and biochemical characterization of a recombinant 3-Deoxy-D-manno-octulosonic acid 8-phosphate synthase from the hyperthermophilic bacterium Aquifex aeolicus.* Biochemical and biophysical research communications., 1999. **263(2)**: p. 346-51.

7. Rick, P.D. and M.J. Osborn, *Lipid A mutants of Salmonella typhimurium. Characterization of a conditional lethal mutant in 3-deoxy-D-mannooctulosonate-8-phosphate synthetase.* J Biol Chem, 1977. **252**(14): p. 4895-903.

8. Munson, R.S., Jr., N.S. Rasmussen, and M.J. Osborn, *Biosynthesis of lipid A. Enzymatic incorporation of 3-deoxy-D-mannooctulosonate into a precursor of lipid A in Salmonella typhimurium.* J Biol Chem, 1978. **253**(5): p. 1503-11.

9. Levin, D.H. and E. Racker, *Condensation of arabinose 5-phosphate and phosphorylenol pyruvate by 2-keto-3-deoxy-8-phosphooctonic acid synthetase.* J Biol Chem, 1959. **234**: p. 2532-9.

10. Radaev, S., et al., *Structure and mechanism of 3-deoxy-D-manno-octulosonate 8-phosphate synthase.* J Biol Chem, 2000. **275**(13): p. 9476-84.

11. Duewel, H.S., et al., *Substrate and metal complexes of 3-deoxy-D-manno-octulosonate-8-phosphate synthase from Aquifex aeolicus at 1.9-A resolution. Implications for the condensation mechanism.* The Journal of biological chemistry., 2001. **276(11)**: p. 8393-402.

12. Kohen, A., A. Jakob, and T. Baasov, *Mechanistic studies of 3-deoxy-D-manno-2-octulosonate-8-phosphate synthase from Escherichia coli.* Eur J Biochem, 1992. **208**(2): p. 443-9.

13. Dotson, G.D., et al., *Stereochemistry of 3-deoxyoctulosonate 8-phosphate synthase.* Biochemistry, 1993. **32**(46): p. 12392-7.

14. Hedstrom, L. and R. Abeles, *3-Deoxy-D-manno-octulosonate-8-phosphate synthase catalyzes the C-O bond cleavage of phosphoenolpyruvate.* Biochem Biophys Res Commun, 1988. **157**(2): p. 816-20.

15. Dotson, G.D., et al., *Overproduction and one-step purification of Escherichia coli 3-deoxy-D-manno-octulosonic acid 8-phosphate synthase and oxygen transfer studies during catalysis using isotopic-shifted heteronuclear NMR.* J Biol Chem, 1995. **270**(23): p. 13698-705.

16. Walsh, C.T., et al., *The versatility of phosphoenolpyruvate and its vinyl ether products in biosynthesis.* Chem Biol, 1996. **3**(2): p. 83-91.

17. DeLeo, A.B. and D.B. Sprinson, *Mechanism of 3-deoxy-D-arabino-heptulosonate 7-phosphate (DAHP) synthetase.* Biochem Biophys Res Commun, 1968. **32**(5): p. 873-7.

18. Sundaram, A.K., et al., *Characterization of N-acetylneuraminic acid synthase isoenzyme 1 from Campylobacter jejuni.* Biochem J, 2004. **383**(Pt 1): p. 83-9.

19. Ganem, B., *From Glucose to Aromatics: Recent Developments in Natural Products of the Shikimic Acid Pathway.* Tetrahedron, 1978. **34**: p. 3353-3383.

20. Shumilin, I.A., R.H. Kretsinger, and R.H. Bauerle, *Crystal structure of phenylalanine-regulated 3-deoxy-D-arabino-heptulosonate-7-phosphate synthase from Escherichia coli.* Structure Fold Des, 1999. **7**(7): p. 865-75.

CHAPTER 2

ALTERNATION OF THE SUBSTRATE SPECIFICITY OF KDOPS

2.1. SUMMARY

As described in Chapter 1, KDOPS and DAHPS are two similar enzymes. One of the main differences between KDOPS and DAHPS is that they use different monosaccharide substrates. The substrate of KDOPS, A5P, is one -CHOH- unit longer than E4P, the substrate of DAHPS. The *E. coli* DAHPS ($DAHPS^{Ec}$) was shown to catalyze the condensation of A5P with PEP albeit at modest rates [1]. The *E. coli* KDOPS ($KDOPS^{Ec}$) is strictly substrate specific for A5P, and is not able to utilize E4P as an alternate substrate (Figure 2-1).

The substrate specificity difference between the KDOPS and DAHPS may be due to the differences in their structure or catalytic mechanism. Altering the substrate specificity of KDOPS to utilize E4P as an alternate substrate may provide valuable information on the role of amino acid residues involved in substrate binding of KDOPS and DAHPS.

To alter the KDOPS substrate specificity, three sets of experiments were utilized: structure-based engineering, domain swapping and directed evolution. Several key substrate binding sites/residues were identified and modified verifying their

importance. However, none of the resulting modified KDOPS is able to utilize E4P as an alternate substrate.

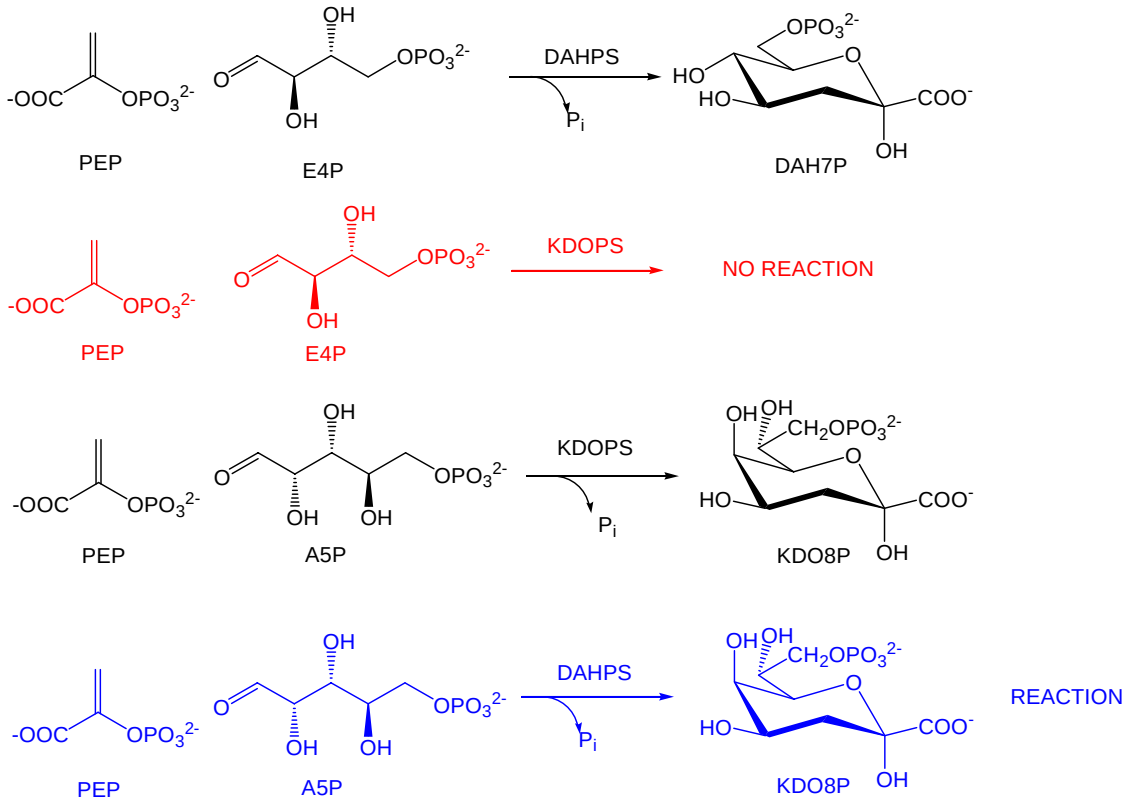

Figure 2-1. Substrate specificity difference between KDOPS and DAHPS.

2.2. STRUCTURE-BASED ENGINEERING

2.2.1. Introduction

The crystal structures of *A. aeolicus* KDOPS (KDOPS^{Aa}) and *Thermotoga. maritima* DAHPS (DAHPS^{Tm}) with both substrates have been solved by our collaborator and our laboratory [2, 3]. Both KDOPS^{Aa} and DAHPS^{Tm} are metallo enzymes and hyperthermophilic enzymes, which display optimal activity at 90-95^{o}C [4]. The phosphorylated monosaccharide biding site structures of the two enzymes were overlaid using PyMol (see Figure 2-2, 2-3, 2-4, 2-5, and 2-6: KDOPS^{Aa} A5P binding site and A5P

are shown in green, DAHPS^{Tm} E4P binding site and E4P are shown in pink). As shown in Figure 2-2, the PEP of both KDOPS^{Aa} and DAHPS^{Tm} binds at a similar position at the bottom of the active site, while A5P in KDOPS^{Aa} binds at a higher place than E4P in DAHPS^{Tm}. Based on the structure overlay of KDOPS^{Aa} and DAHPS^{Tm} as well as sequence alignment between KDOPSs and DAHPSs from several different organisms, four major sites are considered important for the difference in substrate specificity of the two enzymes.

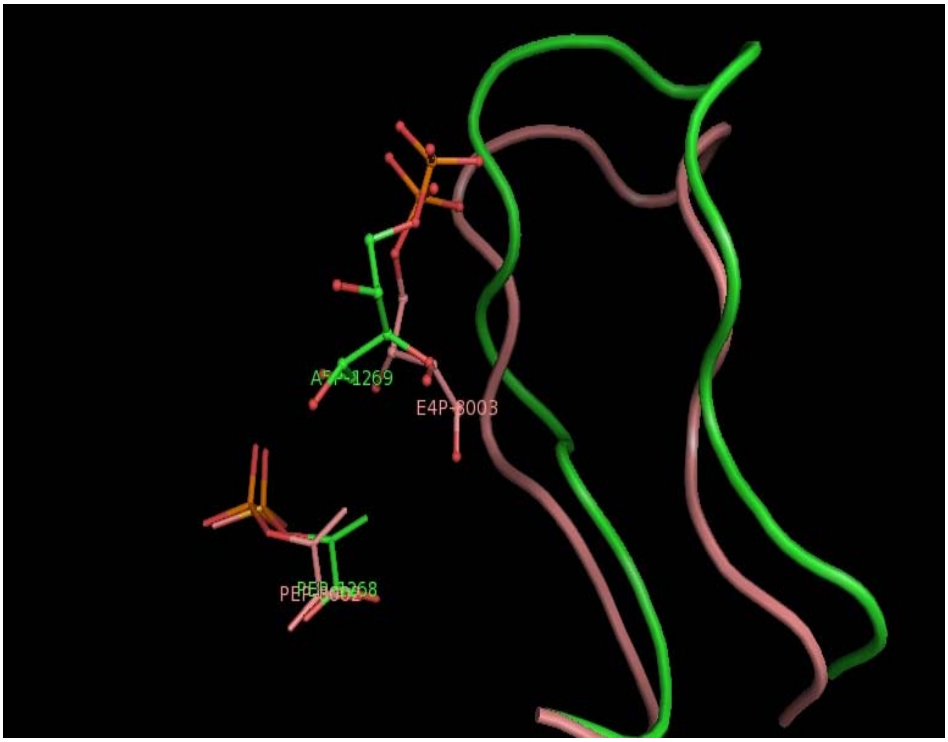

Figure 2-2. PEP and A5P/E4P binding site of KDOPS^{Aa} (shown in green) and DAHPS^{Tm} (shown in pink).

1) An Arg is critical in both KDOPS (R49 in KDOPS^{Aa}) and DAHPS (R133 in DAHPS^{Tm}) (see Figure 2-3).

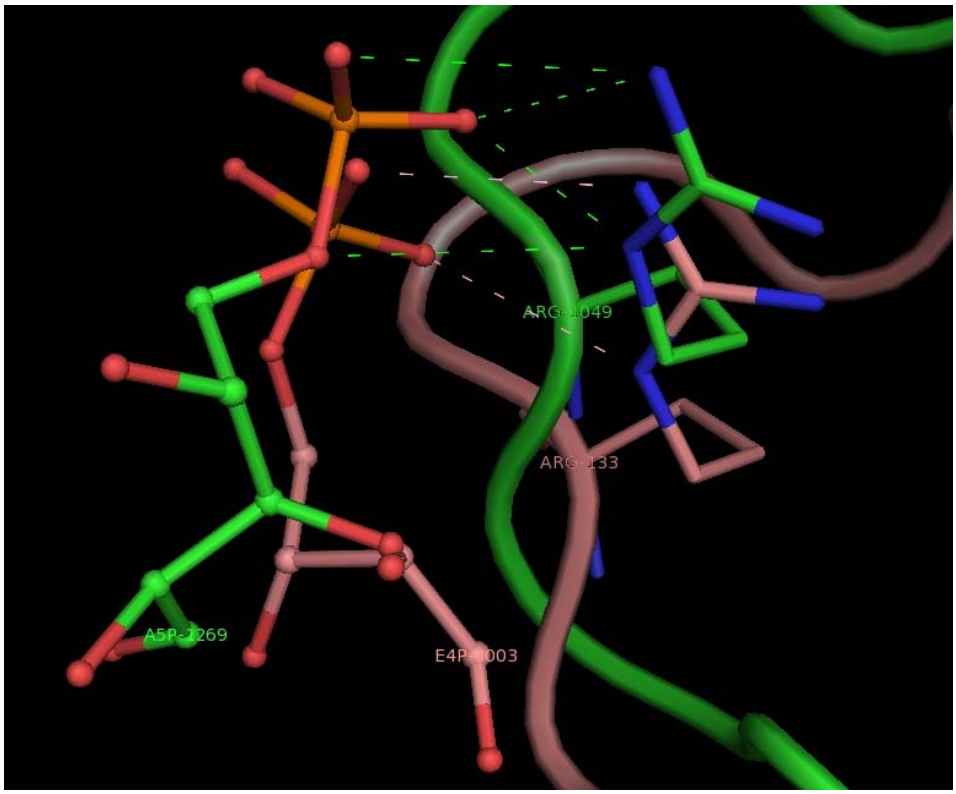

KDOPS^{Aa}	41	KSSFDKANRSSIHSFRGHGL	60
KDOPS^{Ec}	55	KASFEKANRSSIHSYRGPGL	74
DAHPS^{Tm}	126	RGGAYK-PRTSPYSFGGLGE	144
DAHPS^{Ap}	70	RGGAFK-PRTSPYSFQGLGL	88

Figure 2-3. Comparison of R49 in KDOPS^{Aa} (green) to R133 in DAHPS^{Tm} (pink).

The guanidinium group of the side chain of R49 in KDOPS^{Aa} interacts with the phosphate moiety of A5P; while in DAHPS^{Tm}, the corresponding R133 interacts similarly with the phosphate moiety of E4P. This Arg residue is conserved in all known KDOPSs and DAHPS is considered essential in positioning the phosphate moiety of A5P and E4P. Figure 2-2 shows that the PEP in KDOPS^{Aa} and DAHPS^{Tm} binds at similar place. The R49 in KDOPS^{Aa} binds at about 1Å higher than the R133 in DAHPS^{Tm}, which makes the phosphate moiety of E4P in DAHPS^{Tm} 1 Å closer to the C3 of PEP than the phosphate of

A5P in KDOPS^{Aa}. The proposed mechanism of KDOPS/DAHPS involves a nucleophilic attack by the C3 of PEP to the aldehyde of A5P/E4P to form a linear intermediate. This suggests that the reason that KDOPS cannot catalyze the condensation of E4P with PEP might be that the distance between the C1 of E4P and C3 of PEP is too great to form a covalent bond in KDOPS [5]. Conversely, DAHPS may catalyze the condensation between A5P and PEP, since A5P is able to fit within the E4P binding site, and the C1 of A5P is close enough to C3 of PEP for the nucleophilic attack. Mutating this R49 to a Gly in KDOPS^{Aa} will construct a mutant KDOPS^{Aa} in which the E4P might bind loosely and close enough to the PEP to facilitate the nucleophilic attack by C3 of PEP.

2) Active site Ala and Asn in KDOPS (A47 N48 in KDOPS^{Aa}) are replaced by a Pro in DAHPS (P132 in DAHPS^{Tm}) (see Figure 2-4).

The crystal structure overlay in Figure 2-4 shows that the R133 in DAHPS^{Tm} is responsible for binding the E4P phosphate may be held in place by a Pro in position 132. The P132 makes a turn in the loop, and brings the R133 lower and closer to the PEP binding site. The interaction between the side chain of the P132 and E4P also moves the E4P closer to the enzyme. In KDOPS^{Aa}, the R49 responsible for A5P phosphate binding is brought higher and further away from the PEP binding site, probably due to the presence of A47 and N48. The A47 and N48 in KDOPS^{Aa} are conserved in KDOPSs from different organisms, while the P132 in DAHPS^{Tm} is conserved in all known DAHPSs. If the A47 and N48 in KDOPS^{Aa} are replaced with a Pro, this Pro might play the same role as the P132 in DAHPS^{Tm} to hold the substrate binding residue R49 closer to

the PEP, which mimics the E4P binding site in DAHPS^{Tm}. Thus, E4P bound in the resulting mutant KDOPS^{Aa} might be close enough to the PEP for the nucleophilic attack.

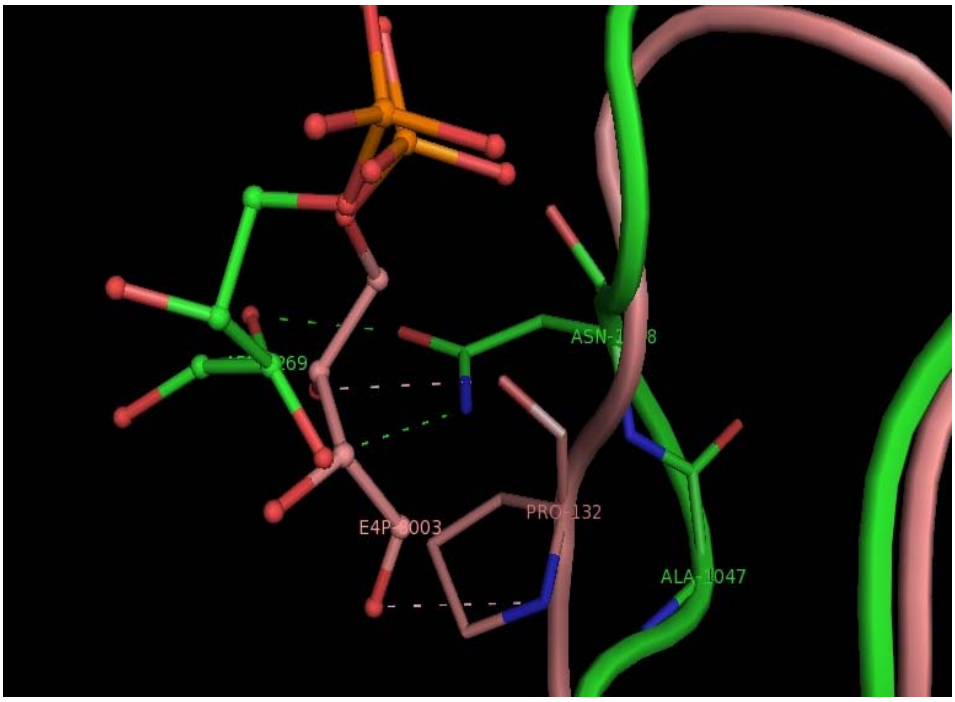

KDOPS^{Aa}	41	KSSFDKANRSSIHSFRGHGL	60
KDOPS^{Ec}	55	KASFEKANRSSIHSYRGPGL	74
DAHPS^{Tm}	126	RGGAYK-PRTSPYSFGGLGE	144
DAHPS^{Ap}	70	RGGAFK-PRTSPYSFQGLGL	88

Figure 2-4. Comparison of A47 N48 in KDOPS^{Aa} (green) to P132 in DAHPS^{Tm} (pink).

3) An Arg in KDOPS (R106 in KDOPS^{Aa}) is replaced by a Gln in DAHPS (Q189 in DAHPS^{Tm}) (see Figure 2-5).

The side chain of R106 in KDOPS^{Aa} from the adjacent subunit points into the active site and interacts with the phosphate moiety of A5P. In DAHPS^{Tm}, this Arg is replaced by Q189, which is shorter and lacks the positively charged guanidinium group to interact with the phosphate moiety of E4P. This R106, which is conserved in all KDOPSs, is considered important in positioning A5P in KDOPS. The Q189 in

DAHPS^{Tm} is conserved in all DAHPSs. Breaking the interaction between R106 and the phosphate moiety in KDOPS might result in looser binding of the phophorylated monosaccharide. If the R196 is mutated to a Gly or Gln in KDOPS^{Aa}, the resulting KDOPS^{Aa} mutant might be able to use E4P as an alternate substrate.

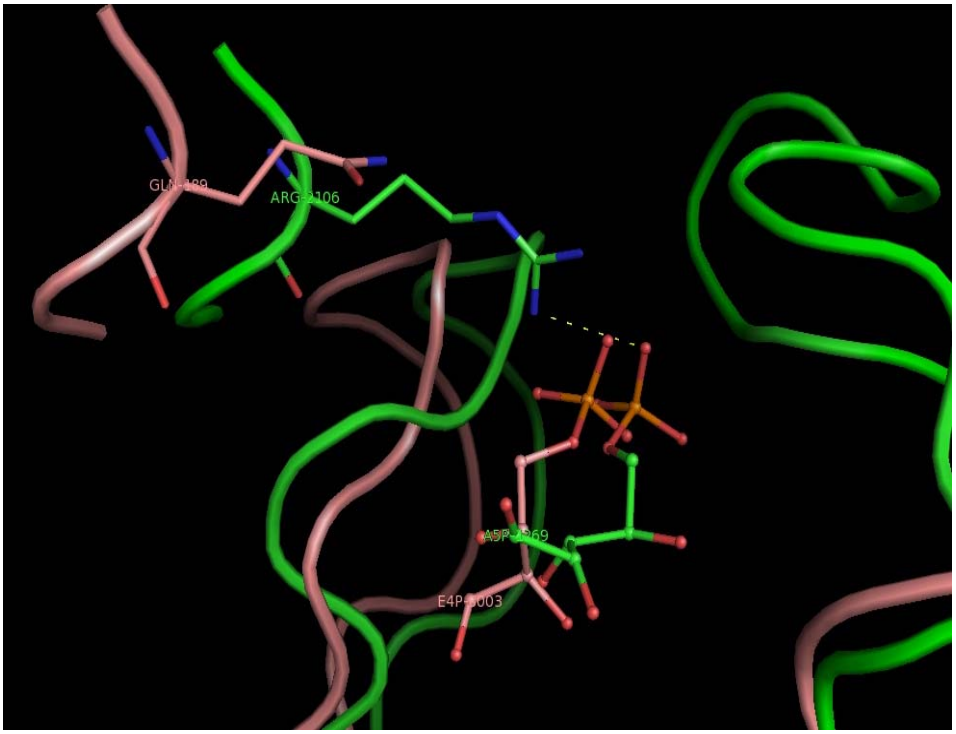

KDOPS^{Aa}	95	ADIIQIPAFLCRQTDLL	111
KDOPS^{Ec}	109	VDVIQLPAFLARQTDLV	125
DAHPS^{Tm}	178	ADIIQIGARNAQNFRLL	194
DAHPS^{Ap}	122	ADMLQIGARNMQNFPLL	138

Figure 2-5. Comparison of R106 in KDOPS^{Aa} (green) to Q189 in DAHPS^{Tm} (pink).

4) Loop 7 in KDOPS (V187—S197 in KDOPS^{Aa}) is absent in DAHPS (see Figure 2-6).

In KDOPS^{Aa}, two residues Q188 and S197 on L7 have interactions with A5P. In DAHPS^{Tm}, this L7 is lacking. Previous studies revealed that the L7 in KDOPS^{Aa} plays an important role in controlling access to the active site cavity [2]. When both PEP (at the bottom) and A5P (on top of PEP) are bound simultaneously, L7 is well

ordered and isolates the active site from bulk solvent [6]. Sequence alignments show that this L7 is conserved in all KDOPSs, while all known DAHPSs lack this loop. Truncating the L7 in KDOPS^{Aa} may make the substrate binding site of KDOPS^{Aa} more similar to that of DAHPS, which may increase the ability of KDOPS^{Aa} to utilize E4P as an alternate substrate.

KDOPS^{Aa}	184	THSVQLPGGLGDKSGGMREFI	204
KDOPS^{Ec}	201	THALQCRDPFGAASGGRRAQV	221
DAHPS^{Tm}	271	SHS----------GGRRDLV	280
DAHPS^{Ap}	215	SHP----------AGRRSLV	224

Figure 2-6. The loop7 (L7) in KDOPS^{Aa} (green) is absent in DAHPS^{Tm} (pink).

2.2.2. Experimental Procedures

Materials – Polymerase chain reaction (PCR) primers were synthesized by Invitrogen. PCR was performed using a MJ Research PTC-200 Peltier Thermal Cycler. The Wizard® Plus SV Minipreps DNA purification kit was utilized for plasmid isolation

and purification. Chemically competent *E. coli* XL1-Blue (Stratagene), chemically competent *E. coli* BL21 (DE3) (Novagen) were used for plasmid transformations. Restriction enzymes, T4 DNA ligase and *Dpn*I were purchased from New England Biolabs. DNA sequencing was performed by the University of Michigan Biomedical Resources Core Facility. Protein dye reagent concentrate was purchased from Bio-Rad. Tris(hydroxymethyl)aminomethane was purchased from Research Organics. Phospho*enol*pyruvate mono(cyclohexyl ammonium) salt, erythrose 4-phophate disodium salt, thiobarbituric acid, and bovine albumin serum (BSA) were purchased from Sigma. Arabinose 5-phosphate was prepared and purified by Dr. Junhua Yan in the Woodard laboratory. Enzyme grade KCl, NaCl, ammonium sulfate, and acetic acid were purchased from Fisher Scientific. DNase I and RNase A were purchased from Roche. High grade spectra/Por® 7 dialysis tubing (10,000 and 15,000 molecular weight cut-off and metal free) was purchased from VWR. The Millex® syringe driven filter units (0.22 μm) were purchased from Millipore. Phenyl Superose (HR 10/10) and Mono Q (HR 10/10) chromatography columns were purchased from Amersham Pharmacia Biotech, and were run in the FPLC® system purchased from Pharmacia.

Sequence Analysis – Database searching of multiple microbial organisms was performed utilizing the BLAST program at the NCBI website (http://ncbi.nlm.nih.gov/BLAST). Multiple sequence alignments were generated using Clustal W (http://www.ebi.ac.uk/clustalw).

Protein Concentration Assay – Protein concentration was determined using the Bio-Rad Protein Assay Reagent assay. BSA served as a standard for this assay.

One Dimensional Polyacrylamide Gel Electrophoresis – Sodium dodecyl

sulfate polyacrylamide gel electrophoresis (SDS-PAGE), used to confirm the weight and purity of proteins, was performed under reducing conditions on a 12% polyacrlamide gel with the Mini-PROTEAN II electrophoresis unit (Bio-Rad). Protein samples of 5-15 µg were used for analysis on the SDS-PAGE gels. Gels were stained and visualized with a 0.25% Commassie Brilliant Blue R-250 solution.

Construction of Mutant KDOPS plasmids – The mutant KDOPS^{Aa} plasmids were prepared by the QuickChange site-directed mutagenesis kit, which utilizes the methodology described by M.P. Weiner (see Figure 2-7) [7].

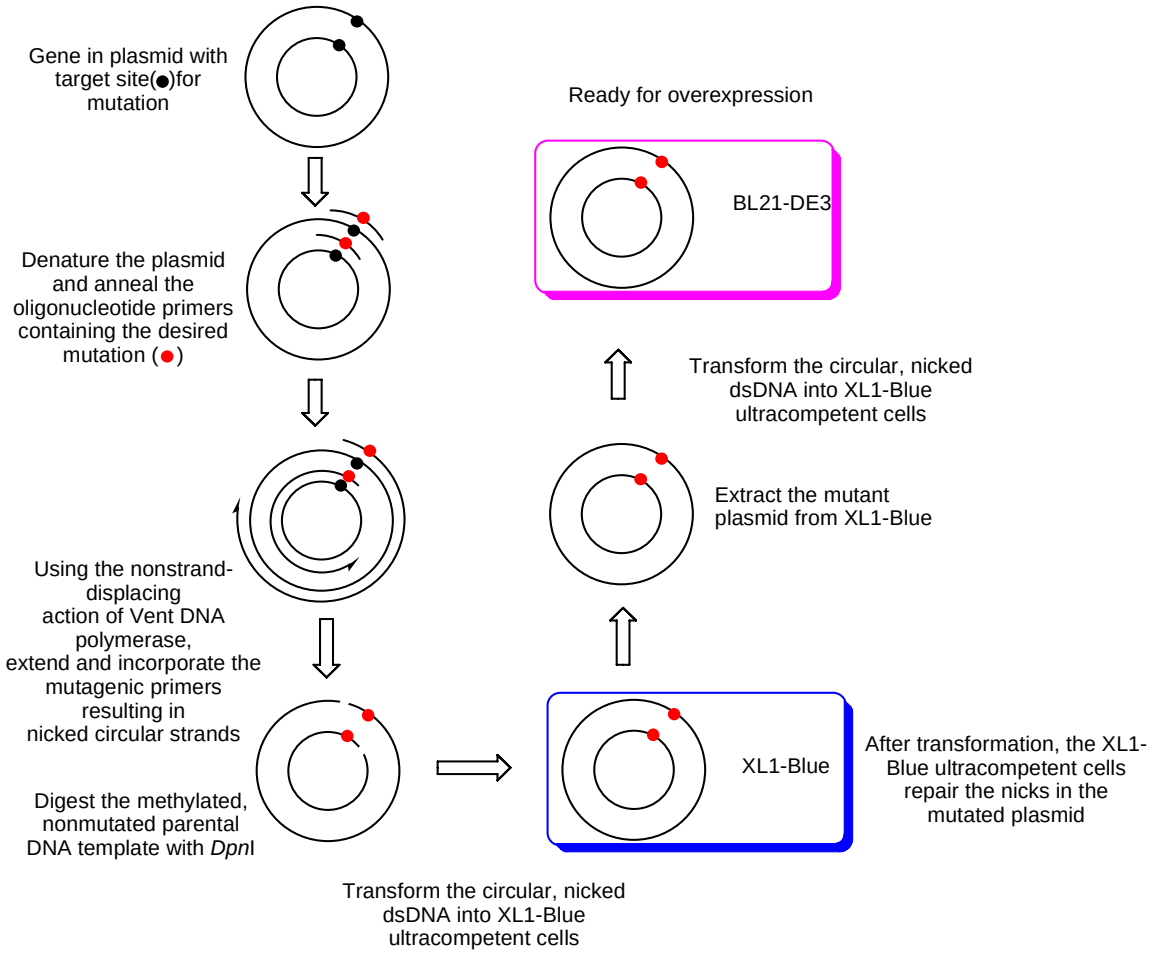

Figure 2-7. Site-directed mutagenesis experiment.

Two oligonucleotide primers (Table 2-1), each containing the desired mutagenic

replacement codon, were designed as forward and reverse primers. PCR was performed in a 50 μL reaction mixture containing 5 μL 10× react ThermolPol buffer, 2 μL 50 mM $MgCl_2$, 1 μL miniprep pT7-7/*kds*A^{Aa} plasmid (wild-type KDOPS^{Aa} expression vector) as a template, 1 μL forward primer, 1 μL reverse primer, 2 μL dNTP mixture, 37 μL H_2O, and 1 μL high-fidelity *Vent* DNA polymerase. Conditions for PCR were as follows: the first step of 3 min at 95°C for one cycle; the second step of 16 cycles of 30 sec at 95°C, 1 min at 55°C, 6.5 min at 72°C; the last step of 5 min at 72°C for one cycle. The PCR product containing the linear mutant plasmid was treated with *Dpn*I to digest the parental methylated pT7-7/*kds*A^{Aa} DNA template. The *Dpn*I digestion reaction mixture, containing the mutagenic DNA, was used to transform supercompetent *E. coli* XL1-Blue cells. Plasmid DNAs were isolated and purified from each of the clones, initially characterized by restriction digestion, and then DNA sequencing (Figure 2-7).

Table 2-1. Oligonucleotides used for the mutagenesis of KDOPS^{Aa}.

Target Amino Acid	Primers 5'→ 3'	Resulting Amino Acid
R49	GATAAAGCGAACGGCTCCTCAATACATTCC GGAATGTATTGAGGAGCCGTTCGCTTTATC	G
A47N48	GTCTTCCTTTGATAAACCGCGCTCCTCAATAC GTATTGAGGAGCGCGGTTTATCAAAGGAAGAC	P
R106	GCCTTTTTATGCGGCCAGACTGAC GTCAGTCTGGCCGCATAAAAAGGC	G
R106	GCCTTTTTATGCCAGCAGACTGAC GTCAGTCTGCTGGCATAAAAAGGC	Q

Construction of truncated KDOPS without L7 – To truncate L7 in KDOPS^{Aa},

a two-step PCR methodology was utilized. The first PCR utilized the 20 base sequence upstream (5') of the *Nde*I site of the pT7-7/*kds*A^{Aa} as a forward primer, a sequence complimentary to the gene fragment encoding for the 5 amino acids before L7 followed by the 5 amino acids after L7 was used as a reverse primer, and pT7-7/*kds*A^{Aa} plasmid as a template. Conditions for PCR were as follows: the first step of 3 min at 95^{o}C for one cycle; the second step of 16 cycles of 30 sec at 95^{o}C, 1 min at 55^{o}C, 6.5 min at 72^{o}C; the last step of 5 min at 72^{o}C for one cycle. The product of the first PCR reaction was applied to a low melting gel, and the desired DNA gene was extracted by QIAquick Gel Extraction kit. The second PCR reaction utilized the purified first PCR product as a forward primer, the reverse cloning primer (containing *BamH*I site) as a reverse primer, and the pT7-7/*kds*A^{Aa} as a template. The purified PCR product was restricted with *Nde*I and *BamH*I. The restricted product was ligated into *Nde*I, *BamH*I and CIAP treated pT7-7 vector, and then transformed into XL1-Blue competent cells. Plasmid DNAs were isolated and purified from each of the clones, and the sequence was verified by DNA sequencing. (All primers used in L7 truncation experiment are shown in Table 2-2)

Table 2-2. Oligonucleotides used for loop7 truncation of KDOPS^{Aa}.

	Primers 5'→ 3'
1st PCR: forward primer	TAATACGACTCACTATAGGG
1st PCR: reverse primer	CTCCCTCATTCCTCCTGAGTGGGTGGCGTCGTATATAAC
2nd PCR: reverse primer	GCATTGGTAACTGTCAGACC

Overexpression and purification of KDOPS – DNA containing the proper mutagenic sequence was used to transform chemically competent *E. coli* BL21 (DE3). The *E. coli* Bl21 (DE3) cells harboring the mutant pT7- 7/*kds*A^{4a} were grown in 2×YT medium (1 L) containing ampicillin (100 μg/mL) at 37^{o}C with orbital shaking (250 RPM). When the culture had reached an absorbance of 1.5 at 600 nm, IPTG was added to a final concentration of 0.4 mM. The culture was grown at 16^{o}C for 16 h, and the cells were collected by centrifugation (18000×g, 20 min, at 4^{o}C) and suspended in buffer A (20 mM Tris-HCl buffer, pH 7.5). The cell suspension was subjected to sonication on ice (4×30 sec, 2 min rests between pulses) and then clarified by centrifugation (18000×g, 40 min, at 4^{o}C) to produce a cell extract. Solid sodium chloride was added to the cell extract to a final concentration of 0.1 M and the solution was heated in a boiling water bath for 2 min and then at 80^{o}C for 10 min with continuous swirling [4]. The suspension was allowed to cool to room temperature and then placed on ice for 15 min. Precipitated protein was removed by centrifugation (18000×g, 20 min, at 4^{o}C). DNase I and RNase A were added to the supernatant, and the mixture was incubated in a 37^{o}C water bath for 30 min. The protein solution was dialyzed against 2 L buffer A overnight. The protein then was applied to a Mono Q (10/10) column previously equilibrated with buffer A. The column was developed at a flow rate of 1 mL/min using a linear gradient from 0 M to 0.3 M potassium chloride in the same buffer (over 60 min). Fractions containing KDOPS, which resolved into a single peak, were pooled and judged by SDS-PAGE (~30 kDa). Solid ammonia sulfate was added to a final concentration of 20% (w/v). The sample was filtered (0.22 μm) and applied to a Phenyl Superose column (10/10) equilibrated with 20% ammonia sulfate in buffer A. The column was developed with a linear

gradient from 20% to 0% (w/v) ammonia sulfate in buffer A (over 120 min). The majority of the protein of interest eluted as a single peak at 0% ammonium sulfate concentration. The purity of the recombinant protein as judged by SDS-PAGE analysis was homogeneous (> 95%). The purified proteins were pooled, dialyzed against 2 L 5 mM Tris-HCl buffer (pH 7.5), and then frozen in dry ice with acetone and stored at -80^{o}C. The total yield of homogenous KDOPS^{Aa} mutant protein was 5-10 mg protein/L of cell culture.

Aminoff colorimetric assay [8] – Enzyme specific activity was measured in a final volume of 50 μL containing PEP (3 mM), A5P or E4P (0.5-10 mM), Tris-acetate buffer (100 mM, pH 7.5) using thin-walled PCR tubes as the reaction vessel. The assay solution was pre-incubated at a desired temperature for 2 min and the reaction was initiated with the addition of enzyme (5 μg) and incubated at the desired temperature. At specified time, the reactions were stopped with the addition of 50 μL 10% ice-cold TCA (to a final concentration of 5%) and then centrifuged to remove precipitated protein. The 100 μL enzymatic reaction mixture was transferred into a 10-mL glass tube and subjected to total oxidation with 0.2 mL 0.025 M $NaIO_4$ in 0.125 M H_2SO_4 at room temperature for 10 min. The excess oxidizing agent was reduced by the addition of 0.4 mL of 2% (w/v) $NaAsO_2$ in 0.5 M HCl. Following the disappearance of the yellow color, 1 mL thiobarbituric acid (0.36% w/v, pH 9.0) was added and the tube was heated at 100^{o}C for 10 min. The amount of KDO8P produced was determined by measuring the absorption at λ = 549 nm ($\varepsilon = 1.03\times10^{5}$ $M^{-1}cm^{-1}$ for the pink chromophore formed between α-formylpyruvate and thiobarbiturate) (Figure 2-8). All assays were performed in triplicate.

Kinetic parameters [9] – A continuous spectrophotometric method for the measurement of the disappearance of the α, β-unsaturated carbonyl absorbance of PEP was used to determine kinetic parameters of KDOPS. The standard assay mixture contained PEP (0.05-1 mM), A5P (0.05-1 mM), 100 mM Tris-acetate buffer (pH 7.5), and 5-15 μg KDOPS in 1 mL. The first three reagents were mixed and pre-heated at 60°C for 2 min. The assay, initiated by the addition of the KDOPS, was monitored for 3 min at λ = 232 nm for a decrease in absorption (ε = 2840 $M^{-1}cm^{-1}$ for the disappeared double bond). K_m and V_{max} values were determined from a nonlinear regression of data pairs (substrate concentration, initial velocity) fit to the Michaelis-Menten equation using KaleidaGraph 3.08d. All assays were performed in triplicate.

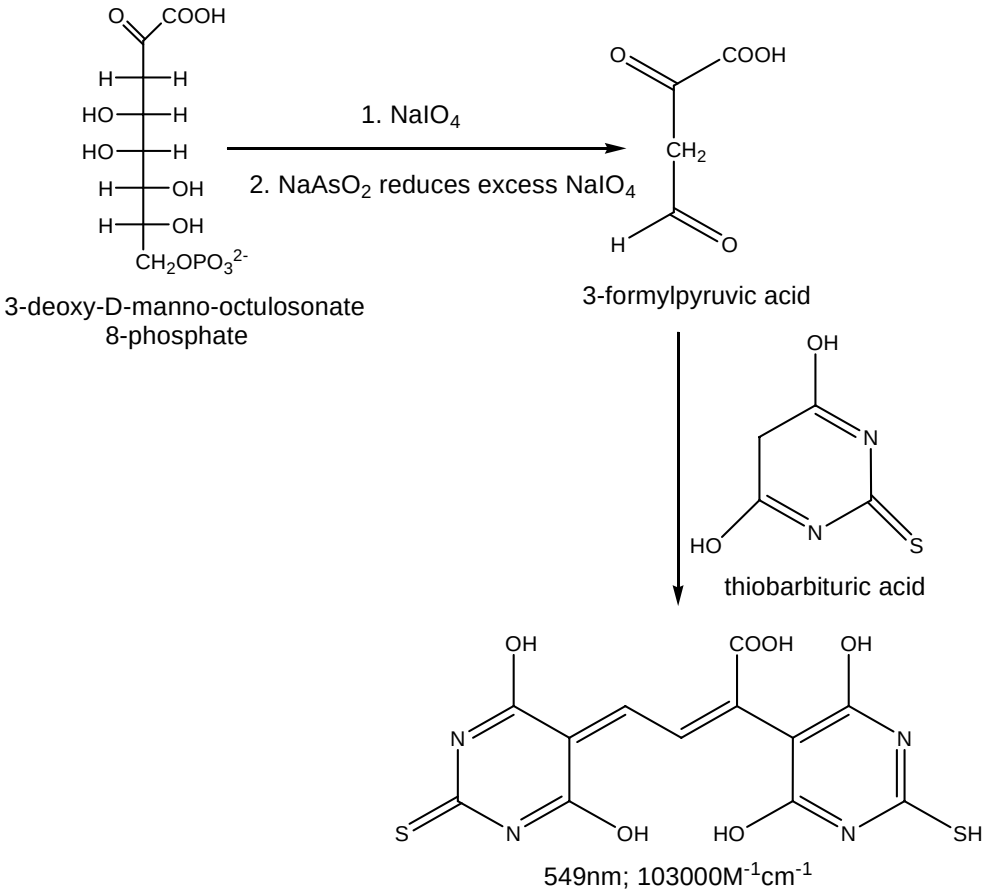

Figure 2-8. Aminoff colorimetric assay.

2.2.3. Results and Discussion

The KDOPS^{Aa} A47N48 to Pro, R49G, R106G, and R106Q mutants were constructed using QuickChange site-directed mutagenesis. The L7 truncated KDOPS^{Aa} was constructed using the two-step PCR methodology described in the experimental procedure section. All mutated and truncated proteins were overexpressed and purified to > 95% homogeneity as demonstrated by SDS-PAGE gel electrophoresis.

Table 2-3. Specific activity of wild-type and modified KDOPS^{Aa}.

KDOPS^{Aa} mutant	Specific activity at 60^{o}C E4P (units/mg)	Specific activity at 60^{o}C A5P (units/mg)
Wild Type KDOPS^{Aa}	0.07	1.88
47AN48 to Pro	0.08	0.64
R49G	0.05	0.32
R106G	0.07	0.36
R106Q	0.09	0.40
L7 truncation	0.06	0.82

All mutant and truncated proteins are still thermal stable similar to the wild-type KDOPS^{Aa}. The activity of each mutant/truncated enzyme was measured at 60^{o}C using the Aminoff colorimetric assay (Table 2-3). First, to determine if the mutation/truncation affect A5P binding, the specific activity of the mutant/truncated KDOPS^{Aa} with A5P and PEP was measured. The results show that compared to the wild-type KDOPS^{Aa}, the activity of all mutant/truncated enzymes is greatly reduced, which indicates that those residues and loop are important in the catalytic mechanism. Furthermore, to determine if the modifications could alter the substrate specificity of

KDOPS^{Aa} to utilize E4P as an alternate substrate, the specific activity of the modified KDOPS^{Aa} with EP4 and PEP was measured. Unfortunately, none of the mutant/truncated enzymes display activity higher than 0.1 units/mg, which is similar to the wild-type KDOPS^{Aa}. None of these mutant/truncated KDOPS^{Aa} can utilize E4P as an alternate substrate.

To further verify that these residues and loop play an important role in A5P binding, the kinetic parameters of the mutant/truncated KDOPS^{Aa} with A5P were measured at 60^{o}C using the continuous assay described in the experimental procedures section (see Table 2-4). There was only a slight increase (within 2 fold) of K_m^{PEP} in the mutant/truncated enzymes compared to the wild-type protein; however, the K_m^{A5P} of the mutant/truncated enzymes was increased dramatically (> 50 fold). These results indicate that these modifications primarily affect the A5P binding.

Table 2-4. Kinetic parameters of wild-type and modified KDOPS^{Aa}.

KDOPS^{Aa} mutant	K_m^{PEP} at 60^{o}C (μM)	K_m^{A5P} at 60^{o}C (μM)	k_{cat} at 60^{o}C (s^{-1})
Wild Type KDOPS^{Aa}	155±8	26±4	0.42±0.06
47AN48 to Pro	210±10	1692±28	0.12±0.02
R49G	180±8	3244±39	0.06±0.01
R106G	202±12	2578±36	0.08±0.01
R106Q	195±9	2327±30	0.09±0.02
L7 truncation	292±14	1168±27	0.17±0.03

The KDOPS^{Aa} A47N48 to Pro, R49G, R106G, R106Q mutants and the truncated L7 KDOPS^{Aa} do not display the desired substrate specificity to utilize E4P as an alternate substrate. These mutant/truncated enzymes still catalyze the condensation of A5P with PEP, however at lower catalytic efficiency. The kinetic parameters prove that these modification sites, selected via structure overlay, are very critical for A5P binding. However, changes to these sites only may not be sufficient to alter the substrate specificity of the enzyme. There might be other trivial changes needed which cannot be found by simply comparing the active site structures. Therefore, a more random experimental approach is demanded in order to potentially alter the substrate specificity of KDOPS.

2.3. DOMAIN SWAPPING

2.3.1. Introduction

Recent analysis of amino acid sequences and X-ray structures suggest that the $(\beta/\alpha)_8$-barrel, which is the most frequently encountered protein fold [10], has potentially evolved by tandem duplication, fusion and mixing of $(\beta/\alpha)_4$-half-barrels [11, 12]. New $(\beta/\alpha)_8$-barrels with novel functions might have evolved by the exchange of $(\beta/\alpha)_4$ half-barrels with distinct functional properties [13, 14]. All structures of KDOPSs and DAHPSs known to date display the $(\beta/\alpha)_8$-barrel topology. If $(\beta/\alpha)_8$-barrels are composed of two independently evolving $(\beta/\alpha)_4$-half-barrels as described above, one could divide any KDOPS or DAHPS into two structural domains, namely the corresponding N- and C-terminal half-barrels. Based on the crystal structures of both KDOPSs and DAHPSs, we found that the phosphorylated monosaccharide binding site is

primarily located at the N-terminal half barrel of the two enzymes; while the PEP binding site is located at the C-terminal half barrel (Figure 2-9) [15]. This suggests that the N-terminal half barrel of KDOPS and DAHPS might be critical for the binding of phosphorylated monosaccharide; while the C-terminal half barrel is responsible for the PEP binding. Since the KDOPS and DAHPS are considered to be evolutionarily related, and these two enzymes mainly differed in utilizing different phosphorylated monosaccharide substrate, we hypothesize that KDOPS may have evolved by some critical changes in the N-terminal half barrel of DAHPS in order to alternate the substrate specificity from E4P to A5P.

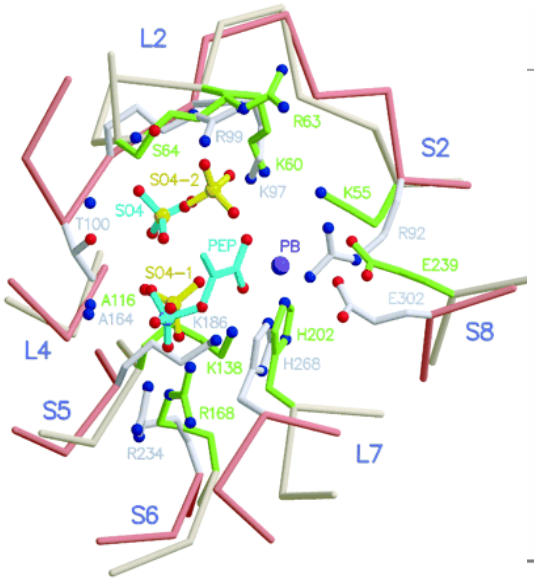

	E.coli DAHP synthase	*E. coli* KDOP synthase
PEP phosphate binding	Ala-164 Lys 186 Arg-234	Ala-116 Lys-138 Arg-168
PEP carboxylate binding	Arg-92 Lys-97 Lys 186	Lys-55 Lys-60 Lys-138
Metal binding	Cys-61 His-268 Glu-302 Asp-326	Asn-26 His-202 Glu-239 Asp-250
E4P/A5P	Arg-99 Thr-100 KP-RT	Arg-63 Ser-64 KANRS

Figure 2-9. Equivalent active site residues in the active sites of KDOPS^{Ec} and DAHPS^{Ec} [15]. The Cα trace and side chains of KDOPS^{Ec} are shown with beige and chartreuse bonds, respectively. The Cα trace and side chains of DAHPS^{Ec} are shown with salmon and gray bonds, respectively.

Based on the half barrel hypothesis, it should be possible to alternate the substrate specificity of KDOPS to E4P by exchanging the N-terminal half barrel between KDOPS and DAHPS. If we keep the C-terminal half barrel, but change the N-terminal

half barrel of KDOPS with the N-terminal half barrel of DAHPS, the resulting KDOPS* might be able to utilize E4P as an alternate substrate.

First, a pair of KDOPS and DAHPS needs to be selected for the half barrel swapping experiments. Since all known DAHPSs are metallo enzymes, the Class II metallo KDOPS should be closer to the DAHPS than the Class I non-metallo KDOPS. There are two reasons for this hypothesis. One is that since we speculate that for KDOPS the loss of metal binding may be the evolutionary driving force, the metallo DAHPS and metallo KDOPS might be more ancient and more closely evolutionary linked to each other than the non-metallo KDOPS. The second reason is that the metallo DAHPS and metallo KDOPS both have metal involved in their catalysis; thus, their catalytic mechanism might be more similar. The *A. aeolicus* KDOPS ($KDOPS^{Aa}$)is a metallo enzyme and was well studied in our laboratory. Thus, $KDOPS^{Aa}$ might be a good candidate for the half barrel swapping experiment. $KDOPS^{Aa}$ is a hyperthermophilic enzyme and displays optimal activity at 95^{o}C. Two hyperthermophilic DAHPSs, *Aeropyrum pernix* DAHPS ($DAHPS^{Ap}$) and *Thermotoga maritima* DAHPS ($DAHPS^{Tm}$), have been studied in our laboratory. $DAHPS^{Tm}$ is feed-back regulated by its downstream products L-phe and L-tyr through a ferredoxin-like (FL) domain appended at the N-terminus. The length of $DAHPS^{Tm}$ is much longer than the unregulated $KDOPS^{Aa}$ due to the extra FL domain. Thus, $DAHPS^{Tm}$ would not be the best choice for the half barrel swapping experiment with $KDOPS^{Aa}$. $DAHPS^{Ap}$ is an unregulated enzyme and has a similar length to the unregulated $KDOPS^{Aa}$. The amino acid sequence alignment shows 22% identity and 37% similarity between the $KDOPS^{Aa}$ and $DAHPS^{Ap}$, which is relatively high among the

pairs of KDOPS and DAHPS we have searched by BLAST. Thus, KDOPS^{Aa} and DAHPS^{Ap} were chosen for the half barrel swapping experiment. Their crystal structures are available in our laboratory, which helped us design the experiments and analyze the results[2, 16]. The protein sequences of KDOPS^{Aa} and DAHPS^{Ap} were compared according to their α-helix (H) and β-strand (S) regions (Figure2-10). The amino acid sequences of these two enzymes aligned very well. The first four $(\beta\alpha)_4$ units and the last four $(\beta\alpha)_4$ units of KDOPS^{Aa} and DAHPS^{Ap} are linked by similar short loops "117TGR119" and "144SGK145", respectively. Thus the N- and C-terminal half barrels of the two enzymes can be defined as KDOPS$^{Aa1\text{-}118}$ and KDOPS$^{Aa119\text{-}267}$, DAHPS$^{Ap1\text{-}145}$ and DAHPS$^{Ap146\text{-}276}$. To exchange half barrels of the two enzymes crosswise, both *in vivo* and *in vitro* experiments were performed.

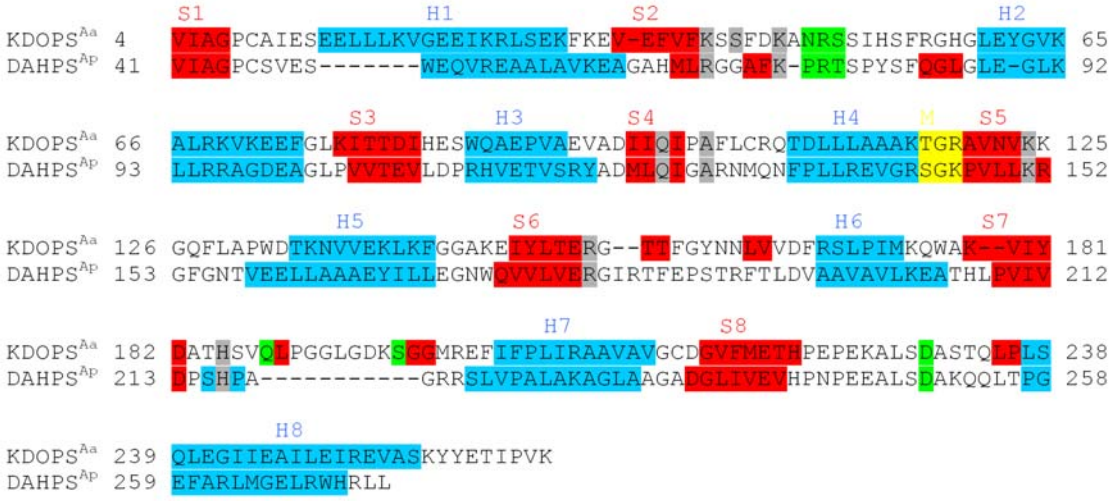

Figure 2-10. Sequence alignment of KDOPS^{Aa} and DAHPS^{Ap}. The α-helix regions are shaded by blue, the β-strand regions are shaded by red. The linkage between the two half barrels are shaded by yellow.

In vitro — The *in vitro* half barrel swapping experiment required the generation of half barrel proteins including the N-terminal half barrel of KDOPS^{Aa} (KDOPS$^{Aa1\text{-}118}$), the C-terminal half barrel of KDOPS^{Aa} (KDOPS$^{Aa119\text{-}267}$), the N-terminal half barrel of

DAHPS^{Ap} (DAHPS$^{Ap1\text{-}145}$), and the C-terminal half barrel of DAHPS^{Ap} (DAHPS$^{Ap146\text{-}276}$). Then, the N-terminal half barrel proteins and the C-terminal half barrel proteins can be mixed together in various combinations. If our hypothesis is true, the results might be as follows:

1) The N-terminal half barrel of KDOPS^{Aa} (KDOPS$^{Aa1\text{-}118}$) + the C-terminal half barrel of KDOPS^{Aa} (KDOPS$^{Aa119\text{-}267}$) would still catalyze the condensation of A5P with PEP to form KDO8P;

2) The N-terminal half barrel of DAHPS^{Ap} (DAHPS$^{Ap1\text{-}145}$) + the C-terminal half barrel of DAHPS^{Ap} (DAHPS$^{Ap146\text{-}276}$) would still catalyze the condensation of E4P with PEP to form DAH7P;

3) The N-terminal half barrel of KDOPS^{Aa} (KDOPS$^{Aa1\text{-}118}$) + the C-terminal half barrel of DAHPS^{Ap} (DAHPS$^{Ap146\text{-}276}$) might be able to catalyze the condensation of A5P with PEP since the N-terminal half barrel of KDOPS^{Aa} normally binds A5P;

4) The N-terminal half barrel of DAHPS^{Ap} (DAHPS$^{Ap1\text{-}145}$) + the C-terminal half barrel of KDOPS^{Aa} (KDOPS$^{Aa119\text{-}267}$) might be able to catalyze the condensation of E4P with PEP since the N-terminal half barrel of DAHPS^{Ap} normally binds E4P.

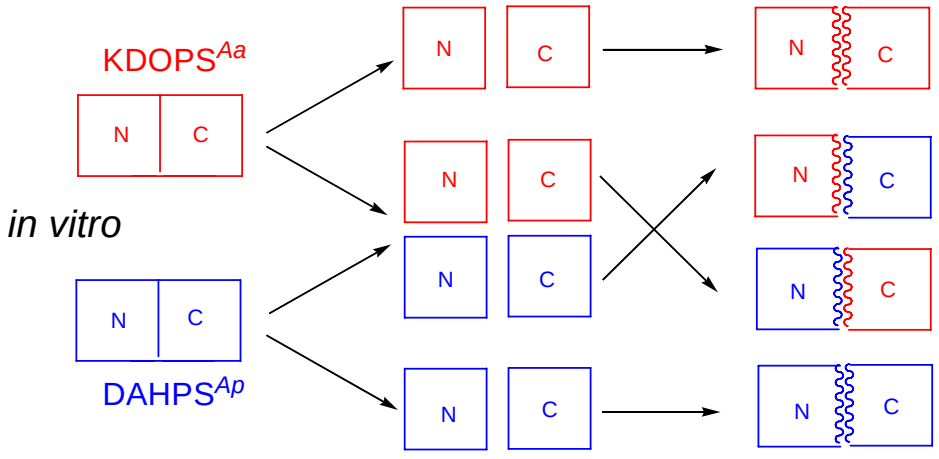

Figure 2-11. Cartoon of *in vitro* half barrel swapping between KDOPS^{Aa} and DAHPS^{Ap}.

In vivo – The *in vivo* half barrel swapping experiment requires two chimeric genes *kds*A$^{Aa1\text{-}118}$*aro*G$^{Ap146\text{-}276}$ and *aro*G$^{Ap1\text{-}145}$*kdsA*$^{Aa119\text{-}267}$, which can be constructed by fusing the genes encoding for the N- and C-terminal half barrels of KDOPS^{Aa} and DAHPS^{Ap} crosswise (*kds*A^{Aa} represents the gene for KDOPS^{Aa}, *aro*G^{Ap} represents the gene for DAHPS^{Ap}). The resulting chimeric protein KDOPS$^{Aa1\text{-}118}$DAHPS$^{Ap146\text{-}276}$, which fuses the N-terminal half barrel of KDOPS^{Aa} to the C-terminal half barrel of DAHPS^{Ap}, may be able to catalyze the condensation of A5P with PEP; while the other chimeric protein DAHPS$^{Ap1\text{-}145}$KDOPS$^{Aa119\text{-}267}$, which fuses the N-terminal half barrel of DAHPS^{Ap} to the C-terminal half barrel of KDOPS^{Aa} may be able to catalyze the condensation of E4P with PEP based on our half barrel hypothesis.

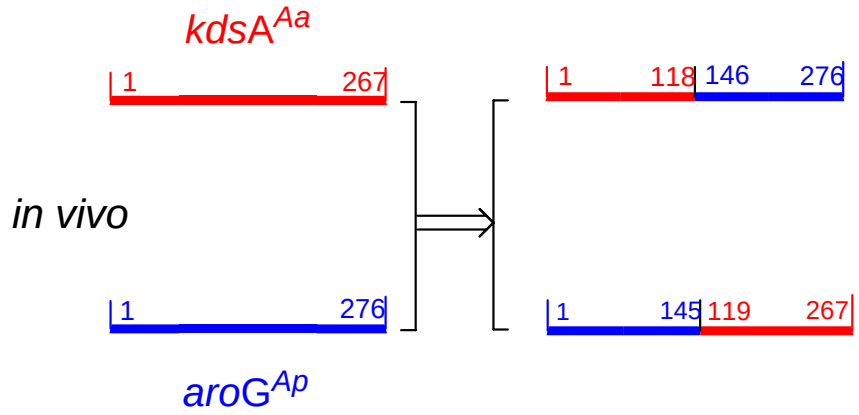

Figure 2-12. Cartoon of *in vivo* half barrel swapping between *kds*A^{Aa} and *aro*G^{Ap}.

Construction of potentially regulated KDOPS – To date, all studies on KDOPSs reported that their enzymatic activity is unregulated by allosteric modifiers, while both unregulated and regulated DAHPSs have been found. Most of the regulated DAHPSs have longer sequences and appear to contain two domains, a catalytic DAHPS domain plus an extra segment with divergent sequences at either the N- or C-terminus responsible for feed-back regulation or allosteric modification [16]. As in the case of

DAHPS^{Tm}, the enzyme is feed-back regulated by L-phe and L-tyr through a ferredoxin-like (FL) domain appended at the N-terminus [17]. Previous experiment to truncate the FL domain from DAHPS^{Tm} resulted in a still active but unregulated DAHPS. This result suggests that the catalytic domain and regulation domain of DAHPS may function independently. Thus, a novel experiment was designed to construct a potentially regulated KDOPS by using the *in vivo* domain swapping methodology. If the FL domain from DAHPS^{Tm} could be fused to the N-terminus of KDOPS^{Aa}, the resulting chimeric KDOPS^{Aa} might also be regulated by L-phe and L-tyr (Figure 2-13).

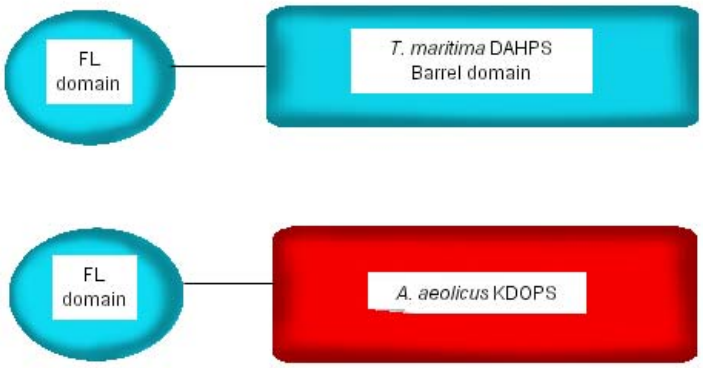

Figure 2-13. Construct a potentially regulated KDOPS by domain swapping.

2.3.2. Experimental Procedures

Construction of half barrel protein plasmids – To construct the plasmids which express either the N- or the C-terminal half barrels of each gene of interest, the following procedure was utilized (Figure 2-14). A pair of complementary primers (shown in Table 2-5) were designed to incorporate a stop codon followed by a *BamH*I restriction site and an *Nde*I restriction site between the codons that were deemed as the end of N-terminal half barrel and the beginning of C-terminal half barrel (inserted sequence: 5' TAAGAATCCCATATG 3'). Standard QuickChange site-directed mutagenesis experiments (described in 2.2.2.) were performed using the primers, with the

pT7-7/gene (wild-type) as the template. The plasmid of the N-terminal half barrel was obtained by self-ligating the *BamH*I digested mutagenesis product. The plasmid of the C-terminal half barrel was obtained by self-ligating the *Nde*I digested mutagenesis product.

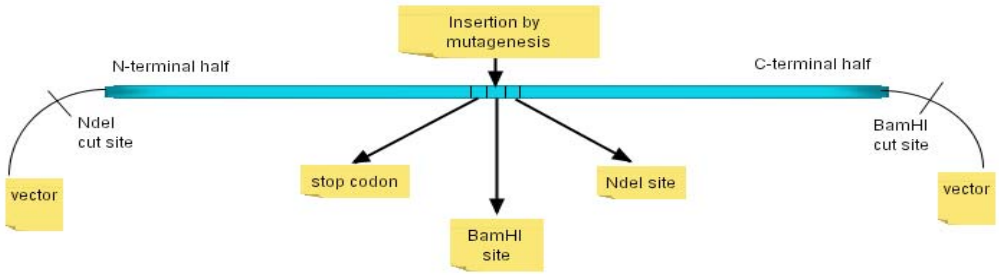

Figure 2-14. Construction of half barrel plasmid.

Table 2-5. Oligonucleotides used for *in vitro* and *in vivo* half barrel swapping.

	Primers 5'→ 3'
In vitro:	
forward	GCTGCAAAAACGGGATAACATATGAGGGCTGTAAACGTG
reverse	CACGTTTACAGCCCTCATATGTTATCCCGTTTTTGCAGC
In vivo:	
kdsA$^{Aa1\text{-}118}$*aroG*$^{Ap146\text{-}276}$	
1st PCR: forward	TAATACGACTCACTATAGGG
1st PCR: reverse	CTTGAGGACAGGCTTTCCCGTTTTTGCAGCCGC
2nd PCR: reverse	GCATTGGTAACTGTCAGACC
In vivo:	
aroG$^{Ap1\text{-}145}$*kdsA*$^{Aa119\text{-}267}$	
1st PCR: forward	TAATACGACTCACTATAGGG
1st PCR: forward	CACGTTTACAGCCCTGCCGGACCTGCCCACCTC
2nd PCR: reverse	GCATTGGTAACTGTCAGACC

Construction of fused half barrel plasmids – To interchange the N- and C-terminal half barrels fragments between KDOPS^{Aa} and DAHPS^{Ap} by *in vivo* expression

of a fused protein, plasmid which fused the N-terminal half barrel of one gene to the C-terminal half barrel of the other gene was constructed using a two-step PCR methodology (Figure 2-15). All PCR primers used in this section are shown in Table 2-5. For example, to fuse the N-terminal half barrel of geneA to the C-terminal half barrel of geneB, the first PCR utilized the 20 base sequence upstream (5') of the *Nde*I site of the geneA as a forward primer, a sequence complimentary to the gene fragment encoding for the last 15 bases of N-terminal half barrel of geneA and the first 15 bases of C-terminal half barrel of geneB as a reverse primer, and the pT7-7/geneA as a template. Conditions for PCR were as follows: the first step of 3 min at 95°C for one cycle; the second step of 36 cycles of 1 min at 95°C, 1 min at 55°C, 1 min at 72°C; the last step of one cycle of 5 min at 72°C. The product of the first PCR reaction was applied to a low melting gel, and the desired DNA was extracted using QIAquick Gel Extraction kit. The second PCR reaction utilized the purified first PCR product as forward primer, the original reverse cloning primer of geneB (containing *BamH*I site) as reverse primer, and the pT7-7/geneB as template. The purified PCR product was restricted with *Nde*I and *BamH*I. The restricted product was ligated into an *Nde*I, *BamH*I and CIAP treated pT7-7 vector. This ligation mixture was transformed into XL1-Blue competent cells. The sequence of the plasmid was verified by DNA sequencing.

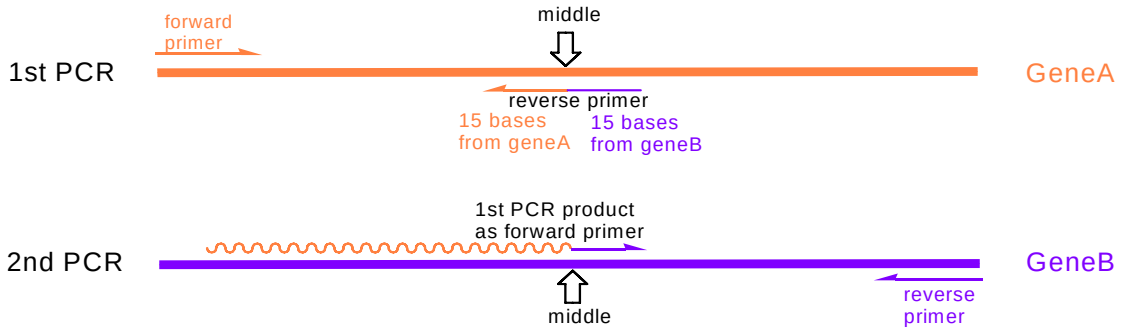

Figure 2-15. Construction of fused half barrel plasmid.

2.3.3. Results and Discussion

***In vitro* half barrel swapping** – The plasmids pT7-7/*kds*A$^{Aa1\text{-}118}$ and pT7-7/*kds*A$^{Aa119\text{-}267}$, which express the N- and C-terminal half barrels of KDOPS^{Aa} respectively, were constructed using the methodology described above. Overexpression of the N-terminal half barrel of KDOPS^{Aa} (KDOPS$^{Aa1\text{-}118}$) and the C-terminal half barrel of KDOPS^{Aa} (KDOPS$^{Aa119\text{-}267}$) were conducted in *E. coli* BL21 (DE3) as described in 2.2.2. Both KDOPS$^{Aa1\text{-}118}$ and KDOPS$^{Aa119\text{-}267}$ were found in the soluble fraction of their respective cell extracts (verified by SDS-PAGE). The two half barrel proteins of KDOPS^{Aa} appeared to retain the wild-type protein thermostability, since they were still soluble after being heated at 100^{o}C for 2 min and 80^{o}C for 10 min as judged by SDS-PAGE. The half barrel proteins were then purified utilizing standard purification procedures by an ion exchange Mono Q column, followed by a hydrophobic interaction Phenyl Superose column.

To determine the ability of the KDOPS^{Aa} half barrel proteins to catalyze the condensation of A5P with PEP, the Aminoff colorimetric assay was used. First, the activity of the two half barrel proteins was measured individually at 37^{o}C and 60^{o}C. The results showed that neither of the half barrel protein individually displayed any catalytic activity at either 37^{o}C or 60^{o}C, which is reasonable since each half barrel can only bind one of the two substrates needed for catalytic reaction. Then, the two half barrel proteins were mixed together and tested for catalytic activity. The half barrel protein mixture still displayed no activity at either 37^{o}C or 60^{o}C.

The reason that the two half barrel KDOPS^{Aa} proteins do not display catalytic activity might be that they could not fold correctly. To probe the folding of the two half

barrel proteins together, several methods were tested. First, the two half barrel proteins were pre-incubated together for 10-30 min at 60^{o}C and then tested by the Aminoff assay. The half barrel proteins might fold together better if a longer pre-incubation period is used. However, no catalytic activity was detected after prolonged incubation. Second, the two crude half barrel proteins were added together during the purification steps, since they may fold together correctly at the initial stage. For example, the cell pellets of the two half barrel proteins were sonicated together, or the two half barrel proteins were heated together during the heat purification step. The co-purified half barrel proteins still displayed no activity. Finally, the two purified half barrel proteins were mixed together for complete unfolding in 8 M urea or 6 M guanidinium chloride, and refolded by removing the chaotropic agent by extensively dialysis against 5 mM of Tris (pH 7.5). This unfold and refold method has been widely used to facilitate correct protein folding [13]. The refolded half barrel proteins were still inactive.

Plasmids encoding the N- and C-terminal half barrels of DAHPS^{Ap} were also constructed by Dr. Mi Zhou in Woodard laboratory using the same methodology. However, no protein overexpression was obtained.

The results above demonstrate that the two half barrels from even the same original full length protein are not able to fold correctly to obtain activity. Even if the half barrel proteins of DAHPS^{Ap} were obtained, the half barrels from KDOPS^{Aa} and DAHPS^{Ap} most likely would not fold together correctly to gain any catalytic activity. If the protein containing half barrel proteins from KDOPS^{Aa} and DAHPS^{Ap} can be expressed from a whole gene, the chimeric protein might be able to fold correctly for catalysis. Thus, the *in vivo* half barrel swapping experiment was performed.

***In vivo* half barrel swapping** – The plasmids pT7-7/*aro*G$^{Ap1\text{-}145}$*kds*A$^{Aa119\text{-}267}$ (fused N-terminal half barrel of DAHPS^{Ap} with C-terminal half barrel of KDOPS^{Aa}), and pT7-7/*kds*A$^{Aa1\text{-}118}$*aro*G$^{Ap146\text{-}276}$ (fused N-terminal half of KDOPS^{Aa} with C-terminal half of DAHPS^{Ap}) were constructed utilizing the 2-step PCR methodology described in the experimental procedures section. The sequences of the two plasmids were verified by DNA sequencing. Neither of the two chimeric proteins could be overexpressed using standard overexpression procedure. Therefore, no further experiments could be performed to determine whether or not the fused half barrel proteins have the desired substrate specificity.

The inability to alter the substrate specificity of KDOPS by half barrel swapping experiments suggests that exchanging the whole half barrel of KDOPS with DAHPS might have changed the protein structure too significantly, so that the resulting chimeric protein could not "digest" those changes correctly by itself to obtain catalytic activity. If only small portion of the enzyme is exchanged, the overall structure of the enzyme would not be disrupted and the modified enzyme may still retain catalytic ability. Thus, experiment was performed to construct a potentially regulated KDOPS by domain swapping.

Construct a potentially regulated KDOPS by domain swapping – Utilizing the *in vivo* domain swapping methodology, the regulation FL domain (residues 1-97) from DAHPS^{Tm} was fused to the N-terminus of KDOPS^{Aa}. The pT7-7/FL$^{Tm1\text{-}97}$*kds*A^{Aa} plasmid was successfully constructed. Only insoluble protein was overexpressed using standard overexpression method, which indicates that the FL+KDOPS^{Aa} might have misfolded. Adding less amount of IPTG (0.05, 0.1, 0.2 or 0.3 mM) did not help overexpress soluble protein. In order to prevent aggregation of the protein, two special

methods were used. One overexpressed the protein in *E. coli* RIL cell instead of the normal *E. coli* BL21-DE3 cell. The *E. coli* RIL cells were used to overexpress proteins that contain R/I/L encoded by rare codons in the first 10 amino acid sequence [18]. The FL+KDOPS^{Aa} protein overexpressed in RIL cell still formed inclusion bodies. Other methods of expressing soluble protein were attempted such as using the Chaperone Plasmid Set purchased from TAKARA for co-expression [19]. The plasmid set consists of five different types of "chaperone team" plasmids which were designed to enable efficient expression of multiple molecular chaperones known to work in cooperation in the folding process. The FL+KDOPS^{Aa} protein was still expressed as an insoluble product.

Neither the *in vitro* nor the *in vivo* half barrel swapping experiments was successful. For the *in vitro* approach, the half barrel proteins were not able to fold correctly. If the two half barrel proteins can be connected by a covalent bond, the resulting linear protein might be able to fold better. For the *in vivo* approach, no fused chimeric proteins were obtained due to either none overexpression or insoluble overexpression. If the protein overexpression problem could be solved, the activity of the chimeric proteins with either A5P or E4P as carbohydrate substrate could be measured by the Aminoff assay.

2.4. DIRECTED EVOLUTION

2.4.1. Introduction

To modify the enzyme substrate specificity, two general routes are normally pursued. One, described in section 2.2., is the structure-based engineering, which relies

on knowledge of an enzyme's three-dimensional structure and an explicit molecular-level understanding of substrate recognition. The other is directed evolution, a process dependent on the availability of a selection process for the desired enhanced or altered enzymatic properties from a created protein library [20]. Utilizing the directed evolution approach, impressive progress has been made in modifying enzyme substrate specificity. For example, the substrate specificity of aspartate aminotransferase was successfully modified by directed molecular evolution using a combination of DNA shuffling and selection in an auxotrophic *E. coli* strain (Yano *et al*.) [21]. A rapid and sensitive selection system is required in directed evolution since the desired activity will be chosen from the enzyme library generated by random mutagenesis containing even > 10^4 mutant enzymes. An ideal selection system must be convenient and reliable, and the sensitivity of the process must be adjustable depending on the progress of the selection steps. Previous reports show that bacterial knockout strain that is deficient in an enzyme with the desired activity is widely used as selection system for directed evolution [21]. Mutant enzymes that can reverse the phenotype of the knockout strain will be selected. The sensitivity of the selection can be adjusted by supplementing the medium with an appropriate amount of the substrate or product.

Since the structure-based engineering approach were not able to alter the substrate specificity of KDOPS as described above, the random methodology, directed evolution, was considered the next experiment to conduct. First, an efficient and reliable selection system was needed.

An auxotrophic *E. coli* CB717 strain that carries knockouts of all three chromosomal DAHPS genes, *aro*F, *aro*G, and *aro*H {C600 Leu Thi Δ (gal-*aro*G-*nad*A) 50,

Δ*aro*H::Kan^{R} Δ*aro*F::Cat^{R} *Tyr*A^{+}/F' *Lac*I^{q}::Tn10 (Tet^{R})} was obtained from Professor Ronald Bauerle at the University of Virginia [22]. For growth on glucose-containing minimal salts medium (M9), the CB717 strain requires supplementation with L-phe, L-tyr, L-trp, L-leu, L-thiamine, nicotinic acid and aromatic vitamins *p*-aminobenzoate (PABA), *p*-hydroxybenzoate (PHBA). Since KDOPS cannot form DAH7P from PEP and E4P, if a mutant of KDOPS can be generated that can use E4P as substrate to form DAH7P, the mutant might also be able to restore aromatic prototrophy of CB717. The auxotrophic *E. coli* CB717 seems to be an effective selection process to monitor the alteration in the substrate specificity of KDOPS to E4P. Recently, *Ran et al*. have used the CB734 strain, a variant of CB717, as a selection tool for modifying the 2-keto-3-deoxy-6-phosphogalactonate aldolase into an aldolase capable of condensing PEP and E4P to form DAH7P [23]. Thus, the methodology should also work for my directed evolution experiment to alter the substrate specificity of KDOPS to E4P.

Alternatively, since DAHPS can catalyze the condensation of A5P with PEP at modest rate, enhancing the ability of DAHPS to utilize A5P as an alternate substrate might be easier and worth trying. An *E. coli* KPM29 (Δ*gut*Q, Δ*kds*D, Δ*kds*A) knockout strain was constructed in our lab by Dr. Timothy Meredith, which knockouts both chromosomal API genes (form A5P) and the KDOPS gene [24]. Growth of the knockout strain is dependent on addition of exogenous A5P. The LPS formation of this *E. coli* knockout strain is dependent on addition of both exogenous A5P and a plasmid containing KDOPS gene. Cells without LPS cannot grow in high concentration bile salts (bio-detergent). This KPM29 strain can grow in high concentration bile salts (> 5000 μg/mL) in the presence of 30 μM A5P, 10 μM G6P (aids in sugar transport), and a

plasmid containing the KDOPS gene. If the KDOPS gene is absent or is replaced by a DAHPS gene, the KPM29 strain can only grow in "extremely" low bile salts concentration (< 200 μg/mL). Thus, this KPM29 strain can be used as the selection system for the directed evolution experiment to enhance the ability of DAHPS to utilize A5P as an alternate substrate. If a mutant of DAHPS can catalyze the condensation of A5P and PEP at a higher rate and have more KDOPS activity, the mutant might be able to grow in higher bile salts concentration.

Logically, the more similar the KDOPS and DAHPS are in amino acid sequence, structure, and mechanism, the easier it should be to alter the substrate specificity of KDOPS to E4P. To select a good pair of KDOPS/DAHPS for the directed evolution experiments, the KDOPS which is the closest to its corresponding DAHPS should be found. Since DAHPSs are all metallo enzymes, the Class II metallo KDOPS should be closer to the DAHPS than the Class I non-metallo KDOPS. There are two reasons for this hypothesis. One is that since we speculate that for KDOPS the loss of metal binding may be the evolutionary driving force, the metallo DAHPS and metallo KDOPS might be more ancient and more closely evolutionary linked to each other than the non-metallo KDOPS. The second reason is that the metallo DAHPS and metallo KDOPS both have metal involved in their catalysis; thus, their catalytic mechanism might be more similar. The *A. aeolicus* KDOPS ($KDOPS^{Aa}$) is a metallo enzyme and its structures with or without substrates have been well studied. Thus, $KDOPS^{Aa}$ seems to be an excellent candidate for the directed evolution experiments. However, *A. aeolicus* is a hyperthermophilic microorganism [4]. Hyperthermophilic enzymes show optimal activity between 60°C and 110°C and typically do not function well below 40°C. Since

the selection systems that will be used are both *E. coli* knockout strains, the directed evolution experiments will be conducted at 37°C. At this temperature, hyperthermophilic KDOPS/DAHPS will not be able to display optimal activity, so a mesophilic pair of enzymes would be a better choice for the substrate alternation experiment utilizing directed evolution. It is also logical to utilize the KDOPS/DAHPS from an organism for which the KDOPS/DAHPS are already available and well studied in our laboratory. Based on the above criteria, the *Porphyromonas gingivalis* KDOPS/DAHPS ($KDOPS^{Pg}$/$DAHPS^{Pg}$) was chosen as templates for the directed evolution experiments. *P. gingivalis* is implicated in periodontal diseases and cardiovascular diseases [16]. An amino acid sequence alignment (Figure 2-16) shows 25% identity and 40% similarity between the $KDOPS^{Pg}$ and $DAHPS^{Pg}$, which is relatively high among the pairs of KDOPS and DAHPS we have searched by BLAST (Figure 2-16).

```
P._gingivalis_KDO8PS     MTNSNSLYERLQTADSFFLMAGPCAIESED------MALRIAERIVEVTS
P._gingivalis_DAH7PS     MKYCDFTPLPLPSEPNTTVIAGPCSAESEEQIMTTARALRDEAGIRIFRA

P._gingivalis_KDO8PS     RLGIPYIFKGSYRKANRSRIDSFTGIGDEKALRILGKVGR----------
P._gingivalis_DAH7PS     GLWKPRTLPGCFEGVGETGLPWLVRVQDELDMLATTEVATREHVEQAMQA


P._gingivalis_KDO8PS     -----EFGVPTVTDIHETHEAA--MAAEYVDVLQIPAFLCRQTDLIVAAA
P._gingivalis_DAH7PS     GIRILWLGARTTSNPFAVQEIADTIGKDESVIVLVKNPISPDLDLWTGAL

P._gingivalis_KDO8PS     YTGRIVNVKKGQFLSGEAMAFVARKCVDSGNSQVILTER-----------
P._gingivalis_DAH7PS     ERLRQSGVRQIGAIHRGFSTYATKTFRNPPHWQIPFDLKRRFPSLTILCD

P._gingivalis_KDO8PS     ----------------GNTFGYTDLVVDYRNIP------AMRSLGFPVV
P._gingivalis_DAH7PS     PSHITGQRDRIESVSQQAMEMNFDGLIIESHCCPDKALSDASQQITPTVL

P._gingivalis_KDO8PS     MDVTHSLQQPNQGSG------------VTGGKPELIETIAKAAIAVGADG
P._gingivalis_DAH7PS     AQILRRLRIPRRQSEKQDEELISWRMQIDQIDESIVELLARRMQVAYEIG

P._gingivalis_KDO8PS     LFIETH------------PDPASAKSDGANMLRLDLLEGLLTKLMRIRAA
P._gingivalis_DAH7PS     LFKKEHNLAVVQNLRYEQLQRNRARTAALLGLDETFISELFSRIHEESVR

P._gingivalis_KDO8PS     IRD-------------
P._gingivalis_DAH7PS     LQTLAPQKPHTDDCIS
```

Figure 2-16. Sequence alignment of $KDOPS^{Pg}$ and $DAHPS^{Pg}$.

If by using directed evolution, any mutant $KDOPS^{Pg}$ plasmids can be selected

that display DAHPS activity or any mutant DAHPS^{Pg} plasmids can be selected to carry enhanced KDOPS activity, the sequences of these mutant plasmids can be compared to the wild-type enzymes in order to identify the primary mutation sites. Important residues that have been mutated can be determined, and these residues might be critical for the substrate specificity. Mutations on these residues only can be constructed to the wild-type enzyme. Further study including *in vitro* characterization, kinetic and crystallography on those mutant enzymes might provide important information on the mechanism of substrate binding.

2.4.2. Experimental Procedures

Materials – Reagents used to make M9 medium including Na_2HPO_4, KH_2PO_4, NaCl, NH_4Cl, $MgSO_4$, $CaCl_2$ and glucose were purchased from Fisher Scientific and Alfa Aesar. Nutrients for the selection plates including L-thiamine, L-leu, nicotinic acid, casein hydrolysate, L-phe, L-tyr, L-trp, PABA, PHBA and bile salts were purchased from Sigma. The pEXP5-CT/TOPO TA Expression kit was purchased from Invitrogen. The gene pulser™ 0.2 cm cuvette and the gene pulser™ II system used for electroporation were purchased from Bio-Rad. XL1-Red competent cells and Mutazyme II® DNA polymerase were purchased from Stratagene.

The general procedure – The procedure used in the directed evolution experiment is shown in Figure 2-17. First, a mutant plasmid library will be generated by random mutagenesis experiments. All the mutant plasmids in the library will then be transformed into the selection/knockout strain using electroporation. If any positive plasmids grow on the selection plates, these plasmids will be purified and used as

templates for the next round of random mutagenesis experiments. Otherwise, if no positive plasmid is selected, the whole mutant plasmid library will be used as template for the next round of random mutagenesis. After several cycles, the mutant plasmids with the highest desired function will be transformed into an overexpression cell line for protein overexpression. The mutant proteins will be characterized *in vitro* and their properties compared to the wild-type enzyme.

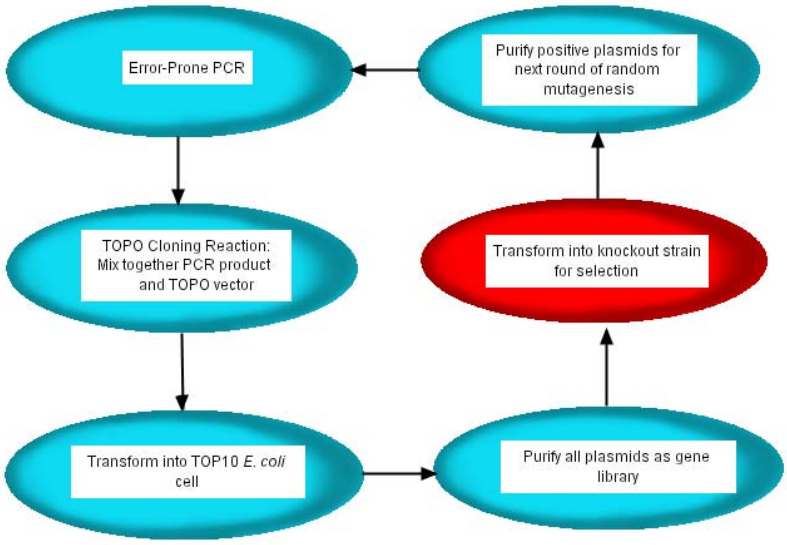

Figure 2-17. General procedure of directed evolution experiment.

Traditional Error-prone PCR – The error-prone PCR methodology described by Cadwell and Joyce produces mutations at a rate of 6.6×10^{-3} per nucleotide [25]. PCR was performed in a 100 µL reaction mixture containing 20 mM Tris-HCl (pH 7.5), 50 mM KCl, 7 mM $MgCl_2$, 0.5 mM $MnCl_2$, 0.2 mM dATP, 0.2 mM dGTP, 1.0 mM dCTP, 1.0 mM dTTP, 5 U *Taq* polymerase, 10 ng gene template (pT7-7/*kds*A^{Pg} or pT7-7/*aro*G^{Pg}) and 50 pmol primers. The primers used for PCR were the original cloning primers (see Table 2-6). Conditions for PCR were as follows: the first step of 3 min at 95°C for one cycle; the second step of 36 cycles of 1 min at 95°C, 1 min at 55°C, 1 min at 72°C; the

last step of one cycle of 5 min at 72°C. The PCR products were digested with *Nde*I and *Bam*HI, and ligated into *Nde*I, *BamH*I and CIAP treated pT7-7 vector. The ligation mixture was transformed into XL1-Blue competent cells. All grown plasmids were extracted and purified to generate the mutant plasmid library.

Table 2-6. Oligonucleotides used for error-prone PCR.

		Primers 5'→ 3'
$KDOPS^{Pg}$	forward	TAATACGACTCACTATAGGG
	reverse	GCATTGGTAACTGTCAGACC
$DAHPS^{Pg}$	forward	TAATACGACTCACTATAGGG
	reverse	GCATTGGTAACTGTCAGACC

XL1-Red competent cell (Stratagene) – A second method for introducing random mutations involves propagating the wild-type $KDOPS^{Pg}$ gene into the XL1-Red *E. coli* mutator strain (Stratagene), which is deficient in three of the primary DNA repair pathways (*mut*S, *mut*D, and *mut*T mutations). The random mutation rate in this triple mutant strain is ~5000 fold higher than that in wild-type *E. coli*. Wild-type $KDOPS^{Pg}$ or $DAHPS^{Pg}$ gene (10-50 ng) was transformed into each 100 μL of XL1-Red competent cells with 1.7 μL of the β-mercaptoethanol added, followed by plating on LB-ampicillin agar plate. The plate was incubated at 37°C for 24-30 h. All the colonies were collected in 5 mL of LB broth with ampicillin and grown overnight at 37°C. For higher mutation rate, the cells were diluted and grown overnight for as many cycles as desired. Plasmids were extracted and purified from 1.5 mL of the overnight culture and transformed into the XL1-Blue competent cells. All grown plasmids were extracted and purified to generate the mutant plasmid library.

Mutazyme II® DNA polymerase – Mutazyme® II DNA polymerase is a novel error-prone PCR enzyme blend, which has been reported to generate 1-16 mutations per kb. PCR was performed in a 50 μL reaction mixture containing 5 μL 10x Mutazyme II® reaction buffer, 1 μL 40 mM dNTP mix (200 μM each final), 0.5 μL primer mix (250 ng/μL of each primer), 1 μL Mutazyme II® DNA polymerase (2.5 U), 1 μL template (100 ng plasmid pT7-7/*kds*A^{Pg} or pt7-7/*aro*G^{Pg}) and 41.5 μL water. The primers used for PCR were the original cloning primers (see Table 2-6). Conditions for PCR were as follows: the first step of 3 min at 95^{o}C for one cycle; the second step of 36 cycles of 1 min at 95^{o}C, 1 min at 55^{o}C, 1 min at 72^{o}C; the last step of one cycle of 5 min at 72^{o}C. The PCR products were digested with *Nde*I and *BamH*I, ligated into an *Nde*I, *BamH*I and CIAP treated pT7-7 vector, and transformed into XL1-Blue competent cells. All grown plasmids were extracted and purified to generate the mutant plasmid library,

Topo vector – To increase the transformation efficiency of the error-prone PCR product, a pEXP5-CT/TOPO® vector (Invitrogen) was used. After the last cycle of the regular PCR program, a 1 h extension step at 72^{o}C was included. After the first 30 min of the cycle, 1 μL *Taq* Polymerase (1 U) was added to the PCR tube in order to add a single deoxyadenosine (A) to the 3' ends of PCR product. The PCR product was purified, 4 μL of which was applied to the TOPO cloning reaction with 1 μL salt solution included in the kit and 1 μL TOPO vector. The linearized TOPO vector has single, overhanging 3' deoxythymidine (T) residues, which allows PCR inserts to ligate efficiently with the vector. The reaction mixture was then transformed into One Shot® TOP10 competent *E. coli* cells. All plasmids grown were extracted and purified to generate the mutant plasmid library.

Electroporation – The mutant plasmid library was transformed into the selection/knockout strain by electroporation. The selection/knockout strains were grown overnight at 37°C in 5 mL LB medium with the proper antibiotics. Part of the overnight culture (~100 μL) was put into another 5 mL fresh LB medium with antibiotics, and was grown at 37°C until the OD_{600} = 0.4~1. The cell was centrifuged at 5000×g for 5 min. The pellet was re-suspended in 1 mL H_2O and centrifuged at 5000×g for 1.5 min. This washing step was repeated for 3 times. After the washed cell pellet was re-suspended using 100-200 μL of H_2O, 5 μL of the plasmid library was added. The cell and plasmid mixture was swirled gently and transferred in to a Bio-Rad gene pulser™ 0.2 cm cuvette on ice. The Bio-Rad gene pulser™ II system was used for electroporation with voltage set at 2.5 V. Immediately after electroporation, 800 μL LB was added to the cuvette. All the solution in the cuvette was then transferred into a 1.5 mL eppendorf tube, shaken for 1 h at 37°C, and plated on the appropriate selection plates.

Selection plates for altering the substrate specificity of KDOPS from A5P to E4P – The plates used to select mutant $KDOPS^{Pg}$ plasmids with DAHPS activity all contained M9-agar with 50 μg/mL Kan, 100 μg/mL Amp, 6 mg/L thiamine, 25 mg/L leu, and 6 mg/L nicotinic acid. Different nutrients were added to the plates to produce a gradient for selection sensitivity as follows: 1) no supplement, 2) 0.2 M IPTG, 3) 0.2 M IPTG + 1 g/L casein hydrolysate, 4) 0.2 M IPTG + 1 g/L casein hydrolysate + 40 mg/L phe, 5) 0.2 M IPTG + 1 g/L casein hydrolysate + 40 mg/L phe +40 mg/L tyr, 6) 0.2 M IPTG + 1 g/L casein hydrolysate + 40 mg/L phe + 40 mg/L tyr + 40 mg/L trp, 7) 0.2 M IPTG + 1 g/L casein hydrolysate + 40 mg/L phe + 40 mg/L tyr + 40 mg/L trp + 40 mg/L PABA + 40 mg/L PHBA.

Selection plates for enhancing the ability of DAHPS to utilize A5P as an alternate substrate – The plates used to select mutant DAHPS^{Pg} plasmids with enhanced KDOPS activity were LB-agar plates with 30 μM A5P, 10 μM G6P, and 100 μg/mL Amp. In addition, bile salts with different concentration were added to the plates which produced a gradient in the selection sensitivity as follows: 1) no bile salts, 2) 100 μg/mL, 3) 250 μg/mL, 4) 500 μg/mL, 5) 1000 μg/mL, 6) 1500 μg/mL, 7) 3000 μg/mL, 8) 4000 μg/mL, and 9) 5000 μg/mL.

2.4.3. Results and Discussion

Random mutagenesis – Three methods were used in the random mutagenesis experiment to generate mutant plasmid library: traditional error-prone PCR, XL1-Red competent cells, and Mutazyme II® DNA polymerase.

Using the XL1-Red competent cells, no mutations were obtained after 7 cycles. The company later reported that the XL1-Red competent cells had mutated back to the parent cell line which could not generate mutations.

When traditional error-prone PCR (which uses Mn^{2+} and low-fidelity *Taq* DNA polymerase to increase the rate of mutation) was tested, over 4 mutations per gene per round were generated. The error generation rate could be adjusted by altering the concentration of Mn^{2+}. However, some of the mutations were conserved in each round of mutagenesis, which restricted the diversity of the mutant plasmid library.

The Mutazyme II® DNA polymerase was able to generate 2-3 mutations per gene in each round. This is a reasonable rate as described by previous directed evolution reports [20]. After each round, over 10 mutant plasmids were purified

individually and DNA sequenced. The results show that there were no conserved mutations generated. Compared to traditional error-prone PCR, Mutazyme II® DNA polymerase turns out to be a better choice for the random mutagenesis experiment. The only problem for using Mutazyme II® DNA polymerase to generate mutant plasmid library was that after the PCR products were digested with *Nde*I and *BamH*I, ligated into similarly digested pT7-7 vector, and transformed into XL1-Blue competent cells, less than 100 colonies grew on the plate after the transformation, probably due to low ligation/transformation efficiency. Therefore, the pEXP5-CT/TOPO® vector was used as described in the experimental procedures section. The PCR products with the additional single deoxyadenosine (A) on the 3' ends were cloned directly into the TOPO vector to generate a large mutant plasmid library. Over 200 mutant plasmids were generated in each round of mutagenesis, and were added to the mutant plasmid library. The updated mutant plasmid library was used as a template for the next round of mutagenesis. After 10 rounds of mutagenesis, an enzyme library containing over 2000 mutant plasmids with an average of 20-28 mutations on each plasmids were obtained.

Alter the substrate specificity of KDOPS from A5P to E4P – The KDOPS^{Pg} gene was used as a starting template to conduct the directed evolution experiments in hopes of generating a mutant KDOPS with DAHPS activity. The mutant KDOPS^{Pg} plasmid library after each round of random mutagenesis was transformed into the CB717 selection/knockout strain and plated on the 7 selection plates containing different supplements. The results are shown in Table 2-7.

A series of control experiments were performed to ensure that the selection system was functional. First, the CB717 selection/knockout strain itself was plated on

the selection plates. Cells only grew on the plate with all nutrients supplied including aromatic amino acids and aromatic vitamins, which is consistent with the selection/knockout strain property. Next, DAHPS genes from different microorganisms (*P. gingivalis*, *E. coli*, *A. pernix*, and *T. maritime*) were transformed into the CB717 strain and individually plated on selection plates. According to our hypothesis, the CB717 selection/knockout strain which contains DAHPS gene can produce aromatic amino acids and aromatic vitamins by itself. The results proved our hypothesis because cells started to grow on plates with only IPTG and casein hydrolysate, and did not need exogenous aromatic amino acids or aromatic vitamins for growth. The last control experiment was to transform the KDOPS^{Pg} and KDOPS^{Ec} genes into the CB717 selection/knockout strain. Since wild-type KDOPS has no DAHPS activity, cells grew only on the plate containing all nutrients supplied similar as the parent CB717 strain. These control experiments verified that the selection system I developed by using CB717 selection/knockout strain is reliable and sensitive, and can be used in the directed evolution experiment to alter the substrate specificity of KDOPS to E4P. If a mutant KDOPS^{Pg} can utilize E4P as an alternate substrate, the mutant should be able to grow without exogenous aromatic amino acids or aromatic vitamins.

Next, the KDOPS^{Pg} mutant plasmid library was screened in the CB717 selection/knockout strain after each round of random mutagenesis. After 10 rounds of mutagenesis, a mutant plasmid library containing > 2000 mutant KDOPS^{Pg} plasmids with an average of 20-28 mutations on each plasmid was obtained. However, all mutant plasmids still only grew on plates supplemented with all nutrients. These results

indicate that no positive mutant KDOPS^{Pg} plasmid with DAHPS activity was generated in the directed evolution.

Table 2-7. Directed evolution of KDOPS^{Pg}. All wild-type and evolved plasmids were transformed into CB717 selection/knockout strain. No growth (-). Growth (+).

	M9	M9+ IPTG	M9+IPTG +Casein Hydrolysate	M9+IPTG +Casein Hydrolysate+ Phe	M9+IPTG +Casein Hydrolysate+ Phe+Tyr	M9+IPTG +Casein Hydrolysate +Phe+Tyr+Trp	M9+IPTG +Casein Hydrolysate +Phe+Tyr+Trp +PABA+PHBA
CB717 ONLY	–	–	–	–	–	–	+
Pg DAHPS WT *Ec* DAHPS WT *Ap* DAHPS WT *Tm* DAHPS WT	–	–	+	+	+	+	+
Pg KDOPS WT *Ec* KDOPS WT	–	–	–	–	–	–	+
1st round RM (2~4 mutations)	–	–	–	–	–	–	+
2nd round RM (5~8 mutations)	–	–	–	–	–	–	+
3rd round RM (6~10 mutations)	–	–	–	–	–	–	+
4th round RM (8~12 mutations)	–	–	–	–	–	–	+
5th round RM (10~15 mutations)	–	–	–	–	–	–	+
6th round RM (12~18 mutations)	–	–	–	–	–	–	+
…….	–	–	–	–	–	–	+
10th round RM (20~28 mutations)	–	–	–	–	–	–	+

Enhance the ability of DAHPS to utilize A5P as an alternate substrate – The DAHPS^{Pg} gene was used as a starting template to conduct the directed evolution experiments in hopes of enhancing the KDOPS activity of DAHPS^{Pg}. The mutant plasmid library after each round of random mutagenesis was transformed into the KPM29

selection/knockout strain and plated on the selection plates which contained different concentration of bile salts. The results are shown in Table 2-8.

A series of control experiments were performed to ensure that the selection system was functional. First, the KPM29 selection/knockout strain itself was plated on the selection plates. Cells only grew on the plate with extremely low bile salts concentration (< 200 μg/mL), which indicates that no LPS was formed in the cell wall. This is consistent with the selection/knockout strain properties, since the KDOPS responsible for the maturation of LPS was absent. Next, the $KDOPS^{Ec}$ and $KDOPS^{Pg}$ were transformed into the KPM29 strain and individually plated on selection plates. According to our hypothesis, the KPM29 selection/knockout strain which contains the KDOPS gene can form LPS; thus, can grow in high concentration of bile salts. The results proved our hypothesis because cells with $KDOPS^{Ec}$ or $KDOPS^{Pg}$ could grow in high concentration bile salts (> 5000 μg/mL). The last control experiment was to transform the $DAHPS^{Ec}$ and $DAHPS^{Pg}$ genes into the KPM29 selection/knockout strain. Since the KDOPS activity of wild-type DAHPS is too weak to form LPS, cells grew only could only grow in low bile salts concentration (< 250 μg/mL). These control experiments verified that the selection system I developed using KPM29 selection/knockout strain is reliable and sensitive, and can be used in the directed evolution experiment to enhance the KDOPS activity in DAHPS. If a mutant $DAHPS^{Pg}$ can catalyze the condensation of A5P and PEP at a higher rate, the mutant might be able to grown in higher bile salts concentration.

The $DAHPS^{Pg}$ mutant plasmid library generated by each round of random mutagenesis was selected in the selection system. After 10 rounds of mutagenesis, a

mutant plasmid library containing > 2000 mutant DAHPS^{Pg} plasmids with an average of 20-28 mutations on each plasmid was obtained. Unfortunately, no mutant DAHPS^{Pg} plasmids could grow in bile salts with concentration at 250 μg/mL or higher. These results indicate that the KDOPS activity of DAHPS^{Pg} was not increased by the mutations generated in the directed evolution.

Table 2-8. Directed evolution of DAHPS^{Pg}. All wild-type and evolved plasmids were transformed into KPM29 selection/knockout strain. No growth (-). Growth (+).

	No Bile salts	100 *u*g/ml Bile Salts	250 *u*g/ml Bile Salts	500 *u*g/ml Bile Salts	1000 *u*g/ml Bile Salts	1500 *u*g/ml Bile Salts	3000 *u*g/ml Bile Salts	4000 *u*g/ml Bile Salts	5000 *u*g/ml Bile Salts
KPM29 ONLY	+	+	–	–	–	–	–	NA	NA
Pg KDOPS WT *Ec* KDOPS WT	+	+	+	+	+	+	+	+	+
Pg DAHPS WT *Ec* DAHPS WT	+	+	–	–	–	–	–	NA	NA
1st round RM (2~4 mutations)	+	+	–	–	–	–	–	NA	NA
2nd round RM (5~8 mutations)	+	+	–	–	–	–	–	NA	NA
3rd round RM (6~10 mutations)	+	+	–	–	–	–	–	NA	NA
4th round RM (8~12 mutations)	+	+	–	–	–	–	–	NA	NA
5th Round RM (10~15 mutations)	+	+	–	–	–	–	–	NA	NA
6th Round RM (12~18 mutations)	+	+	–	–	–	–	–	NA	NA
……	+	+	–	–	–	–	–	NA	NA
10th Round RM (20~28 mutations)	+	+	–	–	–	–	–	NA	NA

Neither of the two directed evolution approaches worked after 10 rounds of experiments. No further rounds were performed since most of the previously reported

success in changing the substrate specificity of enzyme by directed evolution was obtained within 7 rounds of experiments [20]. However, the two selection systems I developed were proved to be reliable and sensitive, and can be used in the future experiments.

2.5. ACKNOWLEDGEMENTS

This research was supported by the National Institute of Health (NIH). I thank Professor Ronald Bauerle at the University of Virginia for generously providing the *E. coli* CB717 knockout strain, Dr. Timothy Meredith for generously providing the *E. coli* KPM29 knockout strain, Dr. Jing Wu for cloning the *P. gingivalis* DAHPS gene, and Dr. Vijayalakshmi Janakiraman for helping study the crystal structures of KDOPS and DAHPS. I would like to also thank members of the Woodard group for their helpful discussions.

2.6. REFERENCES

1. Sheflyan, G.Y., et al., *Enzymatic Synthesis of 3-Deoxy-D-manno-octulosonate 8-Phosphate, 3-Deoxy-D-altro-octulosonate 8-Phosphate, 3,5-Dideoxy-D-gluco(manno)-octulosonate 8-Phosphate by 3-Deoxy-D-arabino-heptulosonate 7-Phosphate Synthase.* J Am Chem Soc, 1998. **120**(43): p. 11027-11032.

2. Duewel, H.S., et al., *Substrate and metal complexes of 3-deoxy-D-manno-octulosonate-8-phosphate synthase from Aquifex aeolicus at 1.9-A resolution. Implications for the condensation mechanism.* The Journal of biological chemistry., 2001. **276(11)**: p. 8393-402.

3. Shumilin, I.A., et al., *Crystal structure of the reaction complex of 3-deoxy-D-arabino-heptulosonate-7-phosphate synthase from Thermotoga maritima refines the catalytic mechanism and indicates a new mechanism of allosteric regulation.* J Mol Biol, 2004. **341**(2): p. 455-66.

4. Duewel, H.S., et al., *Functional and biochemical characterization of a recombinant 3-Deoxy-D-manno-octulosonic acid 8-phosphate synthase from the hyperthermophilic bacterium Aquifex aeolicus.* Biochemical and biophysical research communications., 1999. **263(2)**: p. 346-51.

5. Hedstrom, L. and R. Abeles, *3-Deoxy-D-manno-octulosonate-8-phosphate synthase catalyzes the C-O bond cleavage of phosphoenolpyruvate.* Biochem Biophys Res Commun, 1988. **157**(2): p. 816-20.

6. Xu, X., et al., *The catalytic and conformational cycle of Aquifex aeolicus KDO8P synthase: role of the L7 loop.* Biochemistry, 2005. **44**(37): p. 12434-44.

7. Vandeyar, M.A., et al., *A simple and rapid method for the selection of oligodeoxynucleotide-directed mutants.* Gene, 1988. **65**(1): p. 129-33.

8. Aminoff, D., *Methods for the Quantitative Estimation of N-Acetylneuraminic Acid and their Application to Hydrolysates of Sialomucoids.* Biochem. J., 1961. **81**: p. 384-392.

9. Howe, D.L., et al., *Mechanistic insight into 3-deoxy-D-manno-octulosonate-8-phosphate synthase and 3-deoxy-D-arabino-heptulosonate-7-phosphate synthase utilizing phosphorylated monosaccharide analogues.* Biochemistry., 2003. **42(17)**: p. 4843-54.

10. Pujadas, G. and J. Palau, *Invited Review. TIM barrel fold: structural, functional and evolutionary characteristics in natural and designed molecules.* . Biologia Bratislava, 1999. **54**: p. 231-254.

11. Gerlt, J.A. and F.M. Raushel, *Evolution of function in (beta/alpha)8-barrel*

enzymes. Curr Opin Chem Biol, 2003. **7**(2): p. 252-64.

12. Wise, E.L. and I. Rayment, *Understanding the importance of protein structure to nature's routes for divergent evolution in TIM barrel enzymes.* Acc Chem Res, 2004. **37**(3): p. 149-58.

13. Hocker, B., J. Claren, and R. Sterner, *Mimicking enzyme evolution by generating new (betaalpha)8-barrels from (betaalpha)4-half-barrels.* Proc Natl Acad Sci U S A, 2004. **101**(47): p. 16448-53.

14. Hocker, B., et al., *Dissection of a (betaalpha)8-barrel enzyme into two folded halves.* Nat Struct Biol, 2001. **8**(1): p. 32-6.

15. Radaev, S., et al., *Structure and mechanism of 3-deoxy-D-manno-octulosonate 8-phosphate synthase.* J Biol Chem, 2000. **275**(13): p. 9476-84.

16. Wu, J. and R.W. Woodard, *New Insights into the Evolutionary Links Relating to the 3-Deoxy-D-arabino-heptulosonate 7-Phosphate Synthase Subfamilies.* 2006. **281**(7): p. 4042-4048.

17. Wu, J., et al., *Thermotoga maritima 3-deoxy-D-arabino-heptulosonate 7-phosphate (DAHP) synthase: the ancestral eubacterial DAHP synthase?* The Journal of biological chemistry., 2003. **278(30)**: p. 27525-31.

18. Haddad, et al., *Characterization of Antibody Responses to a Plasmodium falciparum Blood-Stage Antigen Induced by a DNA Prime/Protein Boost Immunization Protocol.* 1999. **49**(5): p. 506-514.

19. Nishihara, K., et al., *Overexpression of trigger factor prevents aggregation of recombinant proteins in Escherichia coli.* Appl Environ Microbiol, 2000. **66**(3): p. 884-9.

20. Tao, H. and V.W. Cornish, *Milestones in directed enzyme evolution.* Curr Opin Chem Biol, 2002. **6**(6): p. 858-64.

21. Yano, T., S. Oue, and H. Kagamiyama, *Directed evolution of an aspartate aminotransferase with new substrate specificities.* Proc Natl Acad Sci U S A, 1998. **95**(10): p. 5511-5.

22. Stephens, C.M. and R. Bauerle, *Essential cysteines in 3-deoxy-D-arabino-heptulosonate-7-phosphate synthase from Escherichia coli. Analysis by chemical modification and site-directed mutagenesis of the phenylalanine-sensitive isozyme.* J Biol Chem, 1992. **267**(9): p. 5762-7.

23. Ran, N., K.M. Draths, and J.W. Frost, *Creation of a shikimate pathway variant.* J Am Chem Soc, 2004. **126**(22): p. 6856-7.

24. Meredith, T.C., et al., *Redefining the requisite lipopolysaccharide structure in Escherichia coli.* ACS Chem Biol, 2006. **1**(1): p. 33-42.

25. Cadwell, R.C. and G.F. Joyce, *Randomization of genes by PCR mutagenesis.* PCR Methods Appl, 1992. **2**(1): p. 28-33.

CHAPTER 3

DETERMINATION OF ALTERNATE CARBOHYDRATE SUBSTRATE FOR KDOPS

3.1. SUMMARY

In this chapter, different A5P analogues were tested as alternate substrates for KDOPS including monosaccharide analogues, phosphorylated monosaccharide analogues, arabinose arsenate ester, arabinose 5-homophosphonate and arabinose 5-difluoromethylenephosphonate. The ability of both *A. aeolicus* KDOPS ($KDOPS^{Aa}$) and *E. coli* KDOPS ($KDOPS^{Ec}$) to utilize these analogues as alternate substrates was measured using the Aminoff colorimetric assay [1]. Only 2-deoxy R5P and arabinose 5-difluoromethylenephosphonate could be utilized as alternate substrates for $KDOPS^{Ec}$. In order to verify that $KDOPS^{Ec}$ can catalyze the condensation of arabinose 5-difluoromethylenephosphonate with PEP to form 3-deoxy-D-*manno*-octulosonate 8-difluoromethylenephosphonate (KDOFP), large amounts of arabinose 5-difluoromethylenephosphonate and PEP were enzymatically reacted with $KDOPS^{Ec}$. The product of this reaction was purified using anion exchange and desalting columns. Both NMR and mass spectrum analysis verify that KDOFP is the product of the reaction, which proves that arabinose 5-difluoromethylenephosphonate is indeed a substrate for KDOPS, but at a much slower rate than the natural substrate A5P.

3.2. INTRODUCTION

KDOPS and DAHPS are two functionally related enzymes. They catalyze similar condensation reactions, have similar tertiary and active site structures, and share similar mechanisms [2, 3]. The carbohydrate substrate of KDOPS, A5P, is one -CHOH- unit longer than E4P, the carbohydrate substrate of DAHPS. DAHPS has been shown to catalyze the condensation of A5P with PEP albeit at modest rate [4], while KDOPS is not able to utilize E4P as an alternate substrate. In chapter 2, different methods were used to alter the substrate specificity of KDOPS from A5P to E4P. However, none of the modified KDOPS can utilize E4P as an alternate substrate. In hopes of gaining more mechanistic information in substrate specificity of KDOPS, finding an alternate substrate for KDOPS from different A5P analogues would be the next reasonable step. Different sets of A5P analogues are listed below.

1) **Monosaccharide analogues** (see Figure 3-1)

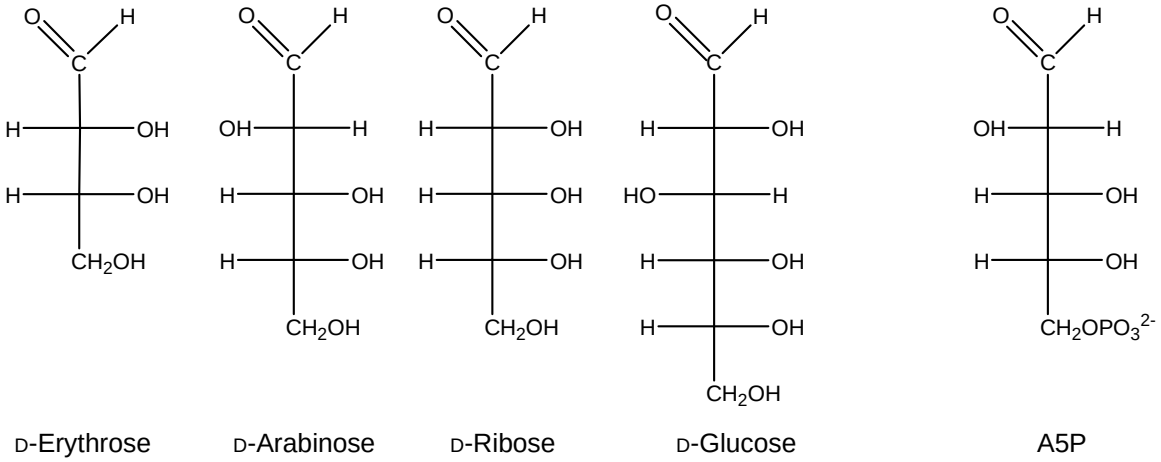

Figure 3-1. Monosaccharide analogues of A5P.

The major differences of these monosaccharide analogues from A5P is the lack of a negatively charged phosphate moiety, which is critical for interacting with the active

site residues of KDOPS to reside A5P. Without the phosphate moiety, the monosaccharide analogues of A5P might not bind the enzyme any longer; thus, they should not be alternate substrates for KDOPS. However, these monosaccharide analogues still contain the aldehyde group, which is also critical for substrate binding. Therefore, these analogues might still bind the enzyme, but less tightly and the chain may be more flexible. The length of these monosaccharide analogues and stereochemistry of C2 may also affect the analogues ability to be utilized as alternate substrates for KDOPS.

2) Phosphorylated Monosaccharide Analogues (see Figure 3-2)

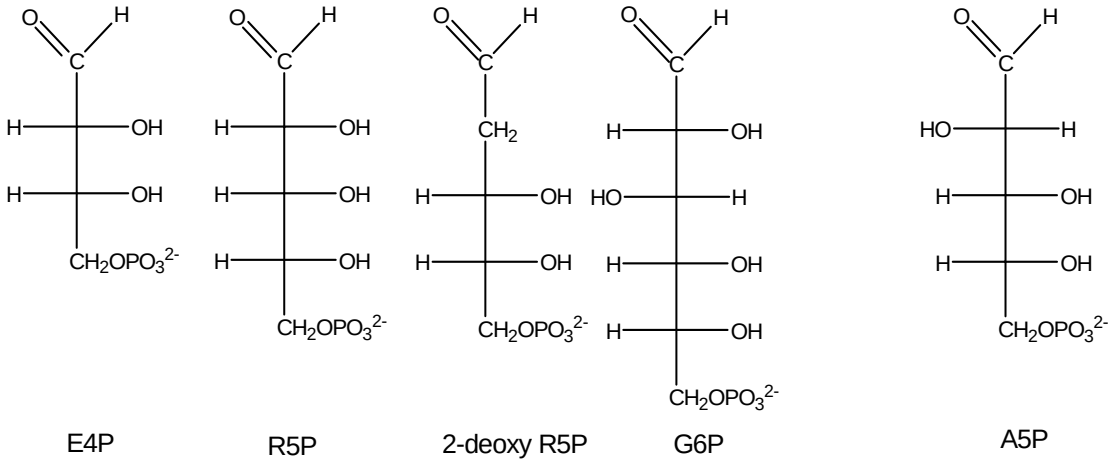

Figure 3-2. Phosphorylated monosaccharide analogues of A5P.

The phosphorylated monosaccharide analogues all contain the phosphate moiety similar to the natural substrate A5P. They are different from A5P in length and in the stereochemistry of C2. The 2-deoxy R5P has the same length as A5P but lacks the C2-OH group. Due to the presence of both aldehyde group and phosphate moiety, these phosphorylated analogues should still be able to bind the enzyme. The difference in length and stereochemistry of C2 however, might prevent these analogues from binding

with the correct orientation, thus affecting their ability to be alternate substrates for KDOPS. Previous studies have shown that DAHPS can utilize R5P and 2-deoxy R5P as alternate substrates [4].

3) Arabinose + Inorganic Arsenate (see Figure 3-3)

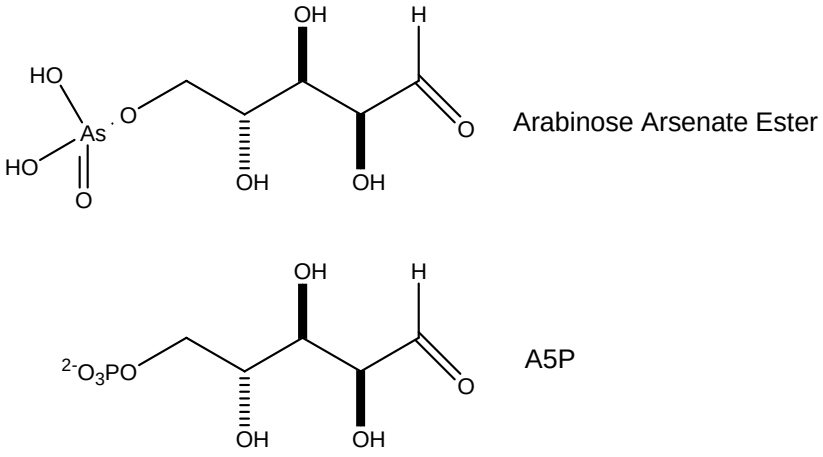

Figure 3-3. Arabinose arsenate ester as A5P analogue.

Sugar and inorganic arsenate are accepted by a wide variety of sugar phosphate utilizing enzymes as alternate substrate and have recently been used in large scale enzymatic synthesis of unphosphorylated carbohydrates [5, 6]. In this process, sugar and inorganic arsenate react reversibly and nonenzymatically *in situ* to form a sugar arsenate ester, which is recognized as an analogue of the phosphorylated sugar. The sugar arsenate ester then serves as a substrate for enzyme. After the enzymatic reaction, the product "ester" can spontaneously hydrolyze to release free sugar product and inorganic arsenate [7]. KDOPS is also a sugar phosphate utilizing enzyme. Based on the mechanism described above, the arabinose arsenate ester might be used to mimic the A5P as an alternate substrate.

The enzyme A5P isomerase (API) is also under investigation in our laboratory. This enzyme forms A5P from ribulose 5-phosphate (Ru5P), which is the first committed step in the KDO biosynthetic pathway. This enzyme is also a sugar phosphate utilizing enzyme. Studies on API show that the ribulose arsenate ester can be utilized as an alternate substrate for this enzyme to form the unphosphorylated arabinose. Thus, the arabinose ester might be able to serve as an alternate substrate for KDOPS to produce the unphosphorylated KDO.

4) Arabinose 5-homophosphonate and Arabinose 5-difluoromethylenephosphonate

(see Figure 3-4)

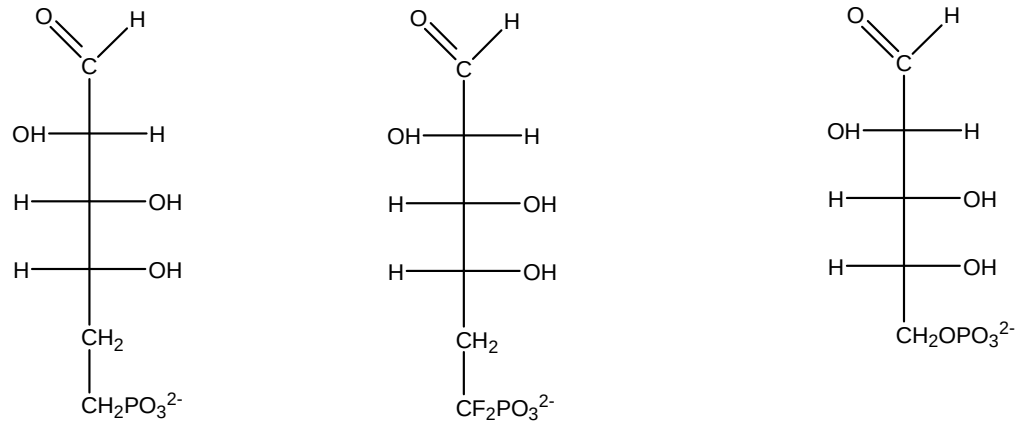

Arabinose 5-homophosphonate

Arabinose 5-difluoromethelynephosphonate

A5P

Figure 3-4. Chemically synthesized A5P analogues.

Arabinose 5-homophosphonate and arabinose 5-difluoromethylenephosphonate were chemically synthesized by our collaborator at Peking University. The phosphate group of A5P in these two analogues was replaced by a homophosphonate and a difluoromethylenephosphonate, respectively. Results from previous studies show that

DAHPS can utilize erythrose 4-phosphonate and erythrose 4-homophosphonate as alternate substrates [8]. Based on the results, we hypothesize that KDOPS might also be able to utilize arabinose 5-homophosphonate as an alternate substrate. Furthermore, fluorine is more electronegative than carbon; thus, arabinose 5-difluoromethylenephosphonate should have a lower pKa than arabinose 5-homophosphonate. The pKa of arabinose 5-difluoromethylenephosphonate should be closer to the natural substrate A5P than that of the 5-homophophonate. If arabinose 5-homophosphonate can be an alternate substrate for KDOPS, arabinose 5-difluoromethylenephosphonate should be an even better substrate.

3.3. EXPERIMENTAL PROCEDURES

Materials – Tris(hydroxymethyl)aminomethane was purchased from Research Organics. Phospho*enol*pyruvate mono(cyclohexylammonium) salt, thiobarbituric acid, D-erythrose, D-arabinose, D-ribose, D-glucose, R5P disodium salt, E4P disodium salt, 2-deoxy R5P disodium salt, G6P disodium salt, sodium arsenate and ferric chloride were obtained from Sigma. Arabinose 5-phosphate was prepared in our laboratory by Dr. Junhua Yan. Acetic acid was purchased from Fisher Scientific. Arabinose 5-homophosphonate (containing 40% sodium acetate and only 55%~60% pure) and arabinose 5-difluoromethylenephosphonate (~70% pure) were chemically synthesized by our collaborator at Peking University. Sodium thiophosphate was purchased from Alfa Aesar. Malachite green carbinol hydrochloride, deuterium oxide (99.99% atom D; D_2O) and orcinol were purchased from Aldrich. The AG-MPI resin was purchased from Bio-Rad. The Sephadex® G10 resin was purchased from Pharmacia Fine Chemicals.

Aminoff colorimetric assay [1] – Enzyme specific activity was measured in a final volume of 50 μL containing PEP (3 mM), A5P or its analogues (0.5-10 mM), Tris-acetate buffer (100 mM, pH 7.5) using thin-walled PCR tubes as the reaction vessel. The assay solution was pre-incubated at a desired temperature for 2 min and the reaction was initiated with the addition of enzyme (5 μg) and incubated at the desired temperature. At specified time, the reactions were stopped with the addition of 50 μL 10% ice-cold TCA (to a final concentration of 5%) and centrifuged to remove precipitated protein. The 100 μL enzymatic reaction mixture was transferred into a 10-mL glass tube and subjected to total oxidation with 0.2 mL 0.025 M $NaIO_4$ in 0.125 M H_2SO_4 at room temperature for 10 min. The excess oxidizing agent was reduced by the addition of 0.4 mL of 2% (w/v) $NaAsO_2$ in 0.5 M HCl. Following the disappearance of the yellow color, 1 mL thiobarbituric acid (0.36% w/v, pH 9.0) was added and the tube was heated at 100^{o}C for 10 min. The amount of KDO8P produced was determined by measuring the absorption at λ = 549 nm ($\varepsilon = 1.03\times10^5$ $M^{-1}cm^{-1}$ for the pink chromophore formed between α-formylpyruvate and thiobarbiturate). All assays were performed in triplicate.

Kinetic parameters [9] **–** A continuous spectrophotometric method for the measurement of the disappearance of the α, β-unsaturated carbonyl absorbance of PEP was used to determine kinetic parameters of KDOPS. The standard assay mixture contained PEP (0.05-1 mM), A5P (0.05-1 mM), 100 mM Tris-acetate buffer (pH 7.5), and 5-15 μg KDOPS in 1 mL. The first three reagents were mixed and pre-heated at desired temperature for 2 min. The assay, initiated by the addition of the KDOPS, was monitored for 3 min at λ = 232 nm for a decrease in absorption (ε = 2840 $M^{-1}cm^{-1}$ for the disappeared double bond). The K_m and V_{max} values were determined from a nonlinear

regression of data pairs (substrate concentration, initial velocity) fit to the Michaelis-Menten equation using KaleidaGraph 3.08d. All assays were performed in triplicate.

Malachite Green Assay [10] – The presence of inorganic phosphate was detected utilizing a malachite green assay. The molybdate/malachite green reagent was prepared by mixing the MG (0.045% malachite green hydrochloride) and AM (4.2% ammonium molybdate in 4 N HCl) solutions at a 3:1 ratio. To 100 μL of the sample, 800 μL of the ammonium molybdate/malachite green colorimetric reagent was added. The solution was mixed and incubated at room temperature for 1 min. The green color development was quenched by the addition of 100 μL of a 34% (w/v) sodium citrate solution. The amount of inorganic phosphate was determined by measuring the absorbance at $\lambda = 660$ nm ($\varepsilon = 20{,}206$ M-1 cm-1), utilizing KH_2PO4 as a standard.

Bial's Test [11] – To detect the presence of D-arabinose 5-difluoromethylenephosphonate, the Bial's test was utilized. To prepare Bial's reagent, 0.3 g orcinol and 0.05 g ferric chloride were dissolved in 100 mL of 12 M HCl. The reagent was stored at 4°C in a brown bottle to protect it from light. During the test, 0.05-0.2 mL sample was added to 1 mL Bial's reagent, and heated in 100°C for 2-5 min. Green color indicates the presence of pentose of hexose, while yellow color indicates the presence of disaccharides.

Enzymatic Synthesis of KDOPF – The 3-deoxy-D-*manno*-octulosonate 8-difluoromethylenephosphonate (KDOFP) was enzymatically synthesized from D-arabinose 5-difluoromethylenephosphonate and PEP in the presence of $KDOPS^{Ec}$. The reaction mixture contained 36 mg of D-arabinose 5-difluoromethylenephosphonate,

21 mg PEP, 500 μg KDOPS^{Ec}, and 2 mL buffer (200 mM BTP, pH 7.5) was incubated at 37^{o}C. Progression of the reaction was monitored by ^{31}P NMR. After every 24 h, another 1.0 mg of KDOPS^{Ec} and 1.0 mg of PEP were added to the reaction mixture. The reaction was quenched after 96 h with 10% trichloroacetic acid to a final concentration of 5%. The final product mixture was lyophilized and reconstituted in 4 mL H_2O. The product was purified on an AG-MP1 anion exchange column utilizing a LiCl gradient (0-400 mM, 500 mL). The fractions positive for the Aminoff assay (indicating the presence of a 3-deoxy monosaccharide), negative for the malachite green assay (indicating the absence of inorganic phosphate), and negative for the Bial's test (indicating the absence of D-arabinose 5-difluoromethylenephosphonate) were pooled and lyophilized. The lyophilized sample was dissolved in 1 mL H_2O and loaded onto a G10 column. The desired product was eluted with water, the Aminoff positive and $AgNO_3$ negative (indicating the absence of salt) fractions were pooled and lyophilized. The lyophilized sample was dissolved in water and frozen at -80^{o}C.

^{31}P NMR and ^{13}F NMR analysis of KDOPF – The purified KDOPF, verified via the Aminoff assay, was further verified via ^{31}P NMR and ^{13}F NMR analysis. NMR tubes consisted of 1 mg KDOPF dissolved in 90% H_2O and 10% D_2O in a total volume of 500 μL. Sample was analyzed via ^{31}P NMR or ^{13}F NMR using a Bruker Advance DRX-300 instrument with the WALTZ16 proton decoupling. A 10 sec delay was used during the acquisition to ensure complete relaxation of the phosphorus nucleus, allowing for direct integration of the peaks. Each spectrum contained 128 scans. As control experiments, inorganic phosphate, PEP and arabinose 5-difluoromethylenephosphonate were analyzed by ^{31}P NMR or ^{13}F NMR.

ESI- mass spectrum analysis of KDOPF – The KDOPF was further analyzed by mass spectroscopy. The molecular weight was determined by electrospray with negative ion detection (ESI-) mass spectrum in the Department of Chemistry using Micromass LCT.

3.4. RESULTS AND DISCUSSION

3.4.1. Monosaccharide Analogues

The specific activities of KDOPS^{Aa} to utilize the monosaccharide analogues of A5P as alternate substrates were measured at 60^{o}C using the Aminoff assay. Similarly, using the Aminoff assay, the specific activities of KDOPS^{Ec} with the monosaccharide analogues of A5P were measured at 37^{o}C. The results are shown in Table 3-1.

Table 3-1. Specific activities of KDOPS with monosaccharide analogues of A5P.

Monosaccharide	Specific Activity at 60^{o}C KDOPS^{Aa} (units/mg)	Specific Activity at 37^{o}C KDOPS^{Ec} (units/mg)
A5P	1.88	12.72
D-Erythrose	0.06	0.08
D-Arabinose	0.05	0.04
D-Ribose	0.03	0.05
D-Glucose	~0	~0

The specific activities of both KDOPS^{Aa} and KDOPS^{Ec} with the monosaccharide analogues of A5P and PEP are all < 0.1 units/mg. These results

indicate that none of the monosaccharide analogues of A5P tested is an alternate substrate for KDOPS.

These monosaccharide analogues differ from A5P mainly in the loss of phosphate moiety. The active site structure of KDOPS^{Aa} with A5P, PEP and metal shows that A5P is mainly stabilized by a network of hydrogen bonds and salt bridges between its phosphate and aldehyde moieties and several active site residues (Figure 3-5) [12]. The phosphate moiety of A5P interacts with R49, S50, R106 and S197. These interactions are considered critical for the A5P binding in KDOPS. Therefore, the reason that these monosaccharide analogues cannot be utilized as alternate substrates for KDOPS may be the lack of phosphate moiety. In this case, the monosaccharide analogues may not be able to bind KDOPS in the active site; or, they can still bind but are not correctly positioned and oriented due to the loss of important interactions between the phosphate moiety and active site residues.

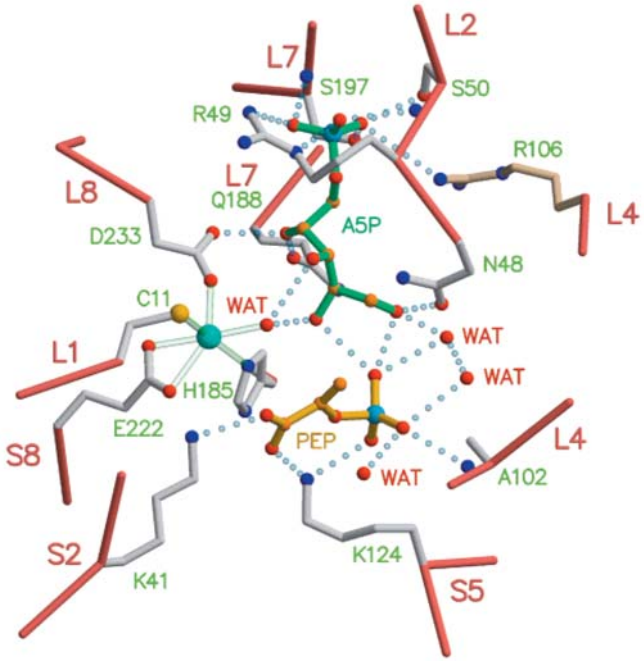

Figure 3-5. Crystal structure of KDOPS^{Aa} active site with PEP, A5P and metal bound [12].

3.4.2. Phosphorylated Monosaccharide Analogues

The specific activities of both KDOPS^{Aa} and KDOPS^{Ec} to utilize phosphorylated monosaccharide analogues of A5P as alternate substrates measured by the Aminoff assay are shown in Table 3-2.

The specific activities of both KDOPS^{Aa} and KDOPS^{Ec} with these phosphorylated monosaccharides and PEP, determined by measuring the absorption at λ = 549 nm in the Aminoff assay, are all < 0.1 units/mg. These results suggest that none of the phosphorylated monosaccharide analogues of A5P is an alternate substrate for KDOPS.

Table 3-2. Specific activities of KDOPS with phosphorylated monosaccharide analogues of A5P.

Phosphorylated Monosaccharide	Specific Activity at 60°C KDOPS^{Aa} (units/mg)	Specific Activity at 37°C KDOPS^{Ec} (units/mg)
A5P	1.88	12.72
E4P	0.07	0.06
R5P	0.03	0.05
2-deoxy R5P*	0.03	0.04
G6P	~0	~0

All the analogues tested herein contain both the phosphate moiety and the aldehyde group, which are considered critical in A5P binding. Thus, they should still bind in the active site of KDOPS by interactions between their phosphate/aldehyde groups and important active site residues. These phosphorylated monosaccharide

analogues differ from A5P mainly in the chain length and stereochemistry of C2. We hypothesize that these differences may prevent the analogues from properly being positioned to accept the nucleophilic attack of C3 of PEP.

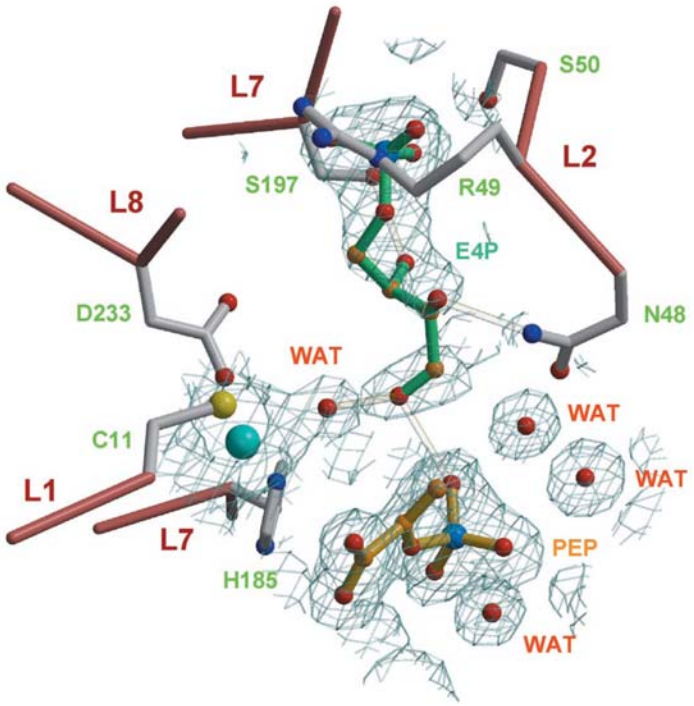

Figure 3-6. Crystal structure of KDOPS^{Aa} active site with PEP, E4P and metal bound [12].

In the active site structure of KDOPS^{Aa} with A5P and PEP, the C2-OH of A5P was hydrogen bonded to a water molecule located at the *si* side of PEP, this interaction might help correctly align the aldehyde group of A5P for the nucleophilic attack by C3 of PEP (Figure 3-5). The crystal structure of KDOPS^{Aa} with PEP and E4P was also solved by our collaborator Dr. Domenico Gatti at Wayne State University (Figure 3-6) [12]. This structure shows that E4P can still bind in the active site of KDOPS^{Aa} with its phosphate and aldehyde groups interacting with active site residues, which is consistent with our hypothesis. Compared to the structure of KDOPS^{Aa} with PEP and A5P, E4P binds in the active site of KDOPS^{Aa} with a different orientation from A5P primarily due

to its different stereochemistry on C2-OH. The C2-OH of E4P does not form hydrogen bond with the active site water molecule, but interacts with N48. Due to this interaction, the aldehyde group of E4P is differently positioned from that of A5P. The different orientation as well as the shorter length of E4P makes the aldehyde group of E4P too far away from the C3 of PEP for the neucleophilic attack. Thus E4P cannot be utilized as an alternate substrate for KDOPS.

The 2-deoxy R5P behaves differently from the other phosphorylated monosaccharide analogues. For 2-deoxy R5P, the Aminoff assay solution does not show absorption at λ = 549 nm (the pink chromophore formed between α-formylpyruvate and thiobarbiturate), however there was a high absorption at λ = 530 nm. The solution displays an orange color instead of the pink color in normal Aminoff assay solution. These phenomena on 2-deoxy R5P suggest that there might be a reaction undergone between 2-deoxy R5P and PEP with the presence of KDOPS, which gives the orange color and the absorption at λ = 530 nm. Thus, a continuous assay which measures the disappearance of the α, β-unsaturated carbonyl absorbance of PEP was used to determine if there is turnover between 2-deoxy R5P and PEP catalyzed by KDOPS^{Ec}. Based on the observation of the loss of absorbance at 232 nm, there appears to be reaction between 2-deoxy R5P and PEP in the presence of KDOPS^{Ec}. The kinetic parameters of the reaction were determined ($K_m^{2d\ R5P}$ = 50 μM, k_{cat} = 0.12 s^{-1}, by David L. Howe in Woodard laboratory) [9]. The K_m for 2-deoxy R5P is approximately 1.5 times greater than the *Km* for A5P (K_m^{A5P} = 30 μM), the k_{cat} for 2-deoxy R5P is about 55 times lower than the k_{cat} of A5P (k_{cat} = 6.8 s^{-1}) [13]. These results indicate that 2-deoxy R5P is an alternate substrate for KDOPS. The product of the condensation reaction between

2-deoxy R5P and PEP catalyzed by KDOPS should be 3,4-dideoxy-D-manno-octulosonate 8-phosphate (see Figure 3-7) instead of KDO8P, which might be the reason for the presence of the unusual absorbance at λ = 530 nm (orange color).

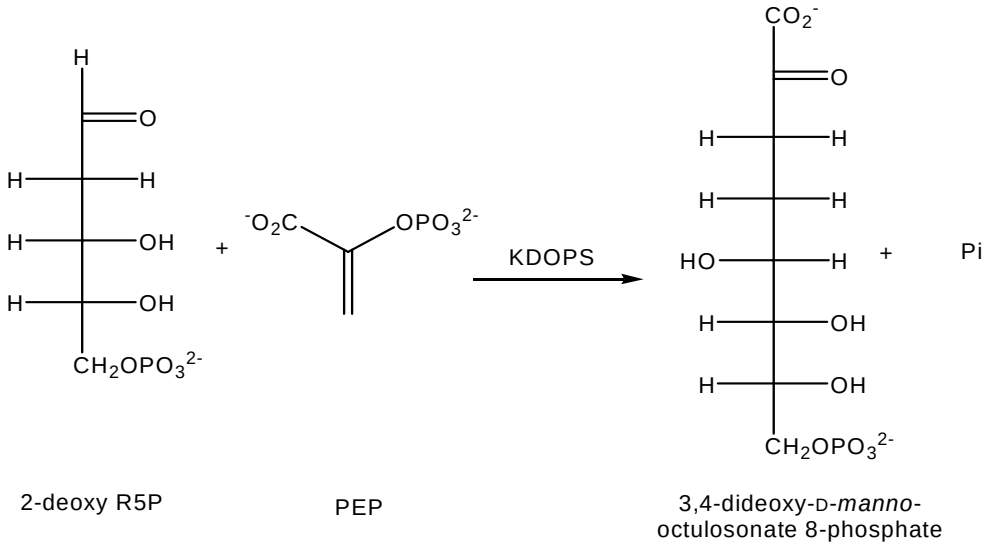

Figure 3-7. Proposed condensation reaction of 2-deoxy R5P and PEP catalyzed by KDOPS.

Both R5P and 2-deoxy R5P have the same length as A5P, the only difference between them is that 2-deoxy R5P does not have a hydroxyl group on C2. The reason that 2-deoxy R5P is an alternate substrate for KDOPS but not R5P might be that the stereochemistry of C2 hydroxyl group in R5P is different from that in A5P. As seen in the structure of KDOPS[Aa] with PEP and E4P (Figure 3-6), the aldehyde group is not correctly oriented due to the different stereochemistry on C2 of E4P from that of A5P. The stereochemistry on C2 of R5P is the same as E4P. Thus, R5P may also not be able to bind with correct orientation for catalysis. In 2-deoxy R5P, the interaction between the C2-OH and the enzyme active site is lost, while interactions between the phosphate/aldehyde group and the enzyme are still present. The 2-deoxy R5P analogue

still binds at the active site with more flexibility and thus undergoes condensation with PEP.

3.4.3. Arabinose + Inorganic Arsenate

To test if an arabinose arsenate ester can serve as an alternate substrate for KDOPS, PEP, arabinose and 120 mM sodium arsenate buffer (pH 7.6) were pre-incubated before the KDOPS was added to initiate the reaction. Specific activities measured by the Aminoff assay are shown in Table 3-3.

Table 3-3. Specific activities of KDOPS with arabinose arsenate ester.

	Specific Activity at 60°C $KDOPS^{Aa}$ (units/mg)	Specific Activity at 37°C $KDOPS^{Ec}$ (units/mg)
A5P + PEP in Tris-HCl buffer	1.86	12.72
A5P + PEP in sodium arsenate buffer	1.94	11.87
Arabinose + PEP in sodium arsenate buffer	0.03	0.07

The specific activities of both $KDOPS^{Aa}$ and $KDOPS^{Ec}$ to utilize arabinose, inorganic arsenate and PEP as substrates are < 0.1 units/mg, which indicates that arabinose arsenate ester is not a substrate for KDOPS.

Results from previous studies report that inorganic phosphate, a product of the KDOPS catalyzed reaction, is a competitive inhibitor for KDOPS due to its ability to bind at the same active site position as the phosphate moieties of PEP [14]. Since

inorganic arsenate has a similar structure to inorganic phosphate, it is likely that inorganic arsenate is also an inhibitor for KDOPS. Thus, a control experiment was performed to determine if inorganic arsenate inhibits KDOPS. The activity of KDOPS with A5P and PEP was measured in 120 mM sodium arsenate buffer (pH 7.6) instead of the normal Tris-HCl buffer. As shown in Table 3-3, the specific activities of both KDOPS^{Aa} and KDOPS^{Ec} in sodium arsenate buffer remained the same as those in the Tris-HCl buffer, which suggests that inorganic arsenate is not an inhibitor for KDOPS.

3.4.4. Arabinose 5-homophosphonate/Arabinose 5-difluoromethylenephosphonate

The ability of both KDOPS^{Aa} and KDOPS^{Ec} to utilize arabinose 5-homophosphonate or arabinose 5-difluoromethylenephosphonate as alternate substrate was measured by the Aminoff assay (Table 3-4).

Table 3-4. Specific activities of KDOPS with arabinose 5-homophosphonate and arabinose 5-difluoromethylenephosphonate.

	Specific Activity at 60^{o}C KDOPS^{Aa} (units/mg)	Specific Activity at 37^{o}C KDOPS^{Ec} (units/mg)
A5P	1.88	12.72
Arabinose 5-homophosphonate	~0	~0
Arabinose 5-difluoromethylene phosphonate	0.08	0.42

The specific activities of KDOPS^{Aa} and KDOPS^{Ec} with arabinose 5-homophophonate and PEP are close to 0 units/mg. This suggests that arabinose 5-homophophonate is not an alternate substrate for KDOPS.

For the condensation of arabinose 5-difluoromethylenephosphonate with PEP, no activity is displayed with KDOPS^{Aa}; however, KDOPS^{Ec} displays an activity of 0.42 units/mg. Although much lower (about 30 fold) than that of the KDOPS^{Ec} with A5P, this specific activity (0.42 units/mg) is still significant, especially compared to that of any other A5P analogues tested above (< 0.1 units/mg). Thus, arabinose 5-difluoromethylenephosphonate is considered to be an alternate substrate for KDOPS^{Ec} but with a slower turnover rate than the natural substrate A5P. The reason that arabinose 5-difluoromethylenephosphonate is an alternate substrate for KDOPS^{Ec} but arabinose 5-homophosphonate is not may be due to their pKa values. Fluorine is more electronegative than carbon; thus, the pKa of arabinose 5-difluoromethylenephosphonate should be lower than the pKa of arabinose 5-homophosphonate, and is closer to that of the natural substrate A5P. Thus, arabinose 5-difluoromethylenephosphonate can be utilized as an alternate substrate for KDOPS^{Ec}.

The condensation reaction between arabinose 5-difluoromethylenephosphonate and PEP catalyzed by KDOPS^{Ec} should produce inorganic phosphate and a KDO8P derivative, 3-deoxy-D-manno-octulosonate 8-difluoromethylenephosphonate (shown in Figure 3-8).

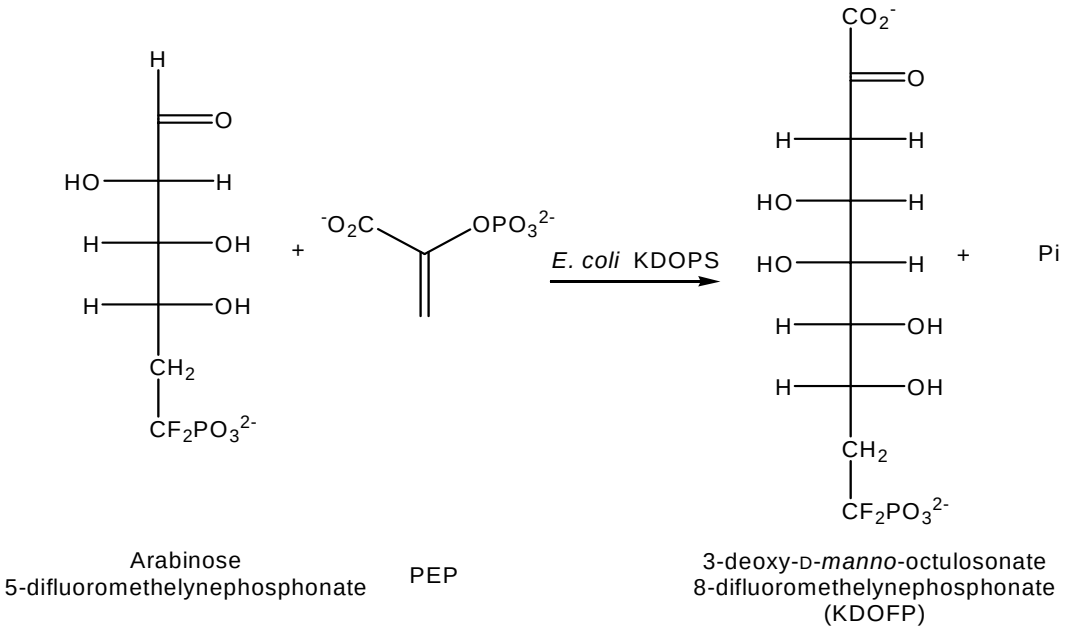

Figure 3-8. Proposed condensation reaction of arabinose 5-difluoromethylene phosphonate and PEP catalyzed by KDOPS^{Ec}.

To further confirm that arabinose 5-difluoromethylenephosphonate is a substrate for KDOPS^{Ec} and that the condensation reaction between arabinose 5-difluoromethylenephosphonate and PEP forms the product 3-deoxy-D-*manno*-octulosonate 8-difluoromethylenephosphonate (KDOFP), a large scale enzymatic synthesis of KDOFP by arabinose 5-difluoromethylenephosphonate, PEP and KDOPS^{Ec} was performed as described in the experimental procedure section. Progression of the reaction was monitored by ^{31}P NMR (Figure 3-9). The triple peak at 4.4, 3.7, and 3.2 ppm corresponds to the coupling between the fluorine and phosphorus in arabinose 5-difluoromethylenephosphonate. The ^{31}P-^{19}F coupling constant in this compound is ~200 Hz. The peak at -2.3 ppm corresponds to the inorganic phosphate product of the reaction. Seen from the spectra, from day1 to day 4, the inorganic phosphate peak increased compared to the arabinose 5-difluoromethylenephosphonate peak, indicating that reaction although slow continued and produced more inorganic

phosphate every day. After 4 days, the reaction was stopped. The reaction mixture was applied to an AG-MP1 anion exchange column. The proposed product KDOFP was separated from the excess reagents and the inorganic phosphate product. The product was then desalted using a G10 sizing column. The purified reaction product was analyzed by ^{31}P NMR, ^{19}F NMR and mass spectrometer. Figure 3-10 shows the ^{31}P NMR spectrum of the purified reaction product. There is a triple peak at 5.6, 4.9, and 4.2 ppm, and the coupling constant is ~210 Hz. This coupling constant is similar to the ^{31}P-^{19}F coupling constant of the starting material, arabinose 5-difluoromethylenephosphonate. The results suggest that the product compound contains phosphorus and fluorine. Figure 3-11 shows the ^{19}F NMR spectrum of the purified reaction product. The peaks in this spectrum indicate that the compound contains fluorine in its structure.

The ^{31}P and ^{19}F NMR spectra can only prove the presence of phosphorus and fluorine in the compound but cannot absolutely confirm that the reaction product is KDOFP since the reagent arabinose 5-difluoromethylenephosphonate displays a somewhat similar spectrum (data not shown). Thus, only the mass spectrum can distinguish between those two compounds. Figure 3-12 shows the mass spectrum of the purified reaction product obtained through electrospray with negative ion detection. The proposed molecular weight of KDOFP is 351.0293 g/mol. The exact mass of the purified product was measured by electrospray through negative ion detection (ESI-) mass spectrometer because of the potentially negative charged carboxyl and phosphonate group of KDOFP. A primary peak at 351.0285 was shown in the mass spectrum, which validates that the product is indeed KDOFP.

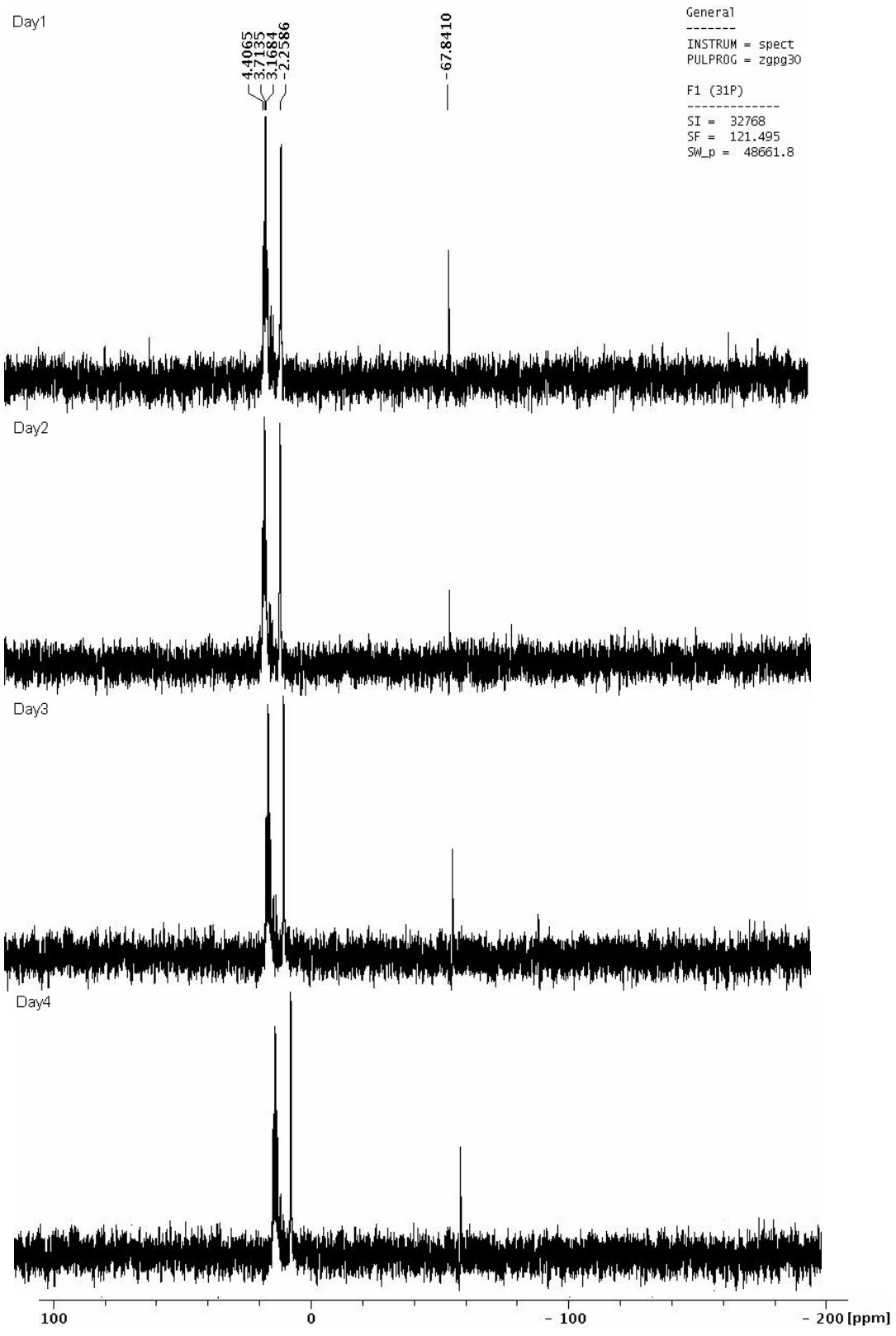

Figure 3-9. Progress of the enzymatic synthesis monitored by ^{31}P NMR.

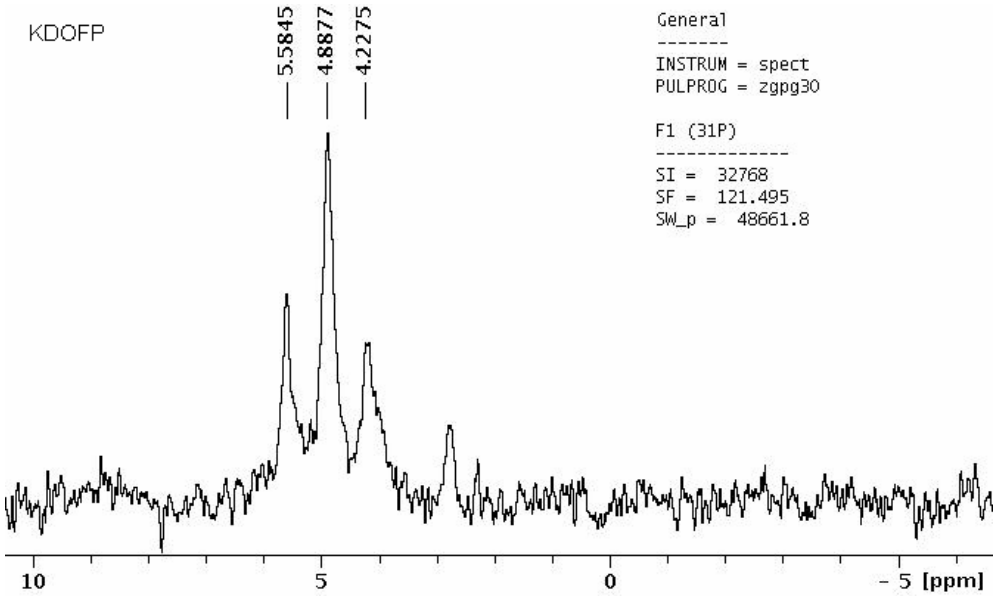

Figure 3-10. ^{31}P NMR spectrum of the purified reaction product.

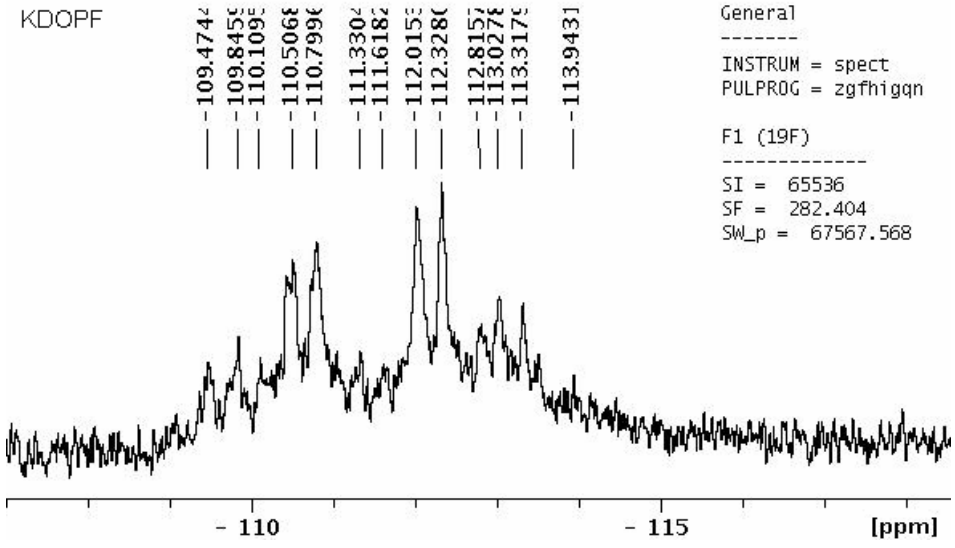

Figure 3-11. ^{19}F NMR spectrum of the purified reaction product.

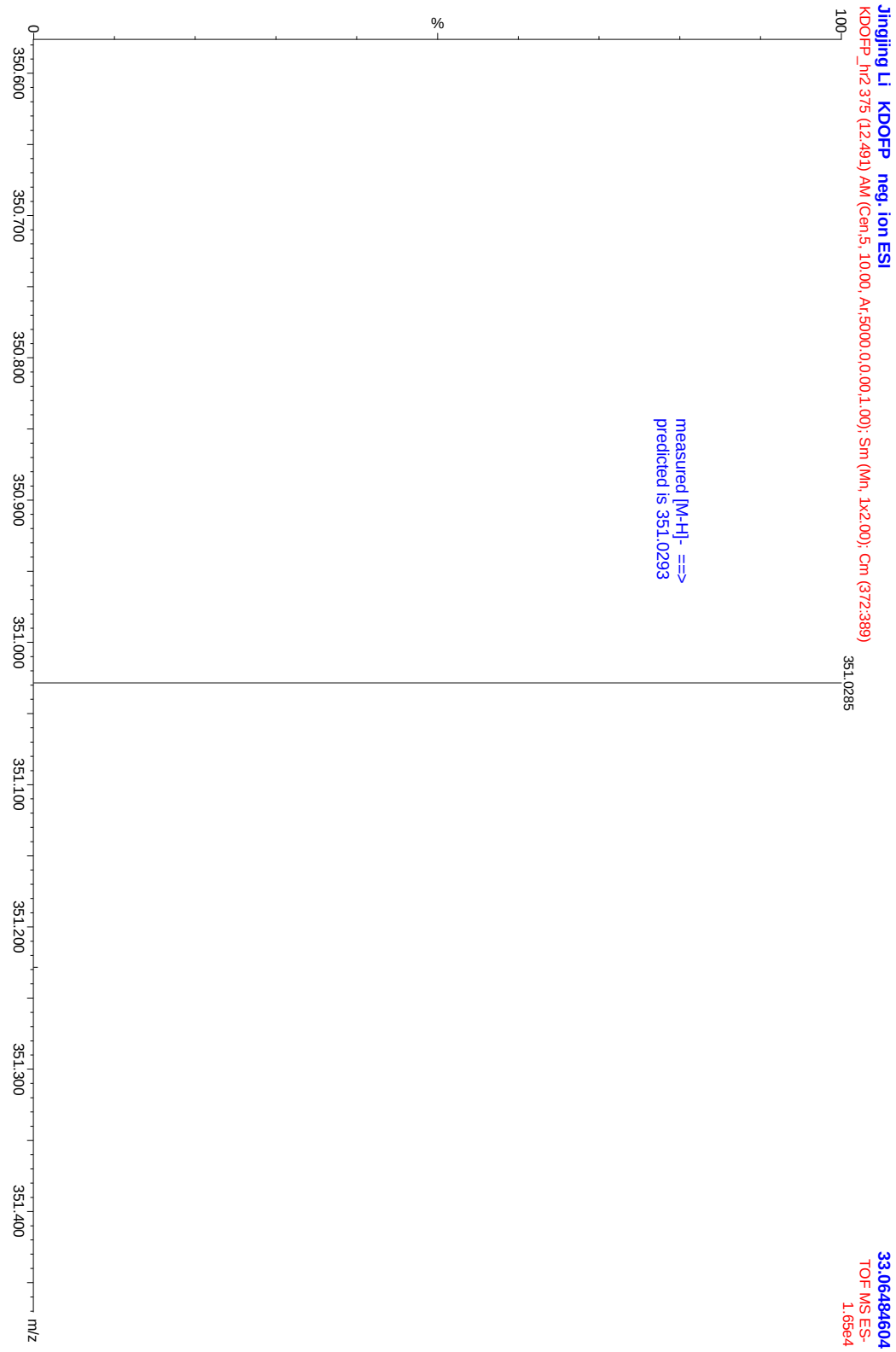

Figure 3-12. Mass spectrum of the purified reaction product obtained using electrospray with negative ion detection (ESI-).

The enzymatic synthesis of KDOFP by KDOPS^{Ec} with arabinose 5-difluoromethylenephosphonate and PEP proves that arabinose 5-difluoromethylenephosphonate is an alternate substrate for KDOPS^{Ec}. However, the enzymatic yield of KDOFP was extremely low (< 2 mg, ~5%). These results suggest that KDOPS^{Ec} might catalyze the condensation of arabinose 5-difluoromethylenephosphonate and PEP at a much slower rate than the natural substrate A5P. Extending the reaction time or increasing the enzyme quantity might help increase the yield of this enzymatic synthesis.

Of all the A5P analogues tested in the present study, only 2-deoxy R5P and arabinose 5-difluoromethylenephosphonate were found to be alternate substrates for KDOPS^{Ec}. Although, the results show that other A5P analogues investigated were not converted to the corresponding 3-deoxy monosaccharide by KDOPS, whether they bind the enzyme active site or not remains unclear. To determine if these A5P analogues bind KDOPS, an isothermal titration experiment might be used in future studies.

3.5. ACKNOWLEDGEMENTS

I thank our collaborator at Peking University for synthesizing arabinose 5-homophosphonate and arabinose 5-difluoromethylenephosphonate, James Patrone for helping me use the Bruker Advance DRX-300 instrument for ^{31}P and ^{19}F NMR analysis, members in Dr. Doston's group for letting me use their lyophilizer, and the Department of Chemistry Technique Service Of Mass Spectrometer for measuring the exact mass of KDOFP. I also want to thank members in Woodard group for their help.

3.6. REFERENCES

1. Aminoff, D., *Methods for the Quantitative Estimation of N-Acetylneuraminic Acid and their Application to Hydrolysates of Sialomucoids.* Biochem. J., 1961. **81**: p. 384-392.

2. Radaev, S., et al., *Structure and mechanism of 3-deoxy-D-manno-octulosonate 8-phosphate synthase.* J Biol Chem, 2000. **275**(13): p. 9476-84.

3. Shumilin, I.A., R.H. Kretsinger, and R.H. Bauerle, *Crystal structure of phenylalanine-regulated 3-deoxy-D-arabino-heptulosonate-7-phosphate synthase from Escherichia coli.* Structure Fold Des, 1999. **7**(7): p. 865-75.

4. Sheflyan, G.Y., et al., *Enzymatic Synthesis of 3-Deoxy-D-manno-octulosonate 8-Phosphate, 3-Deoxy-D-altro-octulosonate 8-Phosphate, 3,5-Dideoxy-D-gluco(manno)-octulosonate 8-Phosphate by 3-Deoxy-D-arabino-heptulosonate 7-Phosphate Synthase.* J Am Chem Soc, 1998. **120**(43): p. 11027-11032.

5. Schoevaart, R., F. van Rantwijk, and R.A. Sheldon, *Facile enzymatic aldol reactions with dihydroxyacetone in the presence of arsenate.* J Org Chem, 2001. **66**(13): p. 4559-62.

6. Durrwacbter, J.R., et al., *Enzymatic Aldol Condensation/Isomerization as a Route to Unusual Sugar Derivatives.* Journal of Organic chemistry, 1986. **108**: p. 7812-7818.

7. Drueckhammer, D.G., et al., *Reversible and in Situ Formation of Organic Arsenates and Vanadates as Organic Phosphate Mimics in Enzymatic Reactions: Mechanistic Investigation of Aldol Reactions and Synthetic Applications.* Journal of Organic chemistry, 1989. **54**: p. 70-77.

8. Hedstrom, L.K., *Studies on the enzymes of the shikimate pathway*, in *Biochemistry*. 1986, Brandeis University. p. 119-121.

9. Howe, D.L., et al., *Mechanistic insight into 3-deoxy-D-manno-octulosonate-8-phosphate synthase and 3-deoxy-D-arabino-heptulosonate-7-phosphate synthase utilizing phosphorylated monosaccharide analogues.* Biochemistry., 2003. **42(17)**: p. 4843-54.

10. Lanzetta, P.A., et al., *An improved assay for nanomole amounts of inorganic phosphate.* Anal Biochem, 1979. **100**(1): p. 95-7.

11. Pramod, S.N. and Y.P. Venkatesh, *Utility of pentose colorimetric assay for the purification of potato lectin, an arabinose-rich glycoprotein.* Glycoconj J, 2006. **23**(7-8): p. 481-8.

12. Duewel, H.S., et al., *Substrate and metal complexes of 3-deoxy-D-manno-octulosonate-8-phosphate synthase from Aquifex aeolicus at 1.9-A resolution. Implications for the condensation mechanism.* The Journal of biological chemistry., 2001. **276(11)**: p. 8393-402.

13. Li, J., et al., *Conversion of Aquifex aeolicus 3-Deoxy-d-manno-octulosonate 8-Phosphate Synthase, a Metalloenzyme, into a Nonmetalloenzyme.* J Am Chem Soc, 2004. **126**(24): p. 7448-9.

14. Asojo, O., et al., *Crystal Structures of KDOP Synthase in Its Binary Complexes with the Substrate Phosphoenolpyruvate and with a Mechanism-Based Inhibitor.* 2001. **40**(21): p. 6326-6334.

CHAPTER 4

INVESTIGATION OF THE METAL REQUIREMENTS OF KDOPS

4.1. SUMMARY

Metal can be considered to be a third substrate of KDOPS. There are two classes of KDOPSs: Class I are non-metalloenzymes (represented by *E. coli*), while Class II (represented by *A. aeolicus*) are metalloenzymes [1]. All DAHPSs studied to date are metalloenzymes. In this chapter, I focused on changing the metal requirements of KDOPSs in order to understand the catalytic or structural function of the metal. The *A. aeolicus* KDOPS ($KDOPS^{Aa}$) C11N mutation successfully converted the wild-type metallo KDOPS into a non-metallo enzyme with comparable activity [2]. The activity of the *E. coli* KDOPS ($KDOPS^{Ec}$) N26C and M25P/N26C mutant enzymes can be increased by the addition of Mn^{2+} or Cd^{2+}, suggesting that these two mutant $KDOPS^{Ec}$ have some properties similar to that of metal-dependent KDOPS.

Crystallography studies on the $KDOPS^{Aa}$ C11N mutant were performed. The crystal structure of the mutant enzyme was determined at a 2.2 Å resolution using molecular replacement. The active site structures of wild-type $KDOPS^{Aa}$ and $KDOPS^{Aa}$ C11N mutant with or without substrates were compared to each other. The restults suggest that the divalent metal plays an important structural role in maintaining correct orientation of A5P for catalysis.

4.2. INTERCONVERSION BETWEEN METALLO AND NON-METALLO KDOPSs

4.2.1. Introduction

In an early phylogenetic study, Birck et al. [1], in our laboratory analyzed the amino acid sequences of KDOPSs and identified two distinct Classes for KDOPSs, labeled Class I and II respectively (see Figure 4-1). Class II KDOPSs originate from more ancient microorganisms than Class I KDOPSs. Later, studies on several KDOPSs from different microorganisms showed that Class I KDOPSs are non-metalloenzymes (represented by *E. coli*), while Class II (represented by *A. aeolicus*) are metalloenzymes. All DAHPSs studied to date are metalloenzymes.

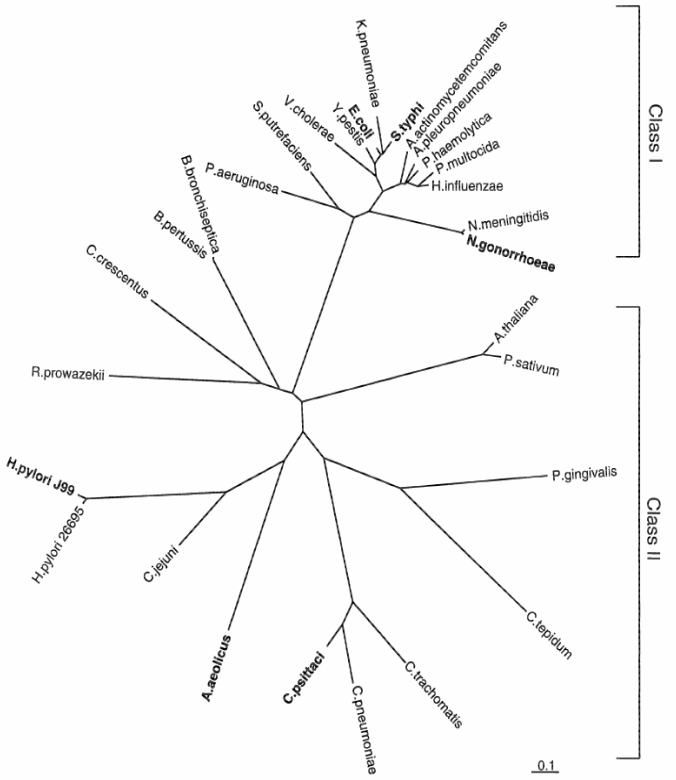

Figure 4-1. Phylogenetic tree generated by maximum-likelihood analysis from the sequences of 29 KDOPS sequences from various organisms [1]. Class I is predicted to maintain the characteristics of the model *E. coli* enzyme (no metal requirement), while Class II, including the *A. aeolicus* enzyme, is predicted to require a divalent metal for catalysis.

Two questions need to be answered in studying the metal requirements of KDOPSs were aksed. One is to determine what causes the differences in the metal requirements of the two classes of KDOPSs. The other is to identify the role of the metal in structure and catalysis.

The crystal structure of KDOPS^{Aa} with Cd^{2+} was solved by Dr. Domenico Gatti at Wayne State University. In the crystal structure of KDOPS^{Aa}, four residues C11, H185, E222, and D233 are found to form the octahedral metal binding site for Cd^{2+} with a water molecule being the sixth ligand (E222 provides two ligands) [3]. (see Figure 4-2)

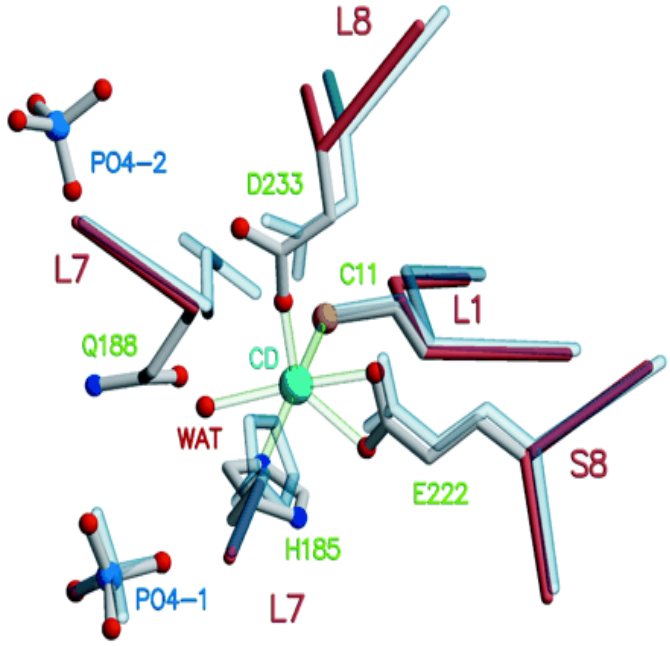

Figure 4-2. Metal binding site of KDOPS^{Aa} [3].

Sequence alignment studied to date (see Figure 4-3) shows that all four of these residues are absolutely conserved in Class II KDOPSs and all DAHPSs (see Figure 4-4).

	Organism	Partial sequence								Accession No.
	E. coli	22	FGGMNV	201	THALQC	237	FIEAHP	249	CDGPSA	P17579
	P. aeruginosa	22	FGGMNV	199	THALQM	235	FLEAHP	247	CDGPCA	AAG07024
Class I	*V. cholera*	22	FAGMNV	201	THSLGM	237	FLEAHP	249	CDGPSA	Q9KQ29
	S. typhimurium	22	FGGMNV	201	THALQC	237	FLESHP	249	CDGPSA	Q8XGR9
	Y. pestis	22	FGGMNV	201	THALQC	237	FLEAHP	249	CDGPSA	CAC90835
	H. influenzae	22	FGGMNV	201	THSLQC	237	FLEAHP	249	CDGPSA	P45251
	A. aeolicus	07	IAGPCA	184	THSVQL	220	FMETHP	232	SDASTQ	O66496
	C. jejuni	07	IAGPCV	194	THSVQM	230	FFETHI	242	CDGPNM	Q9PIB8
Class II	*H. pylori*	14	IAGPCV	203	THSVQM8	239	FAETHI	251	SDGANM	Q9ZN55
	C. psittaci	09	IAGPCV	188	THSVQL	224	FIETHM	236	SDAASM	Q46225
	R. prowazekii	21	IAGPCQ	198	THSVQQ	234	YMEVHQ	246	SDGPCM	NP_220456
	C. pneumoniae	09	IAGPCV	188	THSVQL	224	FIETHT	236	SDAASM	Q9Z7I4

Figure 4-3. Sequence alignment of representative KDOPSs. Sequences were aligned using Clustal W. Invariant residues that are putative metal-binding sites are shaded (C11, H185, E222, and D233 based on amino acid sequence for KDOPS^{Aa}). The conserved N residues in the Class I were shaded in red. The sequences are followed by their NCBI accession numbers.

Organism	Partial sequence								Accession No.
C. pneumoniae	044	AGPCTL	216	DPSHA	243	MIEVH	255	C—-DAK	NP_224680
C. trachomatis	037	AGPCTL	208	DPSHA	235	MIEVH	247	C—-DGS	NP_219891
P. abyssi	031	AGPCAI	201	DPSHP	228	LVEVH	240	S--DSK	B75161
P. furiosus	028	AGPCSI	198	DPSHP	225	MVEVH	237	S--DSQ	NP_579419
T. maritima	099	AGPCSV	269	DPSHS	296	IVEVH	308	S--DGK	E72388
E. faecalis	099	AGPCSI	269	DPSHG	296	IVEIH	308	S--DGP	AAG53674
B. subtilis	123	VGPCAV	293	DVTHS	320	MAEVH	332	S--DSA	P39912
S. pyogenes	020	VGPCSI	190	DVSHS	217	MMEVH	229	S--DAA	AAK34362
C. acetobutyricu	099	AGPCSI	269	DPSHA	296	MIEVH	308	S--DGQ	AAK78868
A. pernis	043	AGPCSV	213	DPSHP	240	IVEVH	252	S--DAK	E72643
H. influenzae	065	IGPCSI	273	DFSHA	308	MVESH	331	SITDAC	P44303
E. coli	058	IGPCSI	265	DFSHA	300	MVESH	323	SITDAC	P00886
P. agglomerans	057	IGPCSL	264	DFSHG	299	MIESF	322	SITDPC	O54459
B. aphidicola	057	IGPCSV	264	DFSHG	299	MIESF	322	SITDAC	P46245
C. glutamicum	066	VGPCSV	271	DASHA	306	MIESF	336	SVTDKC	P35170
P. aeruginosa	059	IGPCSI	267	DCSHA	302	MVESH	326	SITDAC	B83426
V. cholerae	058	VGPCSV	266	DFSHA	301	MAESF	324	SITDPC	AAF73000
S. typhimurium	059	CGPCSI	266	DCSHG	301	MIESN	325	SVTDAC	P21307
S. cerevisiae	067	IGPCSL	278	DCSHG	313	MIESN	339	SVTDAC	NP_010320
A. orientalis	065	TGPCSI	273	DASHD	308	MLESN	331	SITDAC	T17477

Figure 4-4. Sequence alignment of representative DAHPSs. Sequences were aligned using Clustal W. Invariant residues that are putative metal-binding sites are shaded (C61, H268, E302, and D326 based on amino acid sequence for *E. coli* phe-sensitive DAHPS). The sequences are followed by their NCBI accession numbers.

In the non-metallo Class I KDOPSs, three of the four residues (H185, E222, and D233) are conserved, while C11 (*A. aeolicus* numbering) has been replaced by an N26 (*E. coli* numbering) residue. The crystal structures reveal that these key metal binding site

amino acids are similarly arranged in both KDOPS and DAHPS [4].

Based on these analyses, it is postulated that the Cys and Asn may be the key residues responsible for the difference in the metal requirements of the two KDOPS classes. Thus, it should be relatively straight forward to change the metal requirements for the enzymes. To test this hypothesis and verify the role of the Cys, Asn, and metal involved in the mechanism, the KDOPS^{Aa} C11N mutant was constructed to convert the metallo KDOPS^{Aa} into a non-metallo enzyme. As control experiments, the KDOPS^{Aa} C11G, C11S, C11S mutants were constructed. In the C11G mutant, Gly has no side chain, and should not bind metal. The sulfur in Cys is replaced by an O in the C11S mutant to test if the Ser can coordinate with the metal or not. The C11K mutant should not bind metal any longer since Lys is potentially positive charged. But the positive charge introduced by Lys might be able to substitute the positive charge carried by the metal to maintain the active site geometry. The KDOPS^{Ec} N26C mutant was also constructed in order to convert the non-metallo KDOPS^{Ec} into a metallo enzyme.

4.2.2. Experimental Procedures

Materials – Polymerase chain reaction (PCR) primers were synthesized by Invitrogen. PCR was performed using a MJ Research PTC-200 Peltier Thermal Cycler. The Wizard® Plus SV Minipreps DNA purification kit was utilized for plasmid isolation and purification. Chemically competent *E. coli* XL1-Blue (Stratagene), chemically competent *E. coli* BL21 (DE3) (Novagen) were used for plasmid transformations. Restriction enzymes and *Dpn*I were purchased from New England Biolabs. DNA sequencing was performed by the University of Michigan Biomedical Resources Core

Facility. Protein dye reagent concentrate was purchased from Bio-Rad. Tris(hydroxymethyl)aminomethane was purchased from Research Organics. Phospho*enol*pyruvate mono(cyclohexyl ammonium) salt, thiobarbituric acid, and bovine albumin serum (BSA) were purchased from Sigma. Arabinose 5-phosphate was prepared and purified by Dr. Junhua Yan in Woodard laboratory. Enzyme grade KCl, NaCl, ammonium sulfate, and acetic acid were purchased from Fisher Scientific. DNase I and RNase A were purchased from Roche. High grade spectra/Por® 7 dialysis tubing (15,000 molecular weight cut-off and metal free) was purchased from VWR. The Millex® syringe driven filter units (0.22 μm) was purchased from Millipore. Phenyl Superose (HR 10/10) and Mono Q (HR 10/10) chromatography columns were purchased from Amersham Pharmacia Biotech, and were run in the FPLC® system purchased from Pharmacia.

Sequence Analysis – Database searching of multiple microbial organisms was performed utilizing the BLAST program at the NCBI website (http://ncbi.nlm.nih.gov/BLAST). Multiple sequence alignments were generated using Clustal W (http://www.ebi.ac.uk/clustalw).

Protein Concentration Assay – Protein concentration was determined using the Bio-Rad Protein Assay Reagent assay. BSA served as a standard for this assay.

One Dimensional Polyacrylamide Gel Electrophoresis – Sodium dodecyl sulfate polyacrylamide gel electrophoresis (SDS-PAGE) used to confirm the weight and purity of proteins, was performed under reducing condition on a 12% polyacrlamide gel with the Mini-PROTEAN II electrophoresis unit (Bio-Rad). Protein samples of 5-15 μg were used for analysis on the SDS-PAGE gels. Gels were stained and visualized with a

0.25% Commassie Brilliant Blue R-250 solution.

Construction, Overexpression, and Purification of mutant KDOPSs –The plasmids of KDOPS mutants were prepared by the QuickChange site-directed mutagenesis kit described by M.P. Weiner [5]. Two oligonucleotide primers, see Table 4-1, each containing the desired mutagenic replacement codon, were designed as forward and reverse primers. PCR was performed in a 50 μL reaction mixture containing 5 μL 10× react ThermolPol buffer, 2 μL 50 mM $MgCl_2$, 1 μL miniprep pT7-7/*kds*A plasmid (wild-type KDOPS expression vector) as a template, 1 μL forward primer, 1 μL reverse primer, 2 μL dNTP mixture, 37 μL H_2O, and 1 μL high-fidelity *Vent* DNA polymerase. Conditions for PCR were as follows: the first step of 3 min at 95°C for one cycle; the second step of 16 cycles of 30 sec at 95°C, 1 min at 55°C, 6.5 min at 72°C; the last step of one cycle of 5 min at 72°C. The PCR product containing the linear mutant plasmid was treated with *Dpn*I to digest the parental methylated pT7- 7/*kds*A DNA template. The *Dpn*I digestion reaction mixture, containing the mutagenic DNA, was used to transform supercompetent *E. coli* XL1-Blue cells. Plasmid DNAs were isolated and purified from each of the clones and initially characterized by restriction digestion and then DNA sequenced.

DNA containing the proper mutagenic sequence was used to transform chemically competent *E. coli* BL21 (DE3). The *E. coli* Bl21 (DE3) cells harboring the mutant pT7- 7/*kds*A were grown in 2×YT medium (1 L) containing ampicillin (100 μg/mL) at 37°C with orbital shaking (250 RPM). When the culture had reached an absorbance of 1.5 at 600 nm, IPTG was added to a final concentration of 0.4 mM. The culture was grown at 16°C for 16 h, then the cells were collected by centrifugation

(18000×g, 20 min, at 4°C) and suspended in buffer A (20 mM Tris-HCl buffer, pH 7.5). The cell suspension was subjected to sonication on ice (4×30 sec, 2 min rests between pulses) and then clarified by centrifugation (18000×g, 40 min, at 4°C) to produce the cell extract. For mutant KDOPS^{Aa} only, solid sodium chloride was added to the cell extract to a final concentration of 0.1 M and the solution was heated in a boiling water bath for 2 min and then at 80°C for 10 min with continuous swirling [6]. The suspension was allowed to cool to room temperature and then placed on ice for 15 min. Precipitated protein was removed by centrifugation (18000×g, 20 min, at 4°C). DNase I and RNase A were added to the supernatant and incubated in 37°C water bath for 30 min. The protein solution was dialyzed against buffer A overnight. The protein then was applied to a Mono Q (10/10) column previously equilibrated with buffer A. The column was developed at a flow rate of 1 mL/min using a linear gradient from 0 M to 0.3 M potassium chloride in the same buffer (over 60 min). The fractions containing KDOPS, which resolved into a single peak, were pooled and judged by SDS-PAGE (~30 kDa). Solid ammonia sulfate was added to a final concentration of 20% (w/v). The sample was filtered (0.22 μm) and applied to a Phenyl Superose column (10/10) equilibrated with 20% ammonia sulfate in buffer A. The column was developed with a linear gradient from 20% to 0% (w/v) ammonia sulfate in buffer A (over 120 min). The majority of the protein of interest eluted as a single peak at 0% ammonium sulfate concentration. The purity of the recombinant protein was homogeneous as judged by SDS-PAGE analysis (> 95%). The purified proteins were pooled, dialyzed against 5 mM Tris-HCl buffer (pH 7.5), and then frozen in dry ice with acetone and stored at -80°C. The total yield of homogenous KDOPS protein was 5-10 mg protein/L of cell culture.

Table 4-1. Oligonucleotides used for the mutagenesis of KDOPS.

Target Amino Acid	Primers 5'→ 3'	Resulting Amino Acid
C11	GTGATAGCTGGACCCAATGCGATAGAGAGCGAGG CCTCGCTCTCTATCGCATTGGGTCCAGCTATCAC	N
C11	GTGATAGCTGGACCCTCGGCGATAGAGAGCGAGG CCTCGCTCTCTATCGCCGAGGGTCCAGCTATCAC	S
C11	GTGATAGCTGGACCTAAGGCGATAGAGAGCGAGG CCTCGCTCTCTATCGCCTTAGGTCCAGCTATCAC	K
C11	GTGATAGCTGGACCCGGGGCGATAGAGAGCGAGG CCTCGCTCTCTATCGCCCCGGGTCCAGCTATCAC	G
N26	CGTACTGTTGGGCGGTATGTGCGTGTTGGAATCTC GAGATTCCAACACGCACATACCGCCCAACAGTA	C
M25 N26	CGTACTGTTGGGCGGTCCGTGCGTGTTGGAATCTC GAGATTCCAACACGCACGGACCGCCCAACAGTA	P C

Aminoff colorimetric assay [7] – Enzyme specific activity was measured in a final volume of 50 μL containing PEP (3 mM), A5P (3 mM), Tris-acetate buffer (100 mM, pH 7.5) using thin-walled PCR tubes as the reaction vessel. The assay solution was pre-incubated at a desired temperature for 2 min and the reaction was initiated with the addition of enzyme (5 μg) and incubated at the desired temperature. At specified time, the reactions were stopped with the addition of 50 μL 10% ice-cold TCA (to a final concentration of 5%) and centrifuged to remove precipitated protein. The 100 μL enzymatic reaction mixture was transferred into a 10-mL glass tube and subjected to total oxidation with 0.2 mL 0.025 M $NaIO_4$ in 0.125 M H_2SO_4 at room temperature for 10 min. The excess oxidizing agent was reduced by the addition of 0.4 mL of 2% (w/v) $NaAsO_2$ in 0.5 M HCl. Following the disappearance of the yellow color, 1 mL thiobarbituric acid

(0.36% w/v, pH 9.0) was added and the tube heated at 100°C for 10 min. The amount of KDO8P produced was determined by measuring the absorption at λ = 549 nm (ε = 1.03×10^5 $M^{-1}cm^{-1}$ for the pink chromophore formed between α-formylpyruvate and thiobarbiturate). All assays were performed in triplicate.

Kinetic parameters [8] **–** A continuous spectrophotometric method for the measurement of the disappearance of the α, β-unsaturated carbonyl absorbance of PEP was used to determine kinetic parameters of KDOPS. The standard assay mixture contained PEP (0.05-1 mM), A5P (0.05-1 mM), 100 mM Tris-acetate buffer (pH 7.5), and 5-15 μg KDOPS in 1 mL. The first three reagents were mixed and preheated at 60°C for 2 min. The assay, initiated by the addition of the KDOPS, was monitored for 3 min at λ = 232 nm for a decrease in absorption (ε = 2840 $M^{-1}cm^{-1}$). The K_m and V_{max} values were determined from a nonlinear regression of data pairs (substrate concentration, initial velocity) fit to the Michaelis-Menten equation using KaleidaGraph 3.08d. All assays were performed in triplicate.

Temperature optima – The temperature optimum of mutant KDOPS was determined by measuring the activity of the mutant enzyme at different temperature between 30°C and 100°C using the Aminoff assay.

Thermostability – Purified enzyme (2 mg/mL) in 100 mM Tris-acetate buffer (pH 7.5) was constantly maintained at 90°C in thin-walled PCR tubes. At various times, aliquots of enzyme (5 μg) were removed and subjected to the Aminoff assay.

Metal Analysis of KDOPS – The protein from the mutant constructs was isolated and purified as described above. Protein from each of these mutants was divided into three aliquots, one portion (as isolated) was left untreated, the second portion

(apo) was treated with 10 mM EDTA for 2 h at 25ºC to remove metal and dialyzed against metal-free buffer to remove EDTA, while the third portion (all) was obtained by treating the apo enzyme with a mixture of metal salts (Table 4-2) at 100 μM for 2 h at 25^{o}C and passed through a desalting column to remove excess metal ions. The protein fractions were subjected to the Aminoff assay and metal analysis. The amount of bound metal in each portion of the mutant protein as well as in the wild type KDOPSs was determined using high-resolution inductively coupled plasma-mass spectrometry (ICP-MS) [9] in the University of Michigan, Department of Geology by Dr. Ted Huston.

4.2.3. Results and Discussion

The KDOPS^{Aa} mutants C11N, C11S, C11K and C11G as well as the KDOPS^{Ec} mutants N26C were constructed utilizing standard techniques. The proteins from these mutant constructs were isolated and purified as described in the experimental procedures section. The amount of bound metal in each of the mutant and wild-type KDOPSs was determined using ICP-MS. The enzymatic activity of the protein was measured using the Aminoff standard discontinuous assay. The metal content and specific activity of each mutant and wild-type KDOPSs are shown in Table 4-2.

The results demonstrate that the wild-type metallo KDOPS^{Aa} need metal to be active. The KDOPS^{Aa} C11N mutant does not bind metal any longer and is still as active as wild-type KDOPS^{Aa}. The KDOPS^{Aa} C11G, C11S, and C11K mutants also do not bind metal but display minimal activity. The wild-type non-metallo KDOPS^{Ec} does not need metal to be active, and its activity is much higher (> 6 fold) than the wild-type metallo KDOPS^{Aa}. The KDOPS^{Ec} N26C mutant binds metal but has minimal activity.

The data suggests that the KDOPS^{Aa} C11 mutations indeed alter the metal binding ability of the enzyme. The non-metallo active KDOPS^{Aa} C11N mutant was further studied. When individual metal salt was added to the Aminoff assay mixture of the apo KDOPS^{Aa} C11N mutant, no metal ion tested caused an increase in enzyme activity (Table 4-3). The present of metal ions at high concentration however inhibited the C11N mutant catalytic activity.

The KDOPS^{Aa} C11N mutant was kinetically characterized to compare its properties to that of the wild-type KDOPS^{Aa} [6]. To determine kinetic constants, a continuous assay monitoring the disappearance of the PEP double bond was used. The temperature optima, thermal stability and kinetic parameters for both the KDOPS^{Aa} C11N mutant and wild-type KDOPS^{Aa} are summarized in Table 4-4. As seen in the table, the C11N mutant enzyme is still thermol stable. The KDOPS^{Aa} C11N mutant is catalytically more efficient since its k_{cat}/K_m is higher than that of the wild-type KDOPS^{Aa}. The lower K_m^{PEP} value of KDOPS^{Aa} C11N suggests KDOPS^{Aa} C11N binds PEP much tighter compared to the wild-type KDOPS^{Aa}. While the KDOPS^{Aa} C11N mutant displays many of the characteristics of the thermostable metallo family, the kinetic parameters for the KDOPS^{Aa} C11N mutant are more similar to the kinetic values of the non-metallo KDOPS^{Ec} (K_m^{A5P} = 30 μM, K_m^{PEP} = 19 μM, k_{cat} = 6.8 s^{-1}) than that to the wild-type metallo KDOPS^{Aa} values [10].

Table 4-2. Metal analysis of KDOPSs.

Incubation metal salt (Molarequivalentmetal/enzyme subunit)		Zinc	Cadmium	Manganese	Copper	Cobalt	Nickel	Magnesium	Iron	Specific activity (units/mg)
AA Wildtype	As isolated	0.51	----	----	0.02	----	----	0.09	0.06	1.88
	Apo	0.02	----	----	----	----	----	0.05	0.02	0.08
	All	0.12	0.36	0.04	0.24	0.04	0.04	0.11	0.08	1.98
AA C11N	As isolated	0.04	----	----	0.02	----	----	0.04	----	1.47
	Apo	----	----	----	----	----	----	----	----	1.70
	All	0.08	0.03	0.03	0.08	0.04	0.04	0.05	0.06	1.40
AA C11G	As isolated	0.07	----	----	0.01	----	----	----	----	0.08
	Apo	0.02	----	----	----	----	----	----	----	0.04
	All	0.09	0.02	----	0.01	0.02	----	0.02	0.02	0.09
AA C11S	As isolated	0.02	----	----	0.02	----	----	----	----	0.11
	Apo	0.01	----	----	----	----	----	----	----	0.12
	All	0.09	0.02	0.02	0.14	0.02	0.03	0.03	0.07	0.04
AA C11K	As isolated	0.05	----	----	----	----	----	----	----	0.07
	Apo	0.02	----	----	----	----	----	----	----	0.15
	All	0.06	----	----	----	----	----	0.04	----	0.22
EC Wildtype	As isolated	0.02	----	----	0.02	----	----	0.04	0.01	12.72
	Apo	0.02	----	----	----	----	----	0.07	0.02	12.28
	All	0.06	0.02	0.02	0.35	0.03	0.03	0.08	0.03	0.80
EC N26C	As isolated	0.12	----	----	0.10	----	----	0.07	0.04	0.07
	Apo	0.08	----	----	----	----	----	0.05	0.03	0.17
	All	0.17	0.13	0.05	0.54	0.04	0.06	0.10	0.12	0.03
EC M25P/N26C	As isolated	0.65	----	----	0.02	----	----	0.02	0.04	0.35
	Apo	0.02	----	----	----	----	----	0.02	----	0.76
	All	0.04	0.16	0.32	0.02	----	----	----	0.17	0.98
	Blank	----	----	----	----	----	0.02	----	----	----

Table 4-3. KDOPS^{Aa} C11N mutant activity with different metal.

Metal Salt	Specific Activity (units/mg)
Apo	1.70
$MgCl_2$ (0.1 mM)	1.54
$ZnSO_4$ (0.1 mM)	1.38
$FeSO_4$ (0.1 mM)	1.47
$CoCl_2$ (0.1 mM)	1.38
$NiCl_2$ (0.1 mM)	1.50
$MnCl_2$ (0.1 mM)	1.45
$MnCl_2$ (0.5 mM)	1.36
$MnCl_2$ (1.0 mM)	1.24
$MnCl_2$ (3.0 mM)	1.15

Table 4-4. Comparison of kinetic parameters between wild-type KDOPS^{Aa} and C11N mutant.

	Wild-type KDOPS^{Aa}	KDOPS^{Aa} C11N mutant
Optimal temperature (^oC)	95	90
Half-life at 90^{o}C (hr)	1.5	0.5-0.75
k_{cat} at 60^{o}C (s^{-1})	0.42±0.06	0.64±0.04
K_m^{A5P} at 60^{o}C (μM)	26±4	30±4
K_m^{PEP} at 60^{o}C (μM)	155±8	12±2

The metal binding and enzymatic activities of the KDOPS^{Aa} C11 control mutants, namely C11G, C11S and C11K, are shown in Table 4-2. The C11G mutant does not bind metal because of the missing key metal ligand, and has no activity since it has neither a metal at active site nor an Asn at the C11 position. Replacing the sulfur of the Cys metal ligand with an oxygen [11] in the C11S mutant again results in a catalytically inactive KDOPS that does not bind a metal ion. Since it has been speculated that the γ-nitrogen of the Class I N26 may interact with the negatively charged carboxylate moiety of PEP at the active site to adjust the angle of the carboxylate π-electron system with the carbon-carbon double bond π-electron system in order to facilitate the anti-Michael addition to C3 of PEP [12, 13], the C11K mutant was constructed and tested for both enzymatic activity and its ability to bind divalent metal ion. While an unlikely metal binding ligand, the ω-nitrogen of the C11K KDOPS has the potential to be positively charged at the active site and might assist in aligning the orbital angles by interaction with the carboxylate anion as observed for the γ-nitrogen of the N26 of wild-type KDOPS^{Ec}. The C11K mutant does not bind metal and is inactive.

The data presented above demonstrates that the mutation of a single conserved amino acid, C11, in a metallo KDOPS (KDOPS^{Aa}) to an Asn found in non-metallo KDOPS results in a catalytically functional enzyme. Examination of the crystal structure of wild-type KDOPS^{Aa} reveals that the four metal binding ligands are positioned solely on one side of the metal ion, whereas the other side of the metal is facing the substrate PEP [3]. This suggests that the function of the metal may be to orient the PEP in a manner similar to that discussed for the function of the γ-nitrogen of the non-metallo N26. In addition to the loss of the chelating sulfur atom, the exchange of an Asn for the

Cys at position 11 likely destroys the geometry necessary for proper metal binding, and thus the mutant enzyme does not bind metal. Results from *in silico* mutation, utilizing the Swiss-PdbViewer software, suggest that the functional amide group of N11 fills the hole left from the loss of the metal. The carboxamide's carbonyl oxygen appears to be capable of hydrogen bonding to both E222 and D233, which might help maintain the active site geometry; further, the γ-nitrogen of N11 is positioned to interact with PEP similar to that predicted for the N26 of KDOPS^{Ec}. In short, the carboxamide group of the Asn in the C11N mutant may substitute for the function normally performed by the metal. Regardless of the exact role, our results demonstrate that the active site residue occupying position 11 in KDOPS^{Aa} plays a major role directly by interacting with the PEP moiety or indirectly by furnishing a ligand for metal binding needed for catalytic activity. The single amino acid substitution, C11N mutation, in KDOPS^{Aa} successfully converted the metallo wild-type KDOPS into a non-metallo enzyme.

For KDOPS^{Ec}, the change of N26 to Cys only slightly increases the metal binding; however the mutant enzyme displays minimal activity. Therefore, converting a non-metallo enzyme into a metallo enzyme by KDOPS^{Ec} N26C mutant, was not successful. Therefore, a closer examination of the amino acid sequences of the metallo and non-metallo enzymes (see Figure 4-3, 4-4) were perfomed. The results show that the amino acid residues near the metal binding site are very similar in both metallo and non-metallo enzymes. The only exception is that there is a conserved Pro immediately before the Cys in the metallo enzyme families; while for all the non-metallo enzymes, the residue before the Asn is a conserved Met. The crystal structure of the metallo KDOPS^{Aa} shows that the P10 introduces a turn structure in the protein due to the cyclic

nature of its pyrrolidine side group. This Pro residue might play a role in positioning the C11 to the proper orientation that facilitates the metal binding. The M25, instead of Pro, in the KDOPS^{Ec} N26C mutant might likewise be unable to assist in the positioning of the C26 for metal coordination due to the lack of the turn structure. Therefore, the KDOPS^{Ec} M25P/N26C double mutant was constructed.

The specific activities and metal contents of the KDOPS^{Ec} M25P/N26C double mutant enzyme were measured using the same methodology described in the experimental procedures section. The results are shown in Table 4-2. Although still much lower than the wild-type KDOPS^{Ec} , the activity of the KDOPS^{Ec} M25P/N26C double mutant is slightly higher than the KDOPS^{Ec} N26C single mutant. Most interestingly, the activity of the all KDOPS^{Ec} M25P/N26C mutant (0.98 units/mg), which binds Mn^{2+} and Cd^{2+}, is higher than the activity of the as isolated enzyme (0.35 units/mg), which bind Zn^{2+}. These results suggest that the M25P/N26C mutant activity may have different affinities for different metal ions. In order to understand the dependence of the M25P/N26C mutant activity on different divalent metals, the mutant enzyme activity was determined under conditions in which EDTA-treated enzyme was incubated in the Aminoff assay reaction mixture containing various concentrations (0.001-5 mM) of individual metal (Figure 4-5) [9]. The results show that the addition of Mn^{2+} at high concentration increases the mutant enzyme activity slightly, while all other metal ions inhibit the mutant enzyme.

Experiments were next performed to study the dependence of KDOPS^{Ec} N26C mutant activity on divalent metals (see Figure 4-6). The KDOPS^{Ec} N26C apo enzyme has almost no activity; however the addition of Mn^{2+} or Cd^{2+} dramatically stimulates the

mutant enzyme activity by 6 fold or 4 fold, respectively. Other metal ions do not increase the activity of the mutant enzyme.

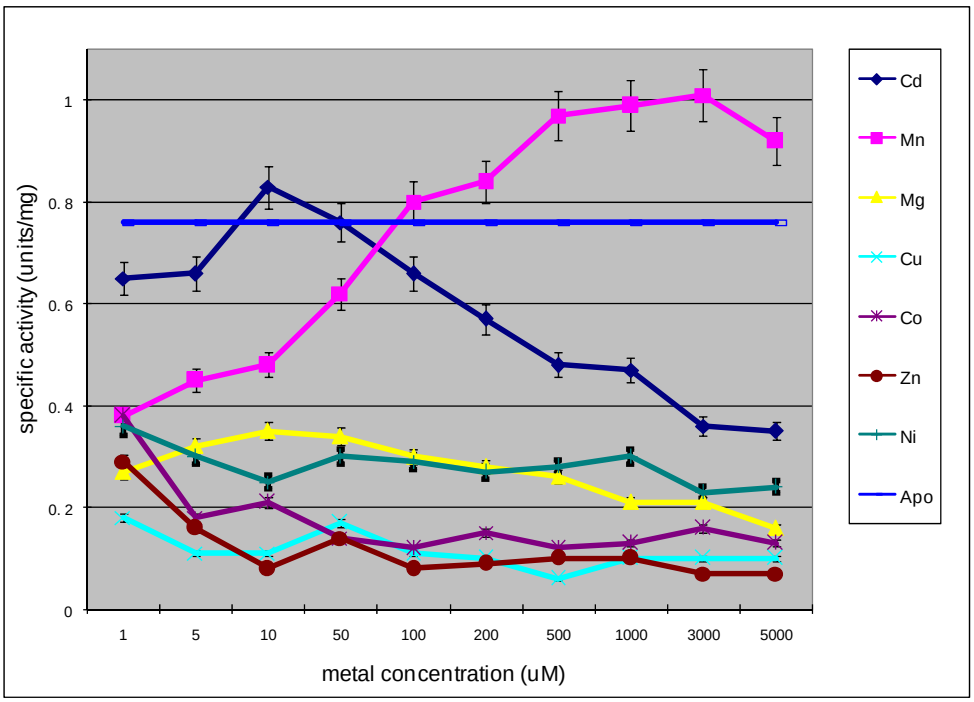

Figure 4-5. Concentration dependence of KDOPS^{Ec} M25P/N26C mutant activity on divalent metals.

The above results suggest that the KDOPS^{Ec} N26C or M25P/N26C mutants are activated by Mn^{2+} or Cd^{2+}. Previous studies show that the highest activation of the metallo wild-type KDOPS^{Aa} was also achieved with Mn^{2+} or Cd^{2+}. Thus, the KDOPS^{Ec} N26C or M25P/N26C mutants have some properties similar to that of the metal-dependent KDOPS, and may be considered as Mn^{2+} or Cd^{2+} dependent enzymes.

Studies on the metal requirements of KDOPS suggest a hypothesis for the evolution of KDOPS. The metallo KDOPSs are more ancient and have lower activity than the non-metallo KDOPSs. Loss of metal can be considered an evolutionary driving force for KDOPS. One amino acid substitution, Cys to Asn, is needed for KDOPS to

survive without metal. This is the reason that the metallo KDOPS^{Aa} can be converted into a non-metallo active enzyme by C11N mutation. Then, some additional secondary structural changes are required for the non-metallo KDOPS to gain higher catalytic activity. The inability to convert the non-metallo KDOPS^{Ec} to a metallo, enzymatically active enzyme by the N26C mutation might be due to these secondary changes in enzyme structure in addition to the single-site amino acid substitution. The Met/Pro might be the most obvious change. However, there are other more subtle changes that cannot be identified by simply comparing the structures or sequences between the two classes of KDOPSs.

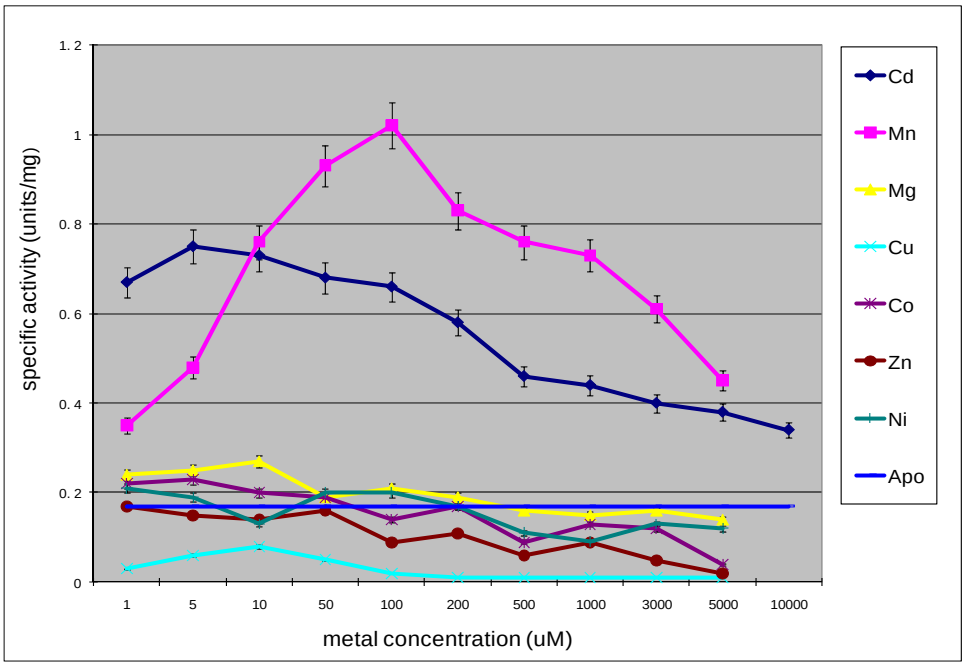

Figure 4-6. Concentration dependence of KDOPS^{Ec} N26C mutant activity on divalent metals.

The results above demonstrate that the Cys and Asn are really critical for the differences in the metal requirements of the two classes of KDOPSs. However, the role of the metal still remains unclear. Thus, the crystal structure of the KDOPS^{Aa} C11N

mutant in the presence of both substrates was solved, which might provide insight into. - the role and function of the metal and Asn.

4.3. THE CRYSTAL STRUCTURE OF *AQUIFEX AEOLICUS* KDOPS C11N MUTANT

4.3.1. Introduction

Several crystal structures of KDOPS^{Ec} and KDOPS^{Aa} were determined by our collaborator Prof. Domenico Gatti at Wayne State University in collaboration with our laboratory [3, 14]. The two proteins both adopt a $(\beta/\alpha)_8$-barrel topology, and share many similarities. The crystal structure of KDOPS^{Aa} with both substrates (A5P and PEP) as well as a metal ion was resolved, since KDOPS^{Aa} is a hyperthermophilic enzyme, it displays optimal activity at 95^{o}C but does not function well below 40^{o}C [6]. However, the crystal structure of KDOPS^{Ec} with both substrates could not be obtained due to turnover of the two substrates under crystallization and/or data collection conditions.

As described above, the KDOPS^{Aa} C11N mutation successfully converted the metallo wild-type KDOPS^{Aa} to a non-metallo KDOPS by single amino acid substitution [2]. Solving the crystal structure of this mutant protein might provide useful information on how the metal and/or Asn functions catalytically or structurally. The crystallization conditions for the mutant KDOPS should be similar to that of the wild-type KDOPS^{Aa}. Since the structure of wild-type KDOPS^{Aa} with both substrates is available, molecular replacement could be used to determine the crystal structure of KDOPS^{Aa} C11N mutant with substrates. In the wild-type KDOPS^{Aa} active site (Figure 4-7), the major role of C11 appears to be helping bind the metal ion with its chelating sulfur atom. The metal

ion is also coordinated to a water molecule bound on the *si* side of PEP. This water molecule is within hydrogen bonding distance to the C2-OH of A5P. How the N11 functions in the non-metallo KDOPS^{Aa} C11N mutant to replace the C and metal ion might be revealed by comparing the active site structure of the KDOPS^{Aa} C11N mutant to that of the wild-type KDOPS^{Aa} [15].

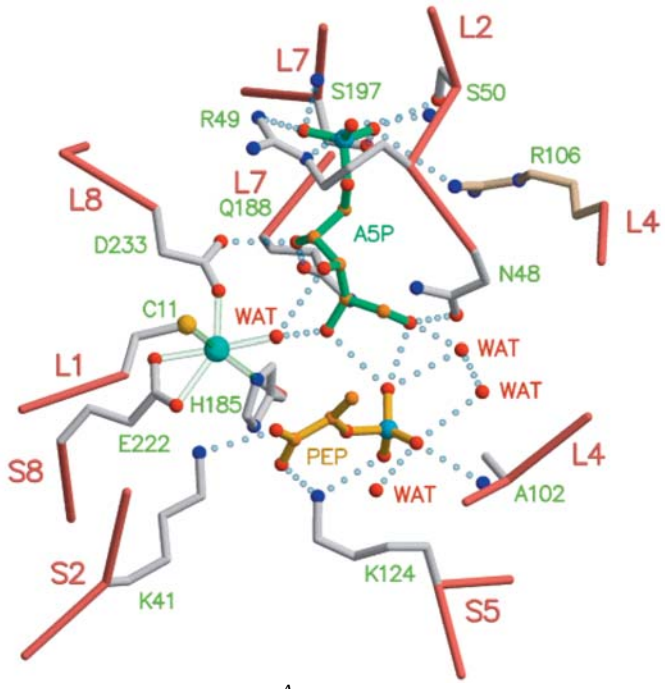

Figure 4-7. The structure of KDOPS^{Aa} active site with A5P, PEP and metal [15].

4.3.2 Experimental Procedures

Materials – Sodium acetate was purchased from J.T.Baker chemical company. Polyethylene glycol (PEG) 4000, Linbro® plate and siliconized glass circle cover slides (22 mm) used for hanging drop crystallization were purchased from Hampton Research. The molecular biology grade glycerol and ethylene glycol were purchased from Sigma. Phospho*enol*pyruvate mono(cyclohexylammonium) salt were obtained from Sigma. Arabinose 5-phosphate was prepared in our laboratory by Dr. Junhua Yan. The

KDOPS^{Aa} C11N mutant protein was prepared as described in 4.2.2, and concentrated to 10 mg/mL in 5mM Tris-HCl buffer (pH 7.5).

Crystal Screening and Crystallization – Purified KDOPS^{Aa} C11N mutant was concentrated to 10 mg/mL. Crystals were obtained by vapor diffusion in hanging drops. A series of conditions were screened [9]. The best condition for crystal growth was that 10 mg/mL protein mixed 1:1 with the reservoir solution containing 100 mM sodium acetate (pH 4.8) and 4-6% polyethylene glycol 4000. The crystallization trays were incubated at room temperature for 2-3 days. Crystals about 0.2-0.6 mm^3 in single were picked with cryoloop and soaked in the holding solution containing 100 mM sodium acetate (pH 4.8), 21% polyethylene glycol 4000, 16% glycerol, and 5% ethylene glycol for 24 h at room temperature. The crystals were then soaked with 8 mM PEP and 10 mM A5P at 4^{o}C for 2 h, and finally frozen in liquid nitrogen.

Data collection, crystal structure determination and refinement – The X-ray diffraction data was collected at the Synchrotron 5ID-B beam line by the Life Sciences Collaborative Access Team (LSCAT) at Advanced Photon Source (APS) in Argonne National Laboratory. The data was processed using d*trek program [16]. The KDOPS^{Aa} C11N mutant crystals belong to C2 space group, with a = 146.017 Å, b = 51.0956 Å, c = 213.5525 Å. The structure of KDOPS^{Aa} C11N mutant was determined at 2.2 Å resolution by molecular replacement using the program Phaser [17], with wild-type KDOPS^{Aa} as a search model. The protein structure was refined iteratively by alternating REFMAC refinement [18], and model building using COOT [19]. The structure contains six monomers of mutant KDOPS^{Aa} in an asymmetric unit (one full tetramer and a half of another tetramer, with the other half generated by a crystal symmetry operation).

The structure also contains six phosphate molecules, each bound at the active sites of the six KDOPS monomers. Water molecules were placed in peaks > 3σ of (Fo - Fc) electron density.

4.3.3. Results and Discussion

The KDOPS^{Aa} C11N mutant crystals, 0.2-0.6 mm^3 in single, from the final crystal screen were selected for data collection (Figure 4-8).

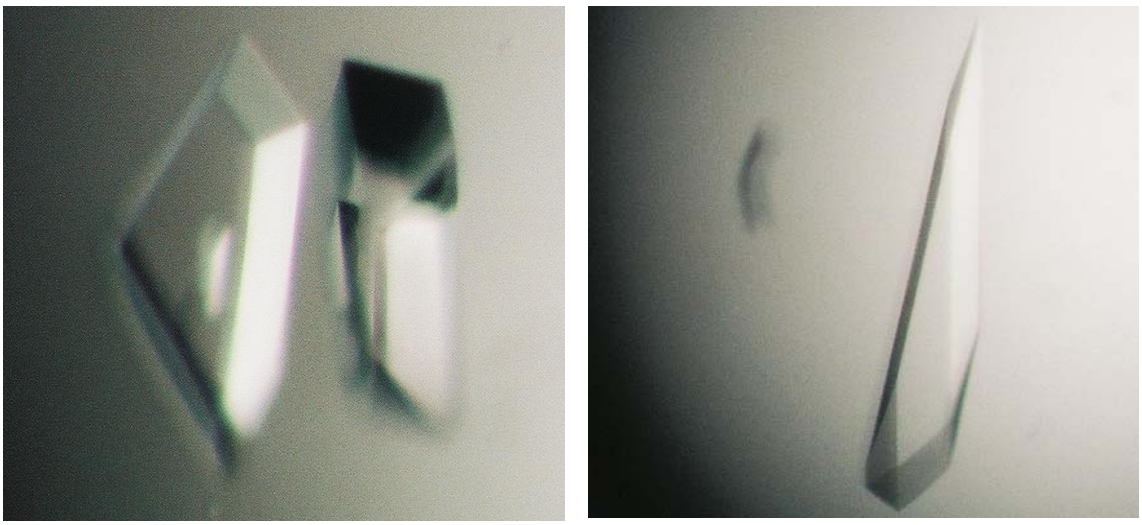

Figure 4-8. Pictures of KDOPS^{Aa} C11N mutant crystals used for X-ray analysis.

Previous crystal structure studies on the wild-type metallo KDOPS^{Aa} report that the crystals of the wild-type KDOPS^{Aa} display a pink color, which is due to the presence of metal ion in the enzyme. The crystals of the C11N mutant KDOPS^{Aa} grown in our laboratory are colorless. The difference in the color of the crystals might indicate that the metal requirement has changed in the mutant enzyme.

Statistics of the data collection and refinement are shown in Table 4-5. The structure contains six monomers (one full tetramer and a half of another tetramer) in the asymmetric unit, and was refined at 2.2 Å. The Ramachandran plot is shown in Figure

4-9, indicating how the crystal data fits into the secondary structure including α-helixes, β-strands and loops.

Table 4-5. Crystallographic data collection and structure refinement statistics for KDOPS^{Aa} C11N mutant. Highest resolution shell values are shown in parentheses.

KDOPS^{Aa} C11N mutant, 6 monomers per asymmetric unit		
Data Collection	Space group	C2
	Cell dimensions a, b, c (Å) α, β, γ (^{o})	 146.017, 51.0956, 213.5525 90, 97.8512, 90
	Resolution(Å)	48.18-2.20 (2.28-2.20)
	R_{merge}	0.071 (0.296)
	I/δ_I	13.8 (5.3)
	Completeness	100% (100%)
	Redundancy	7.84 (7.43)
Refinement	Resolution (Å)	40.00-2.20 (2.26-2.20)
	No. reflections	76047 (5565)
	R/R_{free} (5% test size)	0.22/0.27 (0.25/0.33)
	R.m.s. deviations from ideal geometry Bond length (Å) Bond angles (^{o})	 0.022 1.97

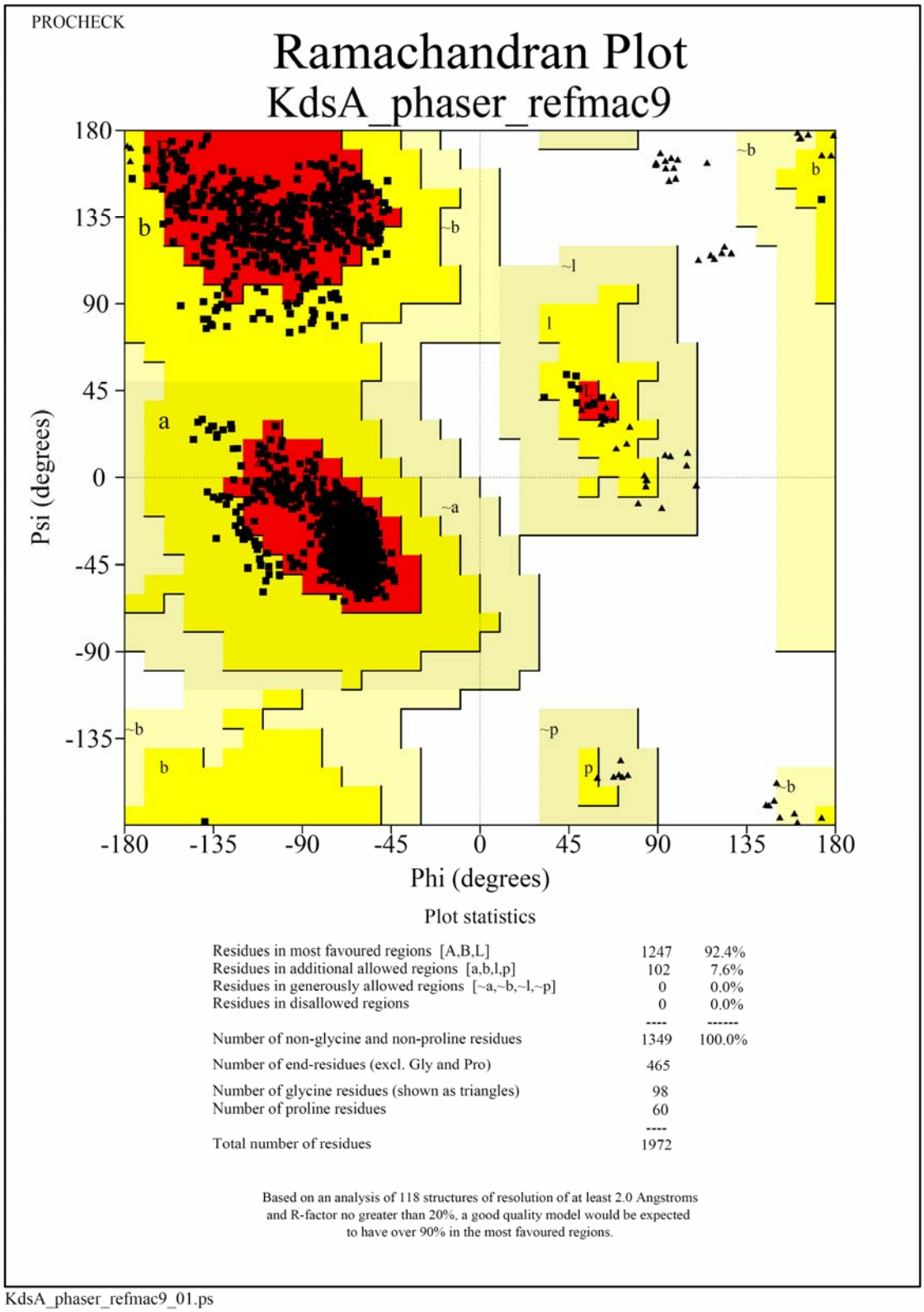

Figure 4-9. Ramachandran plot of KDOPS^{Aa} C11N mutant crystal structure. A represents α-helix. B represents β-strand. L represents loop.

Many similarities are seen in the crystal structure of the KDOPS^{Aa} C11N mutant and the wild-type KDOPS^{Aa} [3]. One asymmetric unit of the KDOPS^{Aa} C11N mutant structure contains one full tetramer and half of another tetramer, while the wild-type KDOPS^{Aa} structure contains one tetramer in one asymmetric unit. Each monomer of the KDOPS^{Aa} C11N mutant folds into a $(\beta/\alpha)_8$ barrel structure: 8 parallel β-strands surrounded by 8 α-helixes. The active site of each monomer is located at the C-terminal end of the barrel in each subunit at the interface of the adjacent subunit. A phosphate molecule is found bound in each of the active sites (Figure 4-10).

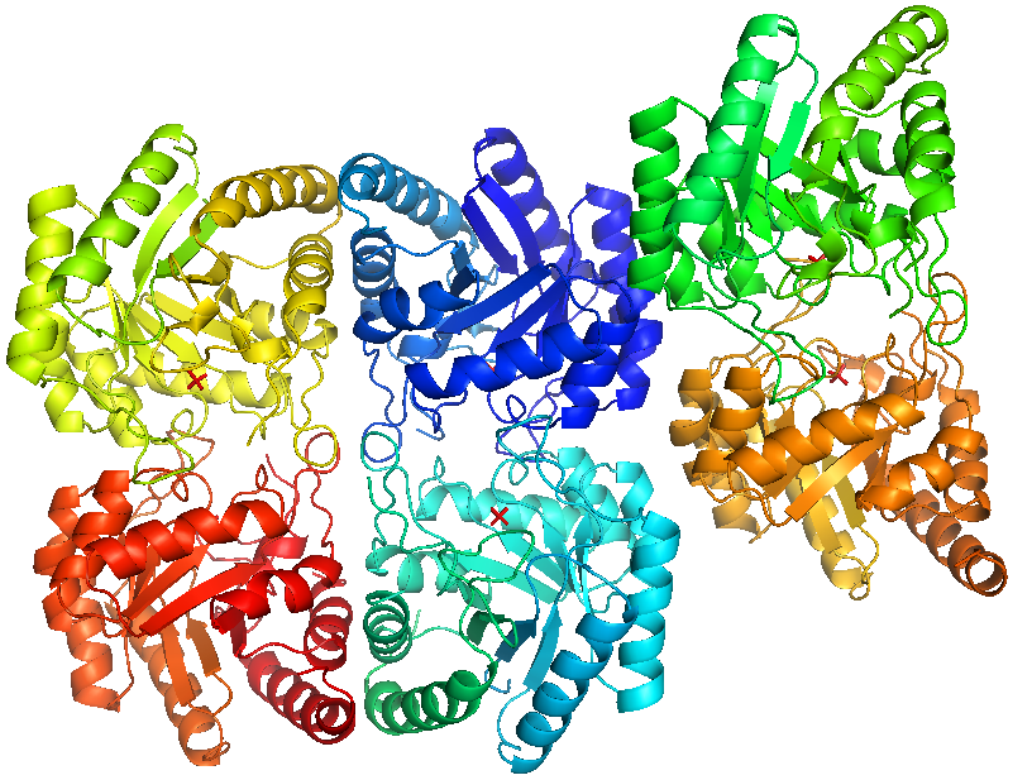

Figure 4-10. Overall structure of one asymmetric unit in KDOPS^{Aa} C11N mutant. The phosphate ions bound in each monomer are shown in red.

The overall feature in the structure of wild-type KDOPS^{Aa} is conserved in the C11N mutant structure. The key difference appears around the replacement position. As expected, no metal is visible in the active site, since KDOPS^{Aa} C11N mutant is a

non-metallo enzyme. As described in the experimental procedures session, during the crystallization procedure, the crystal of KDOPS^{Aa} C11N mutant was soaked in a solution containing PEP and A5P in order to obtain a crystal structure with both substrates in the active site. However, in the final resolved structure, only a phosphate ion is found in the active site. The phosphate ion binds at the same active site position as the phosphate moiety of PEP in wild-type KDOPS^{Aa} structure [3], and is stabilized by a network of electrostatic interactions and hydrogen bonds between the phosphate ion and the back bone of A102 and the side chains of K124 and R154 (Figure 4-11).

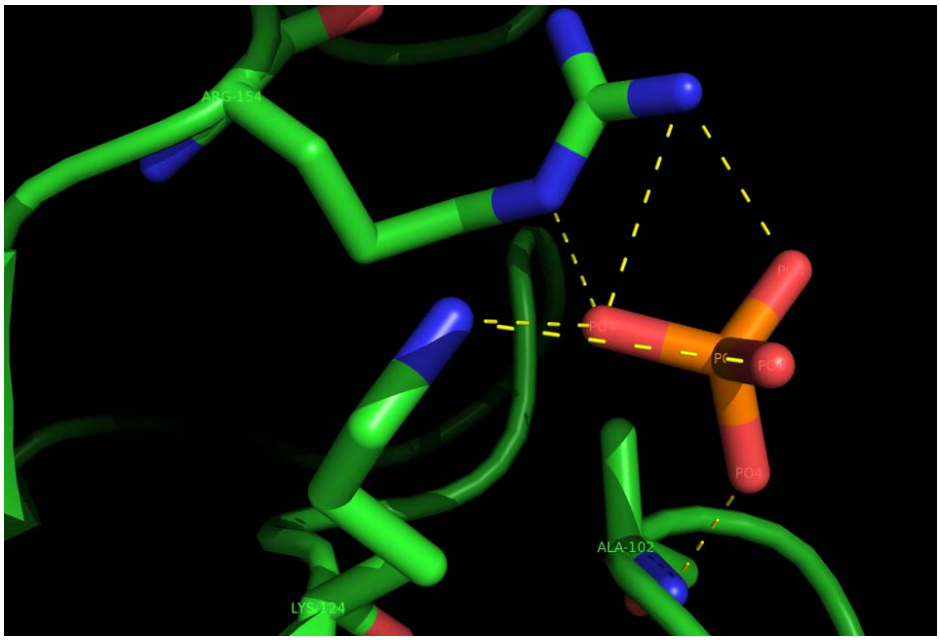

Figure 4-11. The phosphate ion bound in the active site of KDOPS^{Aa} C11N mutant. The protein is shown in green, while the phosphate ion is shown in orange.

No phosphate ion was introduced into the protein during the protein purification or crystallization procedure; thus, the reason that a phosphate ion is present at the active site might be that when PEP and A5P were soaked into the crystal, an enzymatic turnover occurred slowly under the experimental conditions. In this case, a phosphate ion might

be bound at the active site, since the release of inorganic phosphate is the kinetic bottleneck of the catalytic reaction.

While the crystal structure of KDOPS^{Aa} C11N mutant with phosphate ion in the active site was obtained in our laboratory, the crystal structures of KDOPS^{Aa} C11N mutant with both substrates (PEP+A5P) was very recently solved by our former collaborator Professor Domenico Gatti at Wayne State University using different crystallization technology [20]. These two structures are almost identical in both overall structure and active site, which offers an opportunity for us to investigate the structure of the KDOPS^{Aa} C11N mutant in more detail.

In both our and Professor Gatti's structures, the carboxamide group of N11 forms hydrogen bonds with the carboxylate oxygen of E222 (one of the four metal binding residues in metallo KDOPS) and the hydroxyl group of S232. These interactions are not seen in the wild-type enzyme (where C11 is present) and might help maintain the active site geometry. The functional carboxamide group of N11 fills the hole left by the loss of the metal. In the active site of C11N mutant with both substrates (shown in Figure 4-12), a water molecule is located at the *re* side of PEP, and is well positioned for a nucleophilic attack on C2 of PEP. This water molecule is also found in the wild-type KDOPS^{Aa} at a similar place. The most interesting thing in the structure with both substrates is that the carboxamide group of N11 is within hydrogen bonding range to the C2-OH of A5P. Due to this interaction, A5P binds with an orientation different from that of the wild-type KDOPS^{Aa}. In the active site of the wild-type KDOPS^{Aa}, there is a water molecule at the *si* side of PEP, which is coordinated to the divalent metal, and also forms a hydrogen bond to the C2-OH of A5P (see Figure 4-7).

While in the KDOPS^{Aa} C11N mutant, the C2-OH of A5P displaces this water molecule and is hydrogen bonded to N11 and H185 [3]. These results suggest that the metal in the wild-type metallo KDOPS^{Aa} might function by coordinating to a water molecule which forms hydrogen bond with C2-OH A5P and helps correctly orienting A5P for the nucleophilic attack by C2 of PEP. In the KDOPS^{Aa} C11N mutant, no metal is bound; the N11 replaces the metal in helping orient A5P by direct hydrogen bond between the carboxamide group of N11 and C2-OH of A5P. Thus, the metal/Asn might play an important structural role through maintaining correct orientation of A5P in the enzyme active site to allow the catalysis.

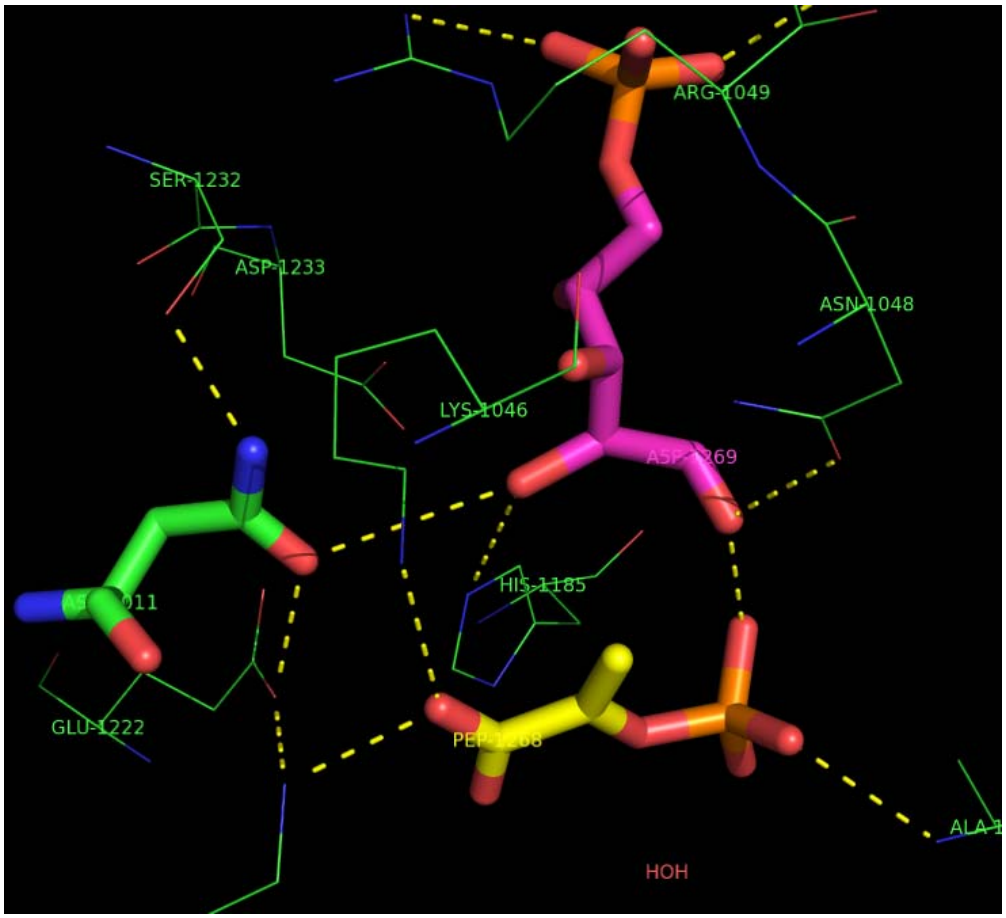

Figure 4-12. Active site structure of KDOPS^{Aa} C11N mutant with both substrates. A5P is shown in purple stick, PEP is shown in yellow stick, and N11 is shown in green stick. Other active site residues are shown in green line.

The results also indicate that the C2-OH group of A5P is important in correctly aligning the aldehyde group of A5P for catalysis. A different stereochemistry on the C2 will not be accepted. Thus, as described in Chapter 3, R5P was an alternate substrate for KDOPS due to its different stereochemistry on C2. The 2-deoxy R5P could be utilized as an alternate substrate since it does not have hydroxyl group on C2, and may not be misoriented.

4.4. ACKNOWLEDGEMENTS

I want to thank Dr. Ted Huston in the University of Michigan, Department of Geology for help determine metal content of KDOPS using high-resolution inductively coupled plasma-mass spectrometry (ICP-MS)., Dr. Oleg Tsodikov and Dr. Tapan Biswas for their help and assistance during the refinement of the crystal structure of KDOPS^{Aa} C11N mutant, Dr. Vijayalakshmi Janakiraman for her help in crystallization and data process, and Prof. Domenico Gatti at Wayne State University for solving the crystal structure of KDOPS^{Aa} C11N mutant with substrates. And I would like to thank members in the Woodard group for all their help.

4.5. REFERENCES

1. Birck, M.R., R.W. Woodard, and C.o.P.U.o.M.C.S.A.A.M.I.U.S.A. Department of Medicinal Chemistry, *Aquifex aeolicus 3-deoxy-D-manno-2-octulosonic acid 8-phosphate synthase: a new class of KDO 8-P synthase?* Journal of molecular evolution., 2001. **52(2)**: p. 205-14.

2. Li, J., et al., *Conversion of Aquifex aeolicus 3-Deoxy-d-manno-octulosonate 8-Phosphate Synthase, a Metalloenzyme, into a Nonmetalloenzyme.* J Am Chem Soc, 2004. **126**(24): p. 7448-9.

3. Duewel, H.S., et al., *Substrate and metal complexes of 3-deoxy-D-manno-octulosonate-8-phosphate synthase from Aquifex aeolicus at 1.9-A resolution. Implications for the condensation mechanism.* The Journal of biological chemistry., 2001. **276(11)**: p. 8393-402.

4. Shumilin, I.A., R.H. Kretsinger, and R.H. Bauerle, *Crystal structure of phenylalanine-regulated 3-deoxy-D-arabino-heptulosonate-7-phosphate synthase from Escherichia coli.* Structure Fold Des, 1999. **7**(7): p. 865-75.

5. Vandeyar, M.A., et al., *A simple and rapid method for the selection of oligodeoxynucleotide-directed mutants.* Gene, 1988. **65**(1): p. 129-33.

6. Duewel, H.S., et al., *Functional and biochemical characterization of a recombinant 3-Deoxy-D-manno-octulosonic acid 8-phosphate synthase from the hyperthermophilic bacterium Aquifex aeolicus.* Biochemical and biophysical research communications., 1999. **263(2)**: p. 346-51.

7. Aminoff, D., *Methods for the Quantitative Estimation of N-Acetylneuraminic Acid and their Application to Hydrolysates of Sialomucoids.* Biochem. J., 1961. **81**: p. 384-392.

8. Howe, D.L., et al., *Mechanistic insight into 3-deoxy-D-manno-octulosonate-8-phosphate synthase and 3-deoxy-D-arabino-heptulosonate-7-phosphate synthase utilizing phosphorylated monosaccharide analogues.* Biochemistry., 2003. **42(17)**: p. 4843-54.

9. Duewel, H.S., R.W. Woodard, and U.o.M.A.A.M.U.S.A. Interdepartmental Program in Medicinal Chemistry, *A metal bridge between two enzyme families. 3-deoxy-D-manno-octulosonate-8-phosphate synthase from Aquifex aeolicus requires a divalent metal for activity.* The Journal of biological chemistry., 2000. **275(30)**: p. 22824-31.

10. Salleh, H.M., et al., *Essential cysteines in 3-deoxy-D-manno-octulosonic acid 8-phosphate synthase from Escherichia coli: analysis by chemical modification and site-directed mutagenesis.* Biochemistry., 1996. **35(27)**: p. 8942-7.

11. Park, O.K., R. Bauerle, and U.o.V.C.V.U.S.A. Department of Biology, *Metal-catalyzed oxidation of phenylalanine-sensitive 3-deoxy-D-arabino-heptulosonate-7-phosphate synthase from Escherichia coli: inactivation and destabilization by oxidation of active-site cysteines.* Journal of bacteriology., 1999. **181(5)**: p. 1636-42.

12. Li, Y., et al., *The hard-soft acid-base principle in enzymatic catalysis: dual reactivity of phosphoenolpyruvate.* Proceedings of the National Academy of Sciences of the United States of America., 1996. **93(10)**: p. 4612-6.

13. Shumilin, I.A., et al., *The high-resolution structure of 3-deoxy-D-arabino-heptulosonate-7-phosphate synthase reveals a twist in the plane of bound phosphoenolpyruvate.* Biochemistry., 2003. **42(13)**: p. 3766-76.

14. Radaev, S., et al., *Structure and mechanism of 3-deoxy-D-manno-octulosonate 8-phosphate synthase.* J Biol Chem, 2000. **275**(13): p. 9476-84.

15. Wang, J., et al., *Structures of Aquifex aeolicus KDO8P synthase in complex with R5P and PEP, and with a bisubstrate inhibitor: role of active site water in catalysis.* Biochemistry., 2001. **40(51)**: p. 15676-83.

16. Broennimann, C., et al., *The PILATUS 1M detector.* J Synchrotron Radiat, 2006. **13**(Pt 2): p. 120-30.

17. McCoy, A.J., et al., *Likelihood-enhanced fast translation functions.* Acta Crystallogr D Biol Crystallogr, 2005. **61**(Pt 4): p. 458-64.

18. Murshudov, G.N., A.A. Vagin, and E.J. Dodson, *Refinement of macromolecular structures by the maximum-likelihood method.* Acta Crystallogr D Biol Crystallogr, 1997. **53**(Pt 3): p. 240-55.

19. Emsley, P. and K. Cowtan, *Coot: model-building tools for molecular graphics.* Acta Crystallogr D Biol Crystallogr, 2004. **60**(Pt 12 Pt 1): p. 2126-32.

20. Kona, F., et al., *Structural and mechanistic changes along an engineered path from metallo to nonmetallo 3-deoxy-D-manno-octulosonate 8-phosphate synthases.* Biochemistry, 2007. **46**(15): p. 4532-44.

CHAPTER 5

CONCLUSIONS AND FUTURE DIRECTIONS

This dissertation focused on studying the substrate specificity and metal requirements of KDOPS through mutagenesis studies, substrate analogue studies, and X-ray crystallography study in order to gain mechanistic insight into KDOPS.

In chapter 2, three methodologies including structure based engineering, domain swapping and directed evolution were used to alter the substrate specificity of KDOPS from A5P to E4P. Although none of the modified KDOPS could utilize E4P (the substrate of DAHPS) as alternate substrate, several important amino acid residues or loop involved in monosaccharide substrate binding in KDOPS were defined. The results show that changes to these residues or loop remarkably affect the A5P binding. For future experiments, the mutations or truncation made to these critical residues or loop could be combined in order to make the KDOPS substrate binding site more similar to that of the DAHPS. Thus, the resulting modified KDOPS might be able to utilize E4P as an alternate substrate.

In chapter 3, different A5P analogues were tested as alternate carbohydrate substrates for KDOPS. Only 2-deoxy R5P and arabinose 5-difluoromethylenephosphonate were found to be alternate substrates for KDOPS albeit at modest rates. Enzymatic synthesis of 3-deoxy-D-manno-octulosonate 8-difluruomethylenephosphonate (KDOFP) was performed using 5-difluoromethylenephosphonate, PEP and *E. coli* KDOPS ($KDOPS^{Ec}$). NMR analysis and mass spectrum of the reaction product verify that 5-difluoromethylenephosphonate is indeed an alternate substrate for $KDOPS^{Ec}$, but with a much lower rate than the natural substrate A5P. The yield of this enzymatic synthesis reaction might be increased by extending the reaction time or supplementing more enzymes in order to synthesize more KDOFP for future studies of other KDO8P utilizing enzymes. Solving the crystal structure of $KDOPS^{Ec}$ with arabinose 5-difluoromethylenephosphonate and PEP might provide more information on how this alternate substrate binds the active site for catalysis.

In chapter 4, the interconversion between metallo and non-metallo KDOPS was conducted in order to gain mechanistic information concerning the two different KDOPS classes. The *A. aeolicus* KDOPS ($KDOPS^{Aa}$) C11N mutant successfully converted the metallo wild-type KDOPS into a non-metallo enzyme by single amino acid substitution. The activity of $KDOPS^{Ec}$ N26C and M25P/N26C mutants can be increased by addition of Mn^{2+} or Cd^{2+}, which suggests that these $KDOPS^{Ec}$ mutants have some properties similar to the metallo KDOPS. The crystal structure of $KDOPS^{Aa}$ C11N was solved in our

laboratory and concurrently by our former collaborator Professor Domenico Gatti at Wayne State University. The combined results suggest that the metal or N11 plays an important structural role in maintaining correct orientation of A5P for catalysis. In future study, solving the crystal structures of KDOPS^{Ec} N26C and M25P/N26 mutants might help better understand the role of these active site residues.

In conclusion, the results in this thesis help better understand the substrate binding modes in KDOPS and help begin to understand the difference between metal and non-metallo KDOPSs. Directions are provided for more in-depth investigation into the mechanism of KDOPS in future mutagenesis and X-ray crystallography studies.